SIMULATION OF A DIODE PUMPED ALKALI LASER; A THREE LEVEL NUMERICAL APPROACH

THESIS

Shawn W. Hackett, Second Lieutenant, USAF

AFIT/GAP/ENP/10-M06

DEPARTMENT OF THE AIR FORCE
AIR UNIVERSITY

AIR FORCE INSTITUTE OF TECHNOLOGY

Wright-Patterson Air Force Base, Ohio

The views expressed in this thesis are those of the author and do not reflect the official policy or position of the United States Air Force, Department of Defense, or the United States Government.

AFIT/GAP/ENP/10-M06

SIMULATION OF A DIODE PUMPED ALKALI LASER; A THREE LEVEL NUMERICAL APPROACH

THESIS

Presented to the Faculty

Department of Engineering Physics

Graduate School of Engineering and Management

Air Force Institute of Technology

Air University

Air Education and Training Command

in Partial Fulfillment of the Requirements for the

Degree of Master of Science in Applied Physics

Shawn W. Hackett, BS

Second Lieutenant, USAF

March 2010

AFIT/GAP/ENP/10-M06

SIMULATION OF A DIODE PUMPED ALKALI LASER; A THREE LEVEL NUMERICAL APPROACH

Shawn W. Hackett, BS
Second Lieutenant, USAF

Approved:

Jeremy C. Holtgrave (Chairman)	Date
Glen P. Perram (Member)	Date
Kevin C. Gross (Member)	Date

AFIT/GAP/ENP/10-M06

Abstract

This paper develops a three level model for a continuous wave diode pumped alkali laser by creating rate equations based on a three level system. The three level system consists of an alkali metal vapor, typically Rb or Cs, pumped by a diode from the ${}^2S_{\frac{1}{2}}$ state to the ${}^2P_{\frac{3}{2}}$, a collisional relaxation from ${}^2P_{\frac{3}{2}}$ to ${}^2P_{\frac{1}{2}}$, and then lasing from ${}^2P_{\frac{1}{2}}$ to ${}^2S_{\frac{1}{2}}$. The hyperfine absorption and emission cross sections for these transitions are developed in detail. Differential equations for intra-gain pump attenuation and intra-gain laser growth are developed in the fashion done by Rigrod. Using *Mathematica* 7.0, these differential equations are solved numerically and a diode pumped alkali laser system is simulated. The solutions of the differential equations are then utilized to characterize the inversion, the gain profile, the output laser intensity, and the pump intensity absorption profile for many different diode pumped alkali laser systems. The results of the simulation are compared to previous experimental results and to previous computational results for similar systems. The absorption profile for the three level numerical model is shown to have excellent agreement with previous absorption models. The lineshapes of the three level numerical model are found to be nearly identical to previous developments excepting those models assumptions. The three level numerical model provides results closer to experimental results than previous systems and provides results which observe effects not previously modeled, such as the effects of lasing on pump attenuation.

Table of Contents

Page

List of Figures

Figure Page

List of Tables

List of Symbols

Symbol — Page

Symbol Page

Symbol Page

Symbol Page

SIMULATION OF A DIODE PUMPED ALKALI LASER; A THREE LEVEL NUMERICAL APPROACH

I. INTRODUCTION

The purpose of this work is to develop a model for the propagation of a Diode Pumped Alkali Laser (DPAL) within a cavity and to use computer modeling software to implement a simulation of this model. The model will be developed to aid in the research and design of new DPAL systems. A DPAL is a relatively new type of laser which relies on laser transitions occurring within an alkali metal. These lasers use electrically driven diodes to create pump photons, which are incident on a gaseous alkali metal. In a process described by Krupke [4], these photons create a population inversion which leads to lasing. Therefore, DPALs are neither solid state not gas phase laser but rather a hybrid.

The vast majority of past and current research within the Air Force has centered around chemical laser systems like the Chemical Oxygen-Iodine Laser (COIL) and Hydrogen Fluoride (HF) lasers. These systems offer high output powers of at least a megawatt or more, but chemical lasers have a finite magazine associated with their reactants and usually require large facilities to create and sustain the conditions needed for lasing. Because of the difficulty in deploying chemical laser systems, the Air Force is studying other types of laser systems to characterize their abilities and their potential to be used in future weapon systems. DPAL systems are attractive as one possible alternative to chemical lasers as they are pumped by electrically driven diodes, and therefore are capable of being powered by a conventional electrical generator or an aircraft's onboard power plant. To date, DPAL systems are not well

characterized compared to other laser systems. Most of the research and development on DPAL modeling has focused on relatively simplistic theoretical models used to make rough estimates and trial and error lab characterization of DPAL systems.

In general, the alkali metal chosen for a DPAL is either cesium (Cs) or rubidium (Rb); however, other alkali metals have been used to successfully create a DPAL. Most DPAL systems currently are three level lasers whereby the ground $^2S_{\frac{1}{2}}$ state is pumped to the excited $^2P_{\frac{3}{2}}$. This is then collisionally relaxed to the $^2P_{\frac{1}{2}}$ state by a buffer gas, which is usually helium or a hydrocarbon such as methane or ethane. Photons in the $^2P_{\frac{1}{2}}$ state proceed to lase to the ground state. The $^2P_{\frac{3}{2}}$ state and $^2P_{\frac{1}{2}}$ state are the analogous features in any alkali corresponding to the well-known doublet in Na. Other, more novel, DPAL systems based on other possible transitions within the alkali metals have been proposed, but have not yet been published. DPAL systems offer a much higher stimulated emission cross section than most laser species, and therefore, have the possibility of delivering sufficient output intensities and power needed for a weapon system. A major drawback to DPAL systems is that they require the ground state to be depopulated by at least half to create an inversion. This is true with any three level laser. To create the required inversion demands that approximately half of the atoms in the $^2S_{\frac{1}{2}}$ be pumped into one of the two upper states. The required inversion will only occur when fewer atoms are in the $^2S_{\frac{1}{2}}$ than in the $^2P_{\frac{1}{2}}$. With modern diode pumping sources this is achievable albeit somewhat difficult. Currently, the theoretical models used by researchers at the Air Force Institute of Technology were developed by Lewis [5] and Hager [3]. The Lewis and Hager models offer many benefits, but do not completely characterize a DPAL system. So, a model has been developed which takes into account a greater amount of parameters and phenomena than [5] and [3]. Throughout this document, "simulation" refers to a computer construct of a "model", which is a theoretical construct of a physical system.

Simulation and model are not interchangeable. The model developed will provide the output power of a DPAL system based on the characteristics of the pump diodes and the lasing cavity. However, this model will not be capable of developing all the necessary physics for the engagement of a target with the DPAL system. Instead this model focuses on developing the output characteristics of a DPAL system which then might be added to current target engagement scenarios or could be used as a research tool to direct the flow of future DPAL research.

II. BACKGROUND

2.1 Overview

DPAL systems are gas electric hybrid lasers. In general, a gaseous cell of an alkali metal has photons incident on it from a narrow banded diode. Alkali atoms are used because of their large absorption cross sections, well-known properties, and similarity to atomic hydrogen [5]. In most current DPAL systems, the diode pumps the ${}^2S_{\frac{1}{2}} \rightarrow {}^2P_{\frac{3}{2}}$ transition (the D2 manifold). The incident light from the diode must have spectral broadening of less than approximately 20 GHz to pump only the ${}^2S_{\frac{1}{2}} \rightarrow {}^2P_{\frac{3}{2}}$ and to ensure that the majority of the pump energy is absorbed by the alkali. A buffer gas is also present in the gaseous cell. This gas serves to collisionally de-excite atoms from the state ${}^2P_{\frac{3}{2}}$ to the ${}^2P_{\frac{1}{2}}$ state [3]. This transition is optically forbidden, so the buffer gas is required for a DPAL to operate. Most often, the gas chosen is ethane, methane, helium or some combination of the three. These gases are generally selected because of their large collisional cross sections with alkali atoms. The alkali metals currently used most often are Rb and Cs. These metals are generally chosen as they have large energy gaps between the ${}^2P_{\frac{3}{2}}$ and ${}^2P_{\frac{1}{2}}$ states [5]. Usually, the laser transition occurs between the ${}^2P_{\frac{1}{2}}$ and the ${}^2S_{\frac{1}{2}}$. The DPAL scheme previously mentioned is the most common method used, but other systems have been theorized and a few have been tested [6]. One such system uses collisional excitation of the alkali to the ${}^2P_{\frac{3}{2}}$ state by a collision of multiple noble gas and alkali pairings. These pairings then dissociate after excitation, and the alkali is then induced to lase by the same process aforementioned [6]. Other proposed systems include pumping to upper states beyond ${}^2P_{\frac{3}{2}}$ with double photon absorption and creating laser transitions in the upper manifold of the alkali atoms. No working demonstration of such a system has been published.

To date, most work on the simulation of DPAL systems has focused on modeling the attenuation of the diode pump upon entering the alkali gain medium and on determining the output lasing intensity of DPAL systems under Continuous Wave (CW) conditions. Two of these simulations were developed by Hager [3] and one by Lewis [5]. In general, the key to developing the output lasing intensity is ascertaining the number densities of each of the three levels in the DPAL system, and then calculating the resulting attenuation of the pump intensity. The intra-cavity lasing intensity is deduced by the attenuation of the pump wave based upon the conservation of energy. To determine these number densities and intensities, a simplifying assumption known as the quasi-two level system is used to some degree by both models. However, later developments of the Hager model are three level and not quasi-two level.

The quasi-two level model approximates that the transition rate between the $^2P_{\frac{3}{2}}$ and $^2P_{\frac{1}{2}}$ level due to the buffer gas is fast enough that no other excitation or de-excitation processes occur to atoms in the $^2P_{\frac{3}{2}}$ state. That is, the number density of the atoms in the $^2P_{\frac{3}{2}}$ level is assumed to maintain an equilibrium distribution in relation to the $^2P_{\frac{1}{2}}$ level based upon statistical mechanics. Thus, the $^2P_{\frac{3}{2}}$ state and the $^2P_{\frac{1}{2}}$ state are essentially one state. This approximation is not completely valid, but vastly simplifies the problem. The Lewis model works under the quasi-two level approximation, but attempts to achieve better fidelity by simulating the effect of the lasing waves in the cavity after threshold have been reached. To actually simulate the true effect of lasing, one must assume that lasing can always effect the number densities. Without this effect the model is not completely accurate. The Hager model assumes that the number density along the alkali cell can be longitudinally averaged, and this number density can be used to formulate the rate equations and the intra-cavity pump and lasing intensities. This is known as Longitudinally Averaged Number Density (LAND). This also, is not a wholly accurate approximation and under certain

conditions will be inaccurate. Indeed, in most cases the LAND approximation is valid. Only in certain regimes near threshold does the LAND approximation begin to fail [3]. Also, the Hager model does not account for spectrally broadband pumping. It is assumed that all pump photons have the same frequency. Therefore, both the Lewis and Hager models are able to give the user of the simulation an idea of how certain systems will perform. Both models offer a great deal of insight into the operation of DPAL systems under many circumstances and regimes. Physical systems cannot be tested to sufficient fidelity to replicate the results of laboratory experiments. Further, these models have been unable to produce results which describe a three level DPAL system to the fidelity required to perform testing and investigation of new systems without the creation of an experimental apparatus. Hence, to better characterize DPAL systems a more accurate model of the DPAL system must be simulated.

2.2 Experimental DPAL Development

One of the earliest developments of a laser system similar to DPAL was done by Beach in 2004 [1]. Beach suggested the use of diodes to pump an optically emitting Rb or Cs laser similar to a diode pumped solid state laser, but using a gas phase alkali. In this paper, Beach used a Ti:S laser to pump a Cs system. Beach then showed that a diode could also be used as a pump source if the diode was able to emit an output sufficiently narrow in frequency to limit the pumping of the lasing transition. To achieve this a diode's pump output must have a lineshape of approximately 10 GHz at 400 $Torr$ of He to successfully pump the Cs D2 line [3]. In practice, this is somewhat difficult to achieve but diodes have been successfully used to pump low power systems [10]. Beach further suggested that such lasers could produce powers comparable to solid state pumped diode lasers in CW operation [1]. A quasi-CW power of 48 W with a 52 percent slope efficiency have been achieved by Zhdanov

by pumping with diode systems [9]. It is believed that DPAL systems can produce even higher output powers as diode technology improves. DPAL systems under pulsed operation have the potential to be the basis of a megawatt class laser system [5] So, as DPAL technology improves it would be extremely advantageous and cost effective to use computer modeling to characterize DPAL systems prior to building such systems.

2.3 Hager Model

The Hager model can be either quasi-two level or three level. The LAND method is utilized to determine the number densities used in the three level rate equations. A two level model cannot create the inversion needed for a laser [8]. The earlier quasi-two level model discussed by Hager assumes that the collisional relaxation rate between ${}^2P_{\frac{3}{2}}$ and ${}^2P_{\frac{1}{2}}$ is fast enough that the two populations are statistically disturbed as aforementioned. This model is, therefore, not a truly 2-level model, but an approximation to simplify analysis. The rate equations are then developed based on these assumptions. It is assumed that the laser is operating in CW conditions. The rate equations are used to develop the pump intensity I_P and the laser intensity I_L as functions of cavity position via Rigrod analysis [3]. The equation for I_P is inherently transcendental. The set of differential equations is solved numerically.

Hager also develops the lineshape g_{ji} of the transitions and their absorption cross sections σ_{ij}. The $g_{ji}(\nu)$ and σ_{ji} derived include the effects from hyperfine structure. The order of the subscripts determines whether σ and g are related to absorption or emission. If i is first then it is absorption; if j is first then it is emission. The effects of hyperfine structure on I_L and I_P are not examined. As I_L and I_P are the main pieces of information required to characterize a DPAL system, I_L and I_P are the focus of this development [3]. Quenching or collisional de-excitation from levels above the ground state to the ground state are not examined. Cavity reflectivities are input parameters

and are utilized to determine loss. The later three-level model developed by Hager assumes that the number densities are still given by LAND, but that the $^2P_{\frac{3}{2}}$ and $^2P_{\frac{1}{2}}$ levels are not given by their statistical relation. Each of these populations must be found independently [3]. Both models developed by Hager assume single frequency pumping, which is, in general, not valid for modern diodes. Hager also assumes that multiple isotopes of the alkali may be present in the gain medium in the quasi-two level and three level cases. The Hager model does simulate the operation of a DPAL system under most cases well. However, the Hager model is not accurate in all cases and can be improved. Further, in some systems the processes not examined by Hager can come to dominate the operation of the DPAL system and must be handled if a complete three level model is to be developed [3].

2.4 Lewis Model

Lewis's model is a quasi-two level model. As mentioned previously this assumes that the $^2P_{\frac{3}{2}}$ state and the $^2P_{\frac{1}{2}}$ state are statistically distributed only. For simplicity, it is assumed that many of the optical transitions are much less likely than the pump and lasing transition. Quenching can be examined, but is not because of a lack of data on the quenching. Several isotopes of common alkalis are examined simultaneously. Lewis also handles the effects of hyperfine structure on $g(\nu)_{ij}$ and σ_{ij} [5]. Lewis develops the three level rate equations and proceeds to solve them for the CW case based upon the quasi-two level approximation. The equation developed for I_P is, again, transcendental. Lewis uses an analytic solution based upon the Product Log function. This is the main benefit of the Lewis model. Because it develops an analytic solution for I_p, Lewis is able to provide the equation for the pump intensity as a function of position for any system. It should be noted that the pump intensity does not account for lasing or the shifting of population densities due to pump in-

tensity. For simplicity it is assumed that lasing is not achievable in general. Lewis modeled lasing as a phenomena that would occur only well above threshold and affected the pump attenuation globally not with any frequency dependence of the input photons. Lewis used this method to show how lasing effects the pump intensity by drastically increasing the attenuation of the pump. The assumptions made to develop this model hinder it from working accurately in regimes near threshold and in cases when processes other than those assumed to occur come to dominate the operation of the DPAL system [5]. Currently, no model has handled the effects of pulsed laser operation, the effects of all possible three level optical and collisional transitions, and the effects of the intra-cavity pump and lasing intensity on the number densities of the populations within the system.

III. DPAL Theory and Model

3.1 Overview

This chapter outlines the theoretical equations and chemical kinetics required to model a DPAL system. The three level system of alkali atoms used by DPAL is explained in detail and the hyperfine structure of the ${}^2P_{\frac{3}{2}}$ and ${}^2P_{\frac{1}{2}}$ manifolds of Rb and Cs is shown. Chemical kinetics are discussed to develop the three level rate equations and their dependencies. A lineshape for the ${}^2P_{\frac{3}{2}}$ and ${}^2P_{\frac{1}{2}}$ transitions is developed using a Voigt profile. The lineshape is used to determine the stimulated emission cross sections and absorption cross sections. The relative intensities of each hyperfine transition are given to find the total stimulated emission cross section. The rate equations are then solved for the population number densities known as N_1, N_2, N_3. For a CW system the differential equations which govern attenuation and growth of lasing and pump intensities in the cavity are given. The gain coefficient for the DPAL is explored, and the cavity mode spacing is given. The combination of these effects and equations constitute a complete picture of a CW DPAL system.

3.2 Three Level System

The three level DPAL system encompasses many possible optical and collisional transitions. For this model, the transitions considered are given in Figure 1 and involve the number densities N_3, N_2, and N_1 of these levels respectively. These transitions are all of those between the ${}^2P_{\frac{3}{2}}$, ${}^2P_{\frac{1}{2}}$, and ${}^2S_{\frac{1}{2}}$ levels which have population number densities N_3, N_2, and N_1. For the remainder of this thesis, a subscript i or j denotes the fine structure energy level. i and j can take on values of 3, 2, or 1 each corresponding to ${}^2P_{\frac{3}{2}}$, ${}^2P_{\frac{1}{2}}$, and ${}^2S_{\frac{1}{2}}$ levels respectively. A_{31} and A_{21} are the spontaneous emission Einstein coefficients (EC) for the ${}^2P_{\frac{3}{2}} \rightarrow {}^2S_{\frac{1}{2}}$ transition and

$^2P_{\frac{1}{2}} \rightarrow {}^2S_{\frac{1}{2}}$ transition respectively. B_{13} and B_{12} are the ECs of absorption for $^2S_{\frac{1}{2}} \rightarrow {}^2P_{\frac{3}{2}}$ transition and $^2S_{\frac{1}{2}} \rightarrow {}^2P_{\frac{1}{2}}$ transition respectively. B_{13} corresponds to the pump transition. B_{31} and B_{21} are the ECs for the stimulated emission. B_{21} corresponds to the lasing transition. All k_{ij}-coefficients are the rates in cycles per second (Hz) of excitation or de-excitation between an alkali and some collision partner (methane, ethane, helium or an alkali) an intitial level indicated by the first subscript and a final level indicated by the second subscript k_{ij} [5]. The k_{ij}-coefficients for excitation k_{13} and k_{12} are approximately 4 orders of magnitude smaller than the corresponding quenching rates k_{31} and k_{21} [5]. The k_{32} and k_{23} rates are the most important for DPAL systems and represent the collisional relaxation between $^2P_{\frac{3}{2}}$ and $^2P_{\frac{1}{2}}$, which allows for lasing to occur. k_{32} and k_{23} are approximately 4 orders of magnitude larger than the quenching rates [5]. Transitions to other atomic states not listed in Figure 1 can occur, but they are much less likely than those listed for a pump source whose wavelength closely matches the wavelength of the $^2P_{\frac{3}{2}} \rightarrow {}^2S_{\frac{1}{2}}$ transition for a given alkali. Note that the transition from $^2P_{\frac{3}{2}} \rightarrow {}^2P_{\frac{1}{2}}$ is optically forbidden, and hence, no ECs are listed on Figure 1. Henceforth "population" and "number density" are used interchangeably

From Figure 1, rate equations for the rate of change in time of each of the number densities N_3, N_2, and N_1 can be constructed in the same manner as done by Lewis [5]. An in depth treatment is given in [8]. For the CW case, these rate equations are set equal to zero [8]. The integrals in Equations (1), (2),and (3) arise from the different possible wavelengths for the pump and laser transitions due to lineshape and hyperfine structure. The sums over species are present to allow for the possibility of different alkali collision partners, such as methane, ethane, and helium, being present simultaneously. Each species corresponds to a different collisional excitation and de-excitation rate and each must be handled separately. $g_p(\nu_p)$ is the lineshape of

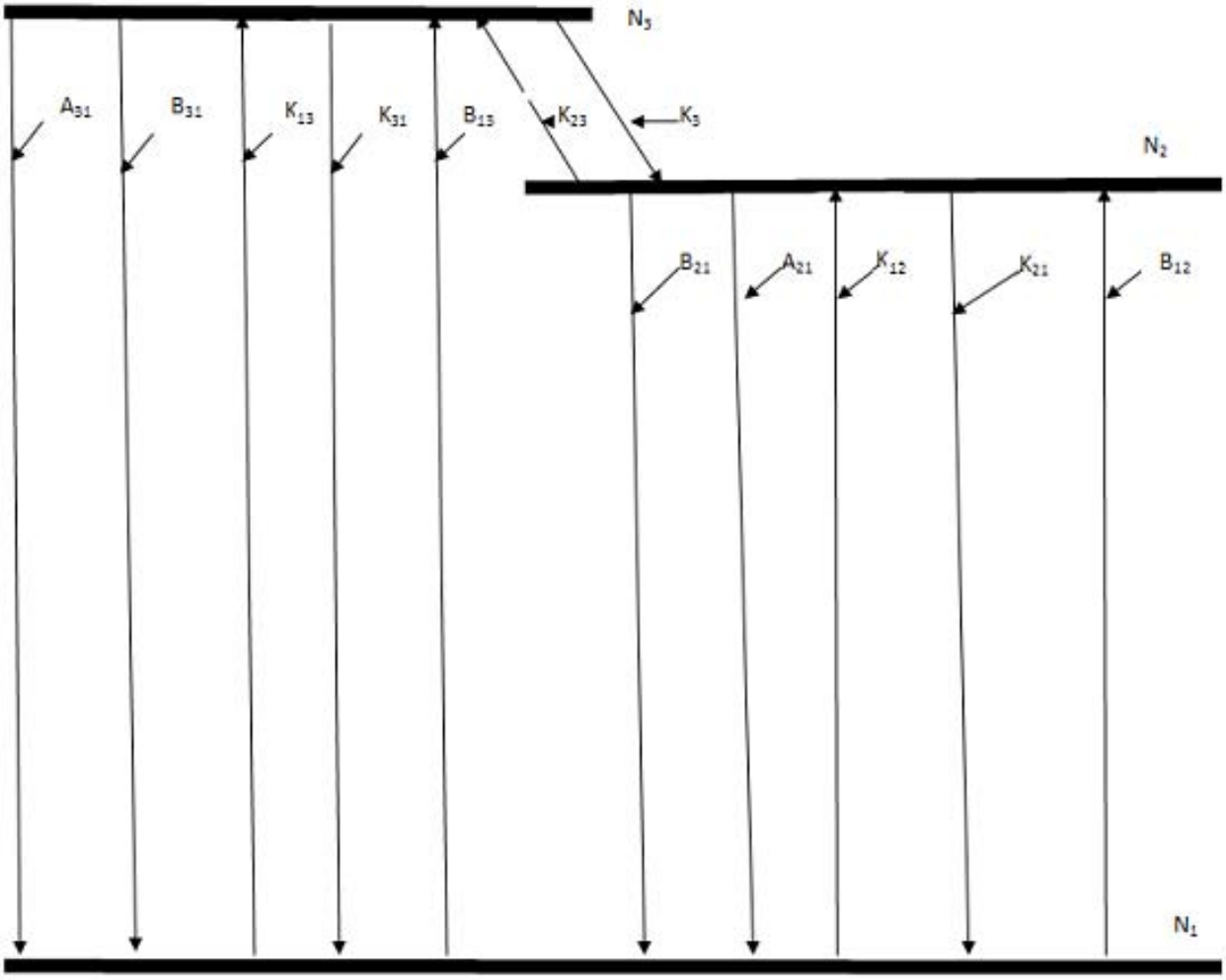

Figure 1. The three level chemical kinetics used for the development of the DPAL model. N_1 corresponds to the population in the $^2S_{\frac{1}{2}}$ state. N_2 corresponds to the population in the $^2P_{\frac{1}{2}}$ state. N_3 corresponds to the population in the $^2P_{\frac{3}{2}}$ state. The pump transition corresponds to B_{13}. The laser transition corresponds to B_{21}.

the input pump as a function of ν_p. The concentration of a given collision partner is $M_{species}$. Also, the excitation rate coeffcients k_{13} and k_{12} are neglected because of their extremely small size under normal temperatures for operation of a DPAL system (less than approximately 1000 K) and for most collision partners typically used (methane, ethane, and helium). However, if one were to use another gas as a collision partner these terms might need to be reinserted. It is suggested that the reader use the list of symbols provided at the outset of this document while reading these equations to avoid confusion. h is Planck's constant.

$$\begin{aligned}\frac{dN_1(z,t)}{dt} &= \sum_{species}[N_3(z,t)A_{31} + N_2(z,t)A_{21} + N_3(z,t)k_{31_{species}}M_{species} \\ &+N_2(z,t)k_{21_{species}}M_{species}] + \int_{-\infty}^{\infty}[-\frac{N_1(z,t)I_P(\nu,z,t)\sigma_{31}(\nu_p)}{h\nu_p} \\ &+\frac{N_3(z,t)I_P(\nu,z,t)\sigma_{31}(\nu_p)}{h\nu_p} + \frac{I_L(\nu,z,t)\sigma_{21}(\nu_l)}{h\nu_l}[N_2(z,t) - \frac{g_2}{g_1}N_1(z,t)]]d\nu \end{aligned} \tag{1}$$

$$\begin{aligned}\frac{dN_2(z,t)}{dt} &= \sum_{species}[N_3(z,t)k_{32_{species}}M_{species} - N_2(z,t)k_{23_{species}}M_{species} - \\ &A_{21}N_2(z,t) - N_2(z,t)k_{21_{species}}M_{species}] \\ &+ \int_{-\infty}^{\infty}[-\frac{I_L(\nu,z,t)\sigma_{21}(\nu_l)}{h\nu_l}[N_2(z,t) - \frac{g_2}{g_1}N_1(z,t)]]d\nu \end{aligned} \tag{2}$$

$$\begin{aligned}\frac{dN_3(z,t)}{dt} &= \sum_{species}[-N_3(z,t)k_{32_{species}}M_{species} + N_2(z,t)k_{23_{species}}M_{species} - \\ &A_{31}N_3(z,t) - N_3(z,t)k_{31_{species}}M_{species}] + \\ &\int_{-\infty}^{\infty}[\frac{N_1(z,t)I_P(\nu,z,t)\sigma_{31}(\nu_p)}{h\nu_p} - \frac{N_3(z,t)I_P(\nu,z,t)\sigma_{31}(\nu_p)}{h\nu_p}]d\nu \end{aligned} \tag{3}$$

Equations (1), (2),and (3) may then be set equal to zero in the CW case. The CW case also eliminates the dependence on time in $I_P(\nu, z, t)$ and $I_l(\nu, z, t)$. These equations constitute two independent equations, not three, as all of the rates between the three levels are present in two of the equations simultaneously. Hence, these equations do not form an independent set of three equations, but only two dependent equations. Therefore, to solve for the corresponding population number densities N_1, N_2, and N_3, which is the ultimate goal of this development, another equation must be added. This is Equation (4), where N_t represents the total number density of alkali in the system.

$$N_t = N_1 + N_2 + N_3 \tag{4}$$

3.3 Cross sections and Lineshapes for DPALs

With three independent equations, N_1, N_2, and N_3 may be solved unambiguously. This is performed via *Mathematica* in Appendix A. With this level of detial in the rate equations, this is a non-trivial task without a computational aide. Armed with N_1, N_2, and N_3 the individual terms within the rate equations must now be developed to actually compute the populations N_1, N_2, and N_3. The stimulated emission cross section σ_{ji} for a DPAL system is given by Equations (5) and (6) where σ_{ij} is the corresponding absorption cross section. If j and i correspond to N_3 and N_1, the pump frequency ν_p is used, and if j and i correspond to N_2 and N_1, the pump frequency ν_l is used. The lineshape $g_{ji}(\nu)$, the natural abundance of hyperfine states $f_{ji}(F'', F')$, and relative intensity of the hyperfine transitions $S(F'', F', iso)$ used all follow the same employment scheme for i and j as σ_{ij}. It is of note, that while the lasing frequency is a single value in CW single mode operation as per [8], the pump frequency ν_p has a lineshape associated with the output of the diode. This requires

that while $\sigma_{21}(\nu_l)$ has a single value, $\sigma_{31}(\nu_p)$ is a continuous function. This point is easily overlooked and is important to accurately model a broadband pumped DPAL system. The functional dependence on a particluar isotope is shown as (iso) and relates to the particular alkali isotope being used. In Equation (5), iso denotes the particular isotope species and its particular $g_{ji}(\nu)$, $S(F'', F', iso)$, and $f_{ji}(F'', iso)$. f_{iso} is the natural abundance of a particular isotope as a fraction out of one.

$$\sigma_{ij}(\nu) = \sum_{iso} \sum_{F''(iso)} \sum_{F'(iso)} \frac{g_j}{g_i} \frac{c^2}{\nu^2 8\pi} A_{ji} S(iso, F'', F') g_{ji}(\nu) f_{ji}(F'', iso) f_{iso} \tag{5}$$

$$\sigma_{ji}(\nu) = \frac{g_i}{g_j} \sigma_{ij}(\nu) \tag{6}$$

The lineshape g_{ji} is a convolution of the Doppler broadening (a Gaussian), the pressure broadening (a Lorentzian), and the lifetime broadening (a Lorentzian)[8]. The lifetime and pressure broadening are known as the homogenous broadening and are given by $\Delta\nu h_{ji}(iso)$ in Equation 7. The Doppler broadening is $\Delta\nu d_{ji}(iso)$ given by Equation (8) [8]. Using these quantities, the Voigt lineshape $g_{ji}(\nu)$ is given by Equation (9) from [8]. k_b is Boltzmann's constant.

$$\Delta\nu h_{ji}(iso) = \frac{1}{2\pi}(\frac{1}{\tau_{rad_{ji}}}) + \sum_{species} \gamma_{species} M_{species} (\frac{T_{species}}{T})^{\frac{1}{2}} \tag{7}$$

$$\Delta\nu d_{ji}(F'', F', iso) = \nu h y_{ji}(F', F'', iso)(\frac{8k_b T * Log(2)]}{m(iso)c^2}) \tag{8}$$

$$g_{ji}(\nu, F'', F', iso) = (\frac{m}{2\pi k_b T})^{\frac{1}{2}} \int_{-\infty}^{\infty} (\frac{\Delta\nu h_{ji}(iso)}{2\pi((\nu - \nu_0 - \nu_0 v_z/c)^2) + (\Delta\nu h_{ji}(iso)/2)^2} exp(-\frac{m v_z^2}{2k_b T}) dv_z) \tag{9}$$

$\Delta\nu d_{ji}(F'', F', iso)$ depends on the particular hyperfine line to which $\Delta\nu d_{ji}(F'', F', iso)$

corresponds as each hyperfine transition has its own associate FWHM. The FWHM depends upon F'', the original transition state in either N_1, N_2, or N_3, and F', the final state in N_1, N_2, or N_3 [5]. Note, $\nu hy_{ji}(F', F'', iso)$ is the hyperfine frequency, in Hz, for a transition from one state to another for a particular F', F'', and isotope. $\nu hy_{ji}(F', F'', iso)$ is not the splitting between hyperfine levels within a single fine level. That is $\nu_{hysplit_j}(F'', iso)$. Figures 2, 3, 4, 5, 6, and 7 show the transitions between each of the hyperfine states of the D1 and D2 transitions for Cs, ^{85}Rb, and ^{87}Rb. The selection rule for F'' to F' is $\Delta F = +1, -1$, or 0 with $F'' = 0$ to $F' = 0$ being forbidden. Figures 2, 3, 4, 5, 6, and 7 are taken from [5].

In practice, Equation (9) is difficult to use. An approximation using an error function can be made as is employed as per [7]. The intermediate quantities given by Equations (10), (11), and (12) are developed in this process. In Equation (12), the i in front of $u_{ji}(\nu, F'', F', iso)$ is the square root of negative one. For the remainder of this thesis, Equation (13) will be used for $g_{ji}(\nu, F'', F', iso)$, not Equation (9).

$$a_{ji}(\nu, F'', F', iso) = Log(2)^{\frac{1}{2}} \frac{\Delta\nu h_{ji}(iso)}{\Delta\nu d_{ji}(iso)} \tag{10}$$

$$u_{ji}(\nu, F'', F', iso) = 2Log(2)^{\frac{1}{2}} \frac{(\nu - \nu hy_{ji}(F'', F', iso))}{\Delta\nu d_{ji}(F'', F', iso)} \tag{11}$$

$$z_{ji}(\nu, F'', F', iso) = a_{ji}(\nu, F'', F', iso) + \imath * u_{ji}(\nu, F'', F', iso) \tag{12}$$

$$g_{ji}(\nu, F'', F', iso) = \frac{4Log(2)}{\pi}^{1/2} \frac{1}{\Delta\nu d_{ji}(F'', F', iso)} Re(e^{z_{ji}(\nu, F'', F', iso)^2} Erfc(z_{ji}(\nu, F'', F', iso))) \tag{13}$$

To calculate the lineshape, the relative strength $S(species, F'', F', iso)$ of a transition between hyperfine levels must be known [5]. The relative intensities of each of

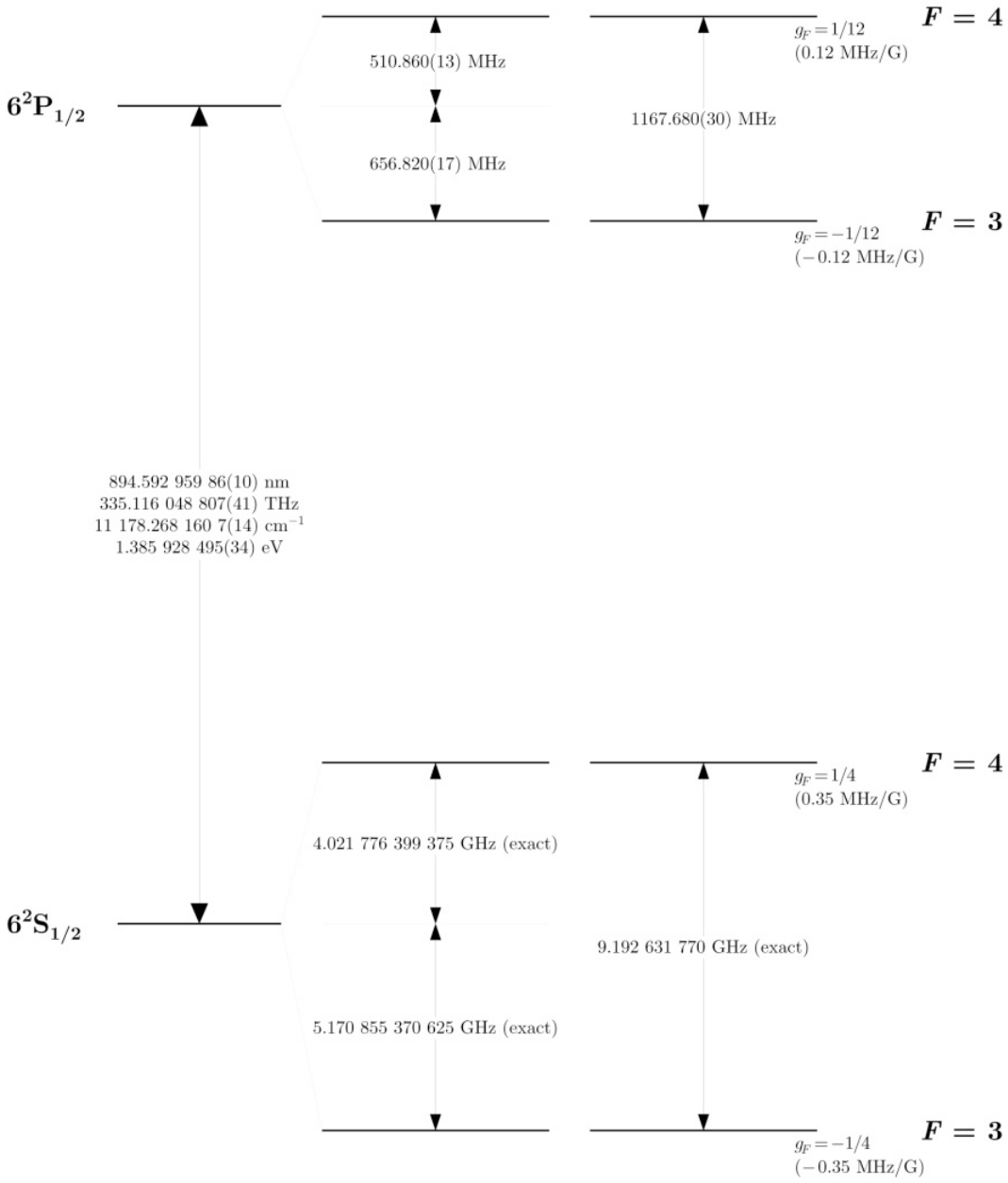

Figure 2. The D1 manifold for ^{133}Cs without possible transitions listed. The frequency spacing of each hyperfine state is listed [5].

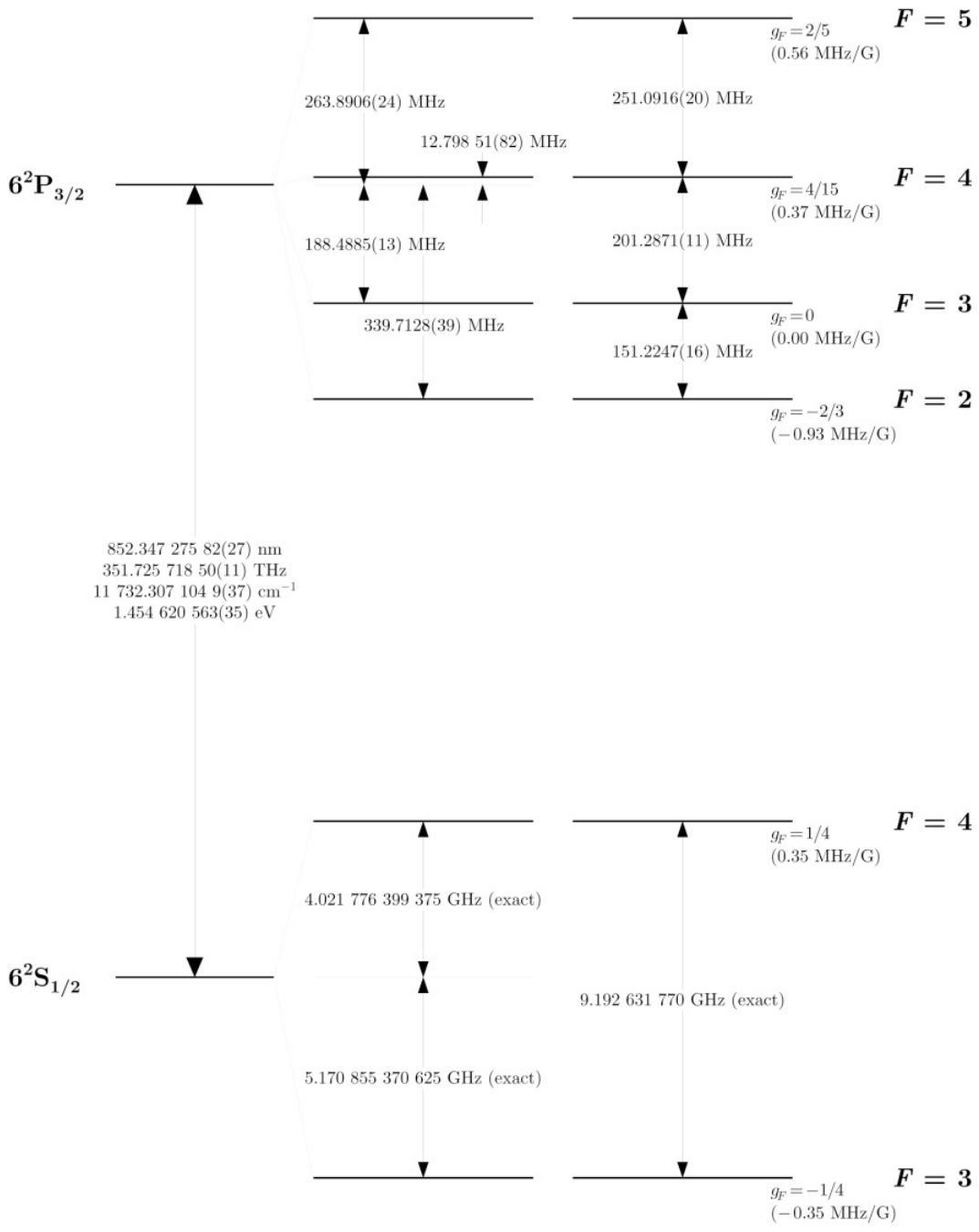

Figure 3. The D2 manifold for ^{133}Cs without possible transitions listed. The frequency spacing of each hyperfine state is listed [5].

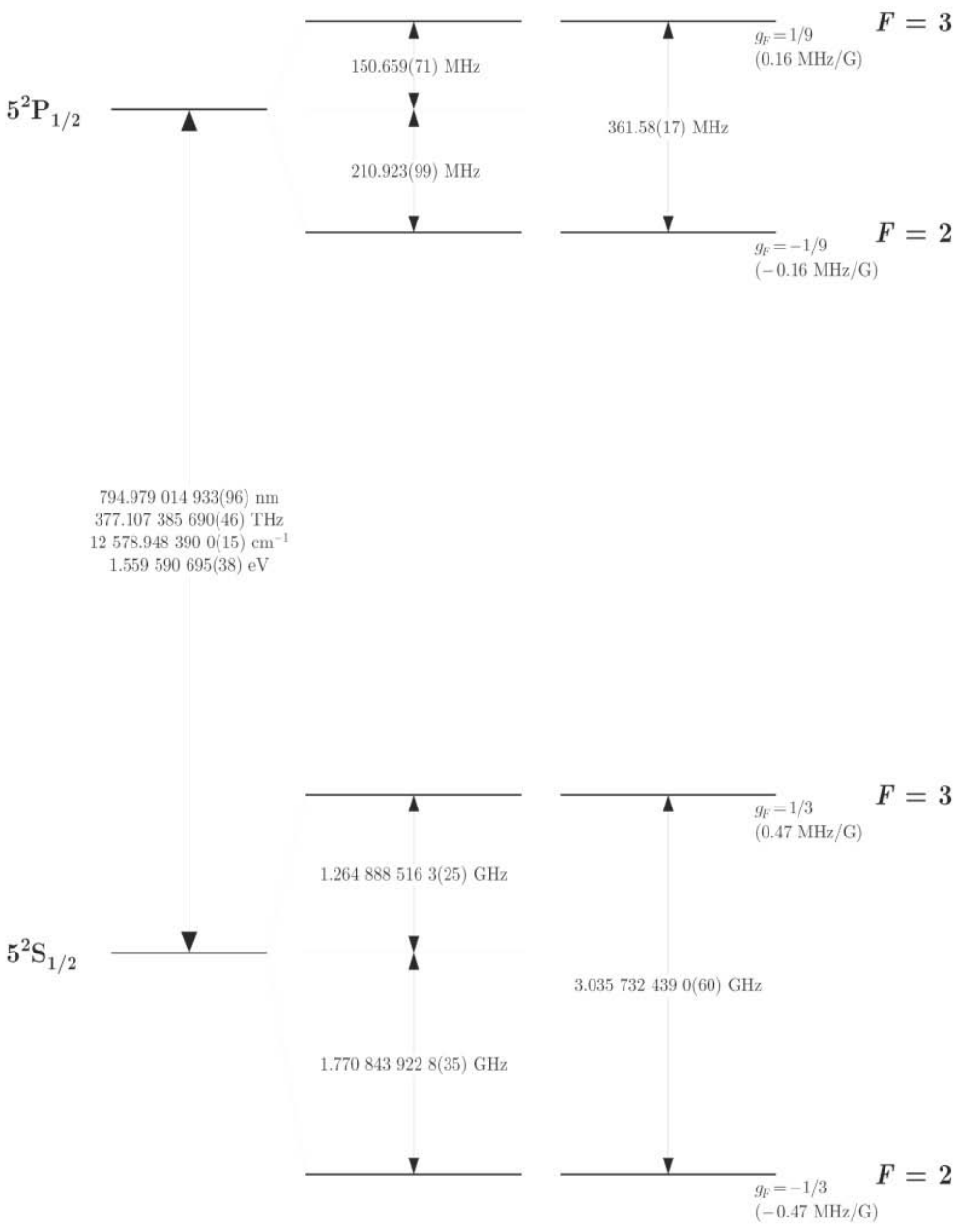

Figure 4. The D1 manifold for ^{85}Rb without possible transitions listed. The frequency spacing of each hyperfine state is listed [5].

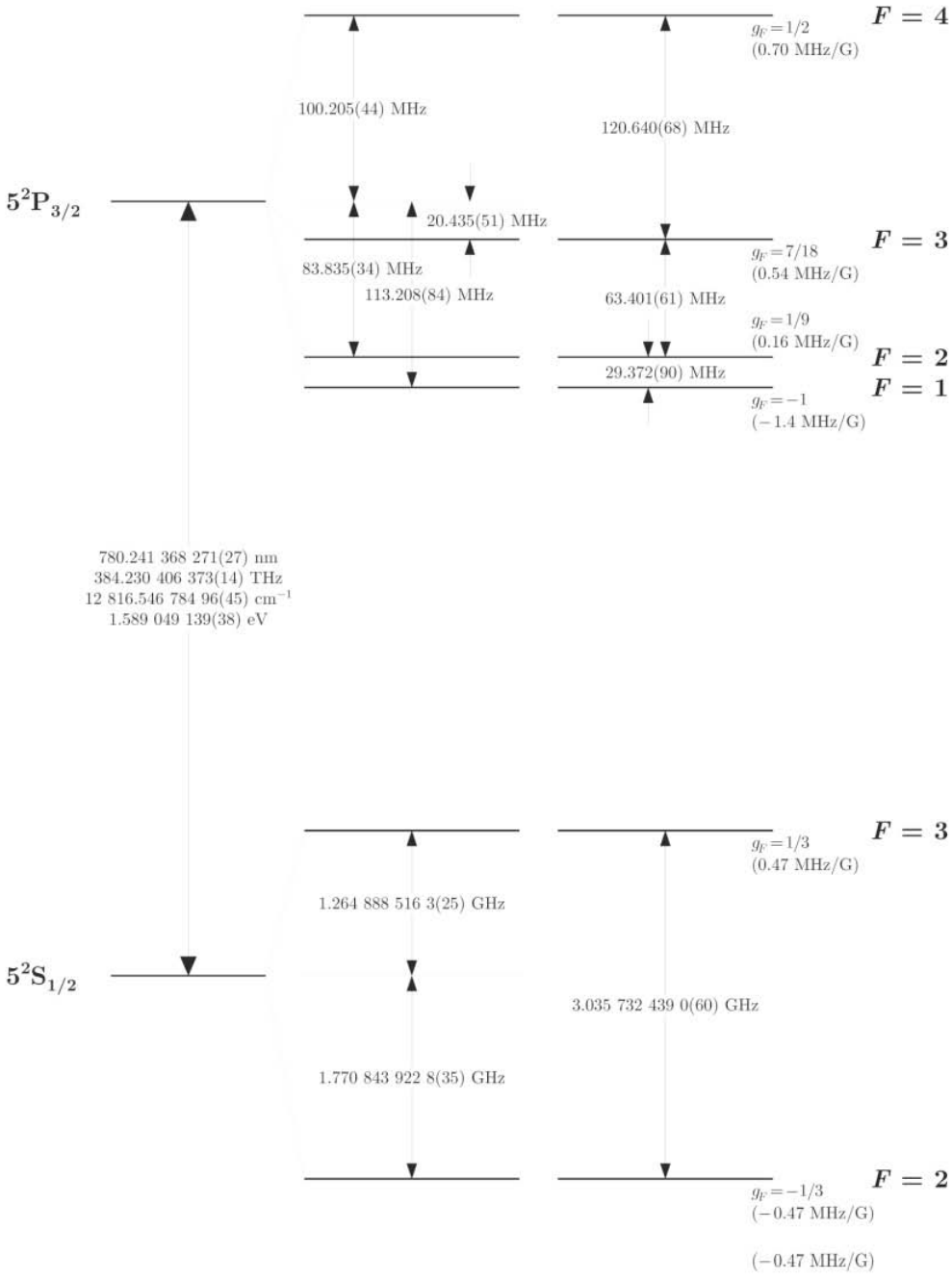

Figure 5. The D2 manifold for ^{85}Rb without possible transitions listed. The frequency spacing of each hyperfine state is listed [5].

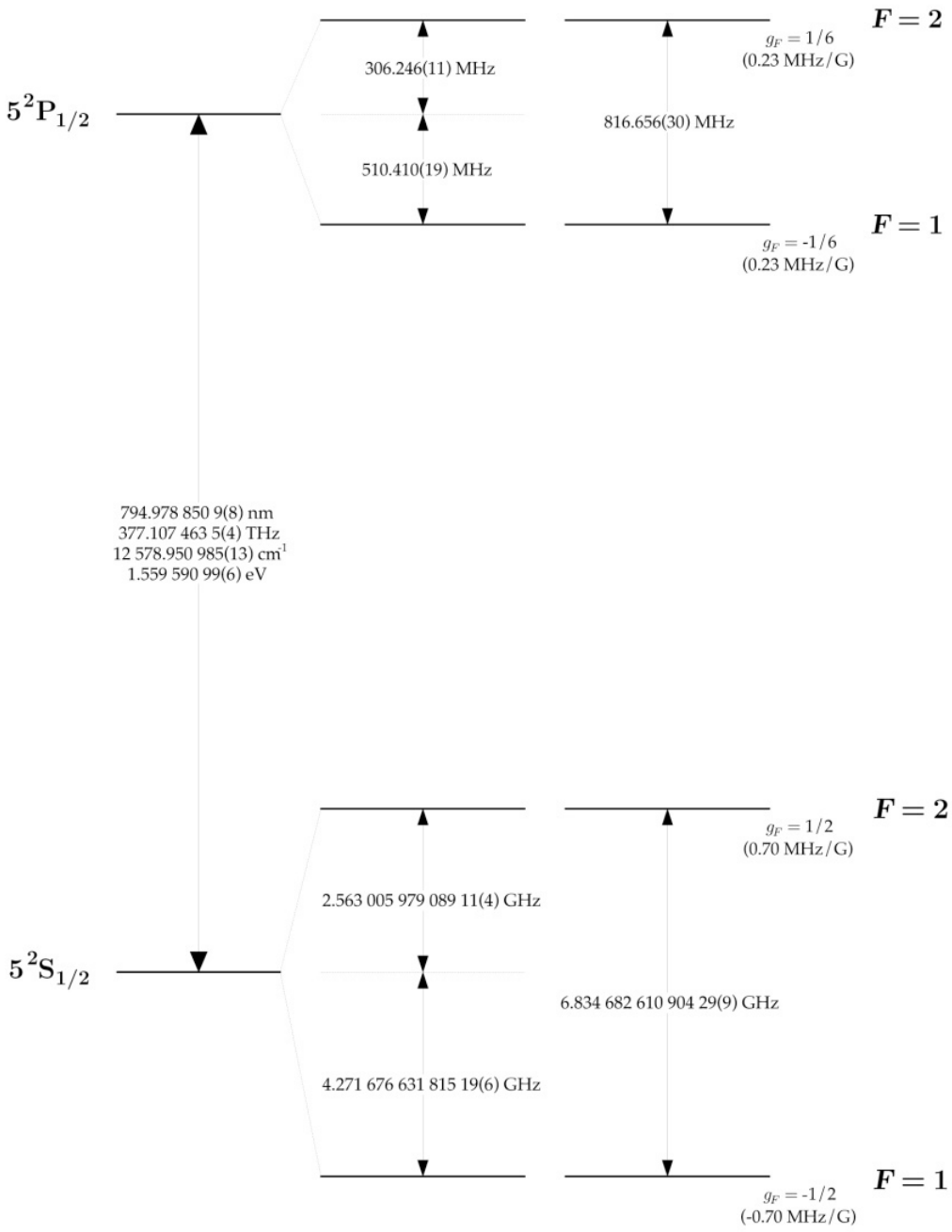

Figure 6. The D1 manifold for ^{87}Rb without possible transitions listed. The frequency spacing of each hyperfine state is listed [5].

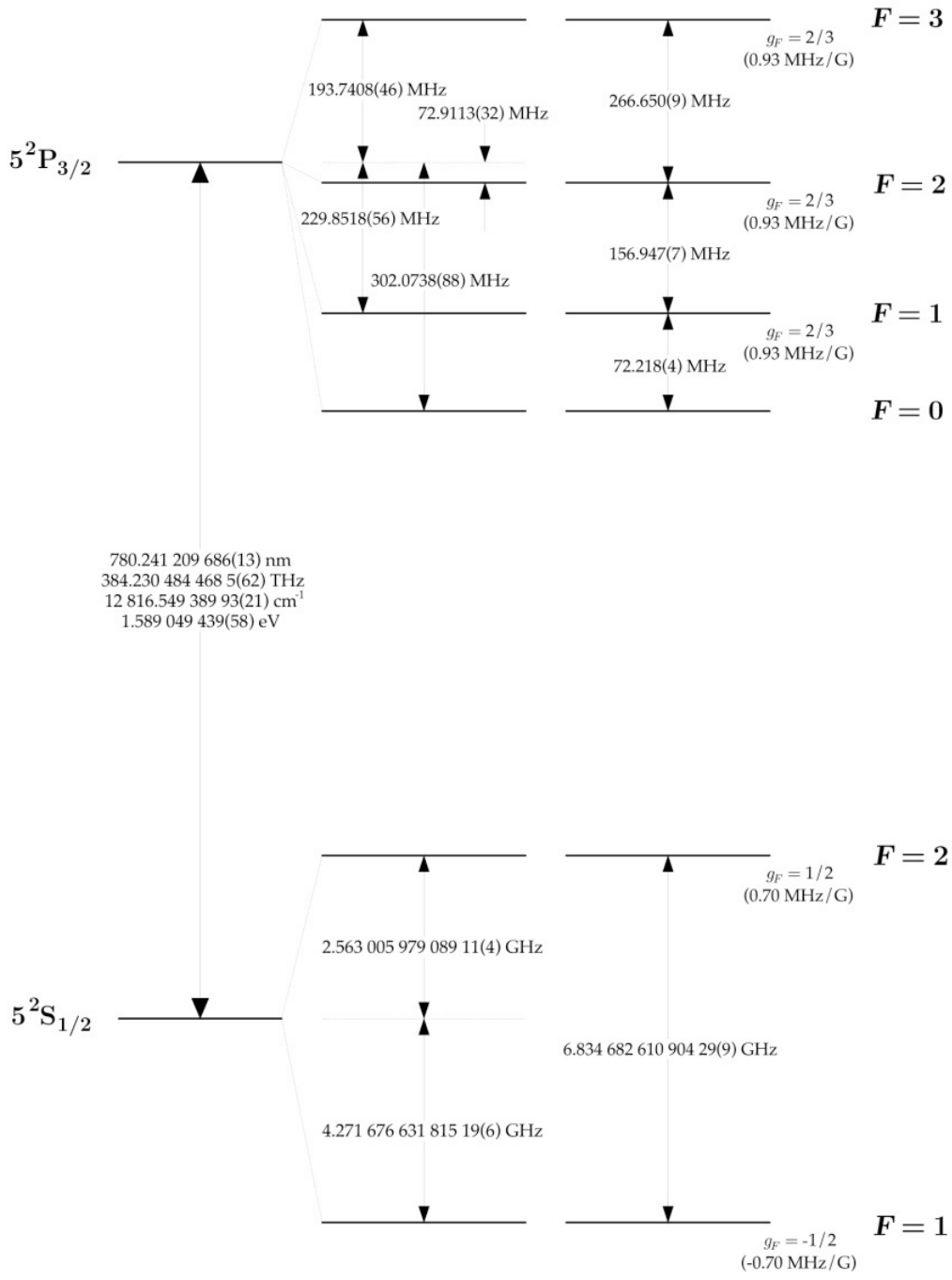

Figure 7. The D2 manifold for ^{87}Rb without possible transitions listed. The frequency spacing of each hyperfine state is listed [5].

the transitions for the D1 and D2 transitions may be found in Tables 1, 2, and 3. The data in Tables 1, 2, and 3 comes from [5].

The relative natural abundance of each hyperfine state as a fraction of one is $f_{ji}(F'', iso)$. $f_{ji}(F'', iso)$ is given by Equation (14). The relative natural abundance is the fraction of atoms in each of the initial hyperfine states F''. It is of note that $\nu_{hysplit_j}(F'', iso)$ is not equal to $\nu_{hy_{ji}}(F'', F', iso)$. $\nu_{hysplit_j}(F'', iso)$ is the frequency in Hz of the splitting between a particular hyperfine level and the center frequency of the fine structure level which the hyperfine level is in. While, $\nu_{hy_{ji}}(F'', F', iso)$ is the frequency in Hz of a $F'' \rightarrow F'$ hyperfine transition between two fine structure levels. Simply put, $\nu_{hysplit_j}(F'', iso)$ is an energy splitting in Hz given on Figures 2, 3, 4, 5, 6, and 7 and $\nu_{hy_{ji}}(F'', F', iso)$ is the absolute difference between two hyperfine levels in different fine structure levels.

$$f_{ji}(F'', iso) = \frac{(2F''+1)exp(\frac{h(\nu_{ji}-\nu_{hysplit_j}(F'',iso))}{k_bT})}{\sum_{iso}\sum_{F''}(2F''+1)exp(\frac{h\nu_{hysplit_j}(F'',iso)}{k_bT})} \tag{14}$$

3.4 Alkali and Collision Partner Properties

Several other important material quantities are needed to calculate Equation (6). Table 4 provides these quantities for Cs and Rb.

From the numbers in Table 4 and using equations from [8], several more needed quantities are developed. These include B_{ji} and k_{ji}.

$$B_{ji}(\nu, iso) = \frac{c^3 A_{ji}(iso)}{n^3 8\pi h\nu^3} \tag{15}$$

$$B_{ij}(\nu, iso) = \frac{g_j}{g_i} B_{ji}(\nu, iso) \tag{16}$$

Table 1. $S(species, F'', F', iso)$ **for** ^{133}**Cs for Hyperfine Structure**

D1 Manifold		D2 Manifold	
$F'' \rightarrow F'$ or $^2S_{\frac{1}{2}} \rightarrow {}^2P_{\frac{1}{2}}$	$S(species, F'', F', iso)$	$F'' \rightarrow F'$ or $^2P_{\frac{1}{2}} \rightarrow {}^2P_{\frac{3}{2}}$	$S(species, F'', F', iso)$
$3 \rightarrow 3$	$1/4$	$3 \rightarrow 2$	$5/14$
$3 \rightarrow 4$	$3/4$	$3 \rightarrow 3$	$3/8$
$4 \rightarrow 3$	$7/12$	$3 \rightarrow 4$	$15/56$
$4 \rightarrow 4$	$5/12$	$4 \rightarrow 3$	$7/72$
-	-	$4 \rightarrow 4$	$7/24$
-	-	$4 \rightarrow 5$	$7/18$

Table 2. $S(species, F'', F', iso)$ **for** ^{85}**Rb for Hyperfine Structure**

D1 Manifold		D2 Manifold	
$F'' \rightarrow F'$ or $^2S_{\frac{1}{2}} \rightarrow {}^2P_{\frac{1}{2}}$	$S(species, F'', F', iso)$	$F'' \rightarrow F'$ or $^2P_{\frac{1}{2}} \rightarrow {}^2P_{\frac{3}{2}}$	$S(species, F'', F', iso)$
$2 \rightarrow 2$	$2/9$	$2 \rightarrow 1$	$3/10$
$2 \rightarrow 3$	$7/9$	$2 \rightarrow 2$	$7/18$
$3 \rightarrow 2$	$5/9$	$2 \rightarrow 3$	$14/45$
$3 \rightarrow 3$	$4/9$	$3 \rightarrow 2$	$5/63$
-	-	$3 \rightarrow 3$	$5/18$
-	-	$3 \rightarrow 4$	$9/14$

Table 3. $S(species, F'', F', iso)$ **for** ^{87}**Rb for Hyperfine Structure**

D1 Manifold		D2 Manifold	
$F'' \rightarrow F'$ or $^2S_{\frac{1}{2}} \rightarrow {}^2P_{\frac{1}{2}}$	$S(species, F'', F', iso)$	$F'' \rightarrow F'$ or $^2P_{\frac{1}{2}} \rightarrow {}^2P_{\frac{3}{2}}$	$S(species, F'', F', iso)$
$1 \rightarrow 1$	$1/6$	$1 \rightarrow 0$	$1/6$
$1 \rightarrow 2$	$5/6$	$1 \rightarrow 1$	$5/12$
$2 \rightarrow 1$	$1/2$	$1 \rightarrow 2$	$5/12$
$2 \rightarrow 2$	$1/2$	$2 \rightarrow 1$	$1/20$
-	-	$2 \rightarrow 2$	$1/4$
-	-	$2 \rightarrow 3$	$7/10$

Table 4. ^{133}Cs, ^{85}Rb, and ^{87}Rb Material Properties

	^{133}Cs	^{85}Rb	^{87}Rb
f_{iso}	1	0.2783[3]	0.7217[3]
I	7/2[5]	5/2[3]	3/2[3]
$A_{21}(Hz)$	n/a	$\frac{1}{27.679\times10^{-9}}$ [5]	$\frac{1}{27.7\times10^{-9}}$ [5]
$A_{31}(Hz)$	n/a	$\frac{1}{26.2348\times10^{-9}}$ [5]	$\frac{1}{26.24\times10^{-9}}$ [5]
g_3	4 [5]	4 [5]	4 [5]
g_2	2 [5]	2 [5]	2 [5]
g_1	2 [5]	2 [5]	2 [5]
γ_{He} for $D1(MHz/Torr)$	26.21[5]	18.9 $\pm$0.2 [9]	18.9 $\pm$0.2 [9]
γ_{He} for $D2(MHz/Torr)$	23.50[5]	20.0 $\pm$0.4 [9]	20.0 $\pm$0.4 [9]
δ_{He} for $D1(MHz/Torr)$	4.46[5]	4.71 $\pm$0.04 [9]	4.71 $\pm$0.04 [9]
δ_{He} for $D2(MHz/Torr)$	0.75[5]	0.37 $\pm$0.06 [9]	0.37 $\pm$0.06 [9]
γ_{CH_4} for $D1(MHz/Torr)$	29.1[5]	29.1 $\pm$0.8 [9]	29.1 $\pm$0.8 [9]
γ_{CH_4} for $D2(MHz/Torr)$	26.2 [5]	26.2 $\pm$0.6 [9]	26.2 $\pm$0.6 [9]
δ_{CH_4} for $D1(MHz/Torr)$	-7.92[5]	-7.9 $\pm$0.1 [9]	-7.9 $\pm$0.1 [9]
δ_{CH_4} for $D2(MHz/Torr)$	-7.0 [5]	-7.0 $\pm$0.1 [9]	-7.0 $\pm$0.2 [9]
$k_{32}(cm^3s^{-1})$	?	3.16×10^{-10} [2]	3.16×10^{-10} [2]
k_{31}	0 [2]	0 [2]	0 [2]
k_{21}	0 [2]	0 [2]	0 [2]

$$k_{ij}(iso) = k_{ji}(iso)\frac{g_i}{g_j}exp(\frac{h\nu_{ji}}{k_bT}) \tag{17}$$

3.5 Lasing and Pump Intensities

To find the output lasing intensity one must first determine the intra-cavity lasing intensity and the intra-cavity pump intensity as functions of ν_p and time. A nearly accurate treatment of this is done by [8] and is known as Rigrod analysis. Rigrod analysis involves the propagation in the cavity of a pump wave, I_P, a forward traveling lasing wave, I_+, and a backward traveling lasing wave, I_- [8]. The saturation intensity I_{sat} is also required to perform Rigrod analysis and is given by Equation (18). Equations (18), (19), (20), and (21) are the initial differential equations for the attenuation or growth of intra-cavity pump and lasing waves. Notice that Equations

(19), (20), and (21) are transcendental. Also, remember that N_1, N_2, and N_3 depend on I_P, I_+, and I_-. This dependence is extremely lengthy and is shown in Appendix A. These two facts greatly increase the solution difficulty of these differential equations. Equations (19), (20), and (21) require numerical differential equation solution techniques to solve. Equations (20) and (21) appear without the terms which go as the inverse of I_+ plus I_- divided by I_{sat} because the population densities (N_1, N_2, and N_3) maintain their dependence on I_P, I_+, and I_- [8].

$$I_{sat}(\nu_p) = \frac{h\nu_p}{\sigma_{31}(\nu_p)} \sum_{iso} (\frac{1}{\tau_{rad}(iso)} f_{iso}) \tag{18}$$

$$\frac{dI_P(z,\nu_l,\nu_p)}{dz} = \sigma_{31}(\nu_p)[N_3(z,\nu_l,\nu_p) - \frac{g_3}{g_1} N_1(z,\nu_l,\nu_p)] I_P(z,\nu_l,\nu_p) \tag{19}$$

$$\frac{dI_+(z,\nu_l,\nu_p)}{dz} = \sigma_{21}(\nu_l)[N_2(z,\nu_l,\nu_p) - \frac{g_2}{g_1} N_1(z,\nu_l,\nu_p)] I_+(z,\nu_l,\nu_p) \tag{20}$$

$$\frac{dI_-(z,\nu_l,\nu_p)}{dz} = -\sigma_{21}(\nu_l)[N_2(z,\nu_l,\nu_p) - \frac{g_2}{g_1} N_1(z,\nu_l,\nu_p)] I_+(z,\nu_l,\nu_p) \tag{21}$$

The crux of the simulation lies in solving Equations (19), (20), and (21). The solution to these differential equations requires three boundary conditions. Initial conditions are not used as the solution is time-independent for the CW case. Equations (22), (23), and (24) provide these boundary conditions as given by [8] for Rigrod analysis, where ν_d is the line center of the diode's spectral profile in Hz. z_0 is the position of the beginning of the gain cell and z_f is the position of the end of the gain cell. Note, that z denotes the functional dependence of an equation upon longitundinal position in m in the alkali gain cell.

$$I_P(z_0,\nu_l,\nu_p) = I_P 0 \frac{g_{31}(\nu_p)}{g_{31}(\nu_d)} \tag{22}$$

$$I_+(z_0, \nu_l, \nu_p) = R_1 T_g^2 I_-(z_0, \nu_l, \nu_p) \tag{23}$$

$$I_-(z_f, \nu_l, \nu_p) = R_2 T_g^2 I_+(z_f, \nu_l, \nu_p) \tag{24}$$

Other important and oft used benchmarks for the system are the gain coefficient γ_ν given by Equation (25), the loss coefficient α given by Equation (26), and the cavity mode spacing $\Delta\nu_{fsr}$ given by Equation (27). Under CW operation, the gain coefficient will equal the loss coefficient once threshold is reached [8]. This forces the gain to operate at the loss. The cavity mode spacing and the gain coefficient are important as they determine what the operating frequency of the laser (ν_l) will be as the mode with the greatest gain coefficient will be selected preferentially over all other modes [8]. By the time threshold is reached, all of the power in the laser will be focused in this single mode. This is the idea of single mode operation. This is only true for lasers operating in a single TEM mode and not multiple modes [8]. n is the index of refraction. c is the speed of light.

$$\gamma_\nu(z, \nu_l, \nu_p) = \frac{dI_+(z_0, \nu_l, \nu_p)}{dz} \frac{1}{I_+(z_0, \nu_l, \nu_p)} = \sigma_{21}(v_l)(N_2(z, \nu_l, \nu_p) - \frac{g_2}{g_1} N1(z, \nu_l, \nu_p)) \tag{25}$$

$$\alpha = \frac{1}{2l_g} ln(\frac{1}{R_1 R_2}) \tag{26}$$

$$\nu_{q+1} - \nu_q = \frac{c}{2nd_{mirror}} \tag{27}$$

These equations constitute a completely-modeled DPAL system.

IV. Simulation Description

4.1 Overview

The simulation of the model developed in Chapter III is performed in *Mathematica 7.0* for Windows XP on a 2.0 GHz AMD processor. The simulation reads in a list of input parameters, then uses all of the equations developed in Chapter III to simulate a DPAL system. Then using the differential equation solving, data analysis, and visualizations packages in *Mathematica* the system is characterized as detailed in Chapter III. The outputs required of the system are $I_p(z, \nu_l, \nu_p)$, $I_+(z, \nu_l, \nu_p)$, $I_-(z, \nu_l, \nu_p)$, $\gamma_\nu(z, \nu_l, \nu_p)$, α, $N_1(z, \nu_l, \nu_p)$, $N_2(z, \nu_l, \nu_p)$, $N_3(z, \nu_l, \nu_p)$, and the output laser intensity, I_{out}, which is the output at the single laser frequency, ν_l

4.2 Assumptions

Without simplifying assumptions simulating the DPAL model discussed in Chapter III would not be practical as a single threaded process on a desktop computer. Assumptions were made to simplify the problem, but these assumptions were chosen such that a high degree of fidelity is maintained in the simulation's outputs. The DPAL system is assumed to be CW in its pump and response. Hence, all time dependence is eliminated. For any system which runs for longer than approximately one ms this is an adequate assumption because the population densities will reach their equilibrium values within that time. Only transitions within the three level system shown in Figure 1 are assumed to occur. All other transitions within the alkali atom are ignored. This assumption is somewhat valid as the absorption and emission cross section for the ${}^2S_{\frac{1}{2}} \rightarrow {}^2P_{\frac{3}{2}}$ and ${}^2P_{\frac{1}{2}} \rightarrow {}^2S_{\frac{1}{2}}$ are much larger (approximately 10^4 times larger) than any of the other transitions.

It is assumed that no forbidden hyperfine transitions occur within or between the

sublevels. The effects of the hyperfine structure beyond its effects on the lineshape $g_{ji}(\nu)$ are neglected. The hyperfine structure in a physical system does play a part in the rate between each sublevel. Hence, a fully complete model would need to create rate equations, such as Equations (1),(2), and (3), for each possible (including the forbidden transitions) hyperfine transition. The populations of each hyperfine level would also have to be independent of one another. Transitions between hyperfine levels due to collisions, absorption, and emission would also have to be tracked. Further, the lasing intensity would not be single quantity but a set of intensities each associated with a transition on the D1 manifold. Each intensity would require an individual plus wave and minus wave differential equation like Equations (20) and (21). Thus, the system would contain not three coupled non-linear ODEs, but instead 13. Also, the collisional excitation and de-excitation rates between hyperfine levels are unknown. Adding this complexity to the model is both extremely complicated and computationally difficult without the use of multi-threading. The laser modeled is assumed to operate only in the TEM(0,0) mode and to not operate in any other modes. The mode volume is assumed to be completely filled. The energy lost because of unfilled mode volume is not considered. This assumption is only somewhat valid, but it is difficult to simulate the effects of partially filling the mode volume of a DPAL because these effects are not yet fully characterized in the literature.

4.3 Simulation Input Parameters

The inputs to the simulation are listed in Table 5. Each parameter is given with its normal range of values. The input parameters are not physical constants, but are rather variables which are dynamic between different DPAL systems. Collisional relaxation rate coefficients such as k_{32} are not considered input parameters. These are considered physical constants of the system and are not input by the user. The

simulation has the ability to include more collisional relaxation rates than those for methane and helium, but does not currently. Appendix B shows a list of the physical parameters used by the code. It is of note that the three level numerical model takes all inputs in meters, kilograms, and seconds (mks) and the derived units of the mks system. Units with metric prefixes other than kilograms should not be used. Table 5 presents the inputs with prefixes for simplicity.

Table 5. Simulation Input Parameters

Input Parameter	Units required	Normal Range	Symbol
Temperature of Cell	K	250-2000	T
Temperature of Methane	K	250-2000	T_{meth}
Temperature of Helium	K	250-2000	T_{He}
Temperature of Alkali	K	250-2000	T_{alk}
Partial Pressure of Methane	kPa	20-2000	M_{meth}
Partial Pressure of Helium	kPa	20-2000	M_{He}
Partial Pressure of Alkali	kPa	2-200	M_{alk}
Total Alkali Number Density	m^{-3}	10^{18}-10^{24}	N_t
Length of gain medium	m	0.005-0.5	l_g
Transmission of windows around gain	Unitless	0.95-1.0	T_g
High Reflector Reflectivity	Unitless	0.95-1.0	R_1
Output Coupler Reflectivity	Unitless	0.2-1.0	R_2
Initial Pump Intensity at linecenter	Wcm^{-2}	$10^2 - 10^6$	I_p0
Diode Pump Line Center frequency	THz	$384.0 - 384.4$	ν_d
Diode Pump FWHM frequency	GHz	10^{-1} - 10^2	$\nu_{p_{fwhm}}$
Space Between Cavity Mirrors	m	0.01-1.0	d_{mirror}

4.4 Simulation Outline

The simulation begins by reading the input parameters in Table 5. Then the program develops each equation listed in Chapter III from Equation (1) to (27) except Equation (9), to which an approximation was used as detailed in Chapter III. These equations are supplemented by the physical parameters of the system given in Tables 1 - 4 and Figures 2 - 7. During this development the assumptions listed above are made by the simulation or were made during the simulation's design. The code then

constitutes a fully-developed model of a DPAL system. If the differntial equations (19), (20), and (21) can be solved numerically for this system, then all of the parameters needed to characterize the system can be developed from that solution. In practice, the solution of Equations (19), (20), and (21) is difficult and requires the use of *Mathematica*'s innate numerical differential equation solver. The differential equation solver is utilized with a shooting method and the boundary conditions of Equations (22), (23), and (24). To solve Equations (19), (20), and (21) requires that a shooting method be performed for different initial values for I_+ and I_- at z_0. Each shot is then solved by the numerical differential equation solver for a solution to the differential equations in z or position. An algorithm then assigns the best starting I_+ and I_- values based upon the occurrence of gain above loss and on the degree of adherence to Equation (24). This solution architecture is then utilized for a select set of pump frequencies spanning three times the pump's full width at half max (FWHM). The solutions which best match the boundary condition for each discrete pump frequency are then interpolated between by *Mathematica*'s data analysis software and are plotted. This architecture is detailed in Figure 8. The complete *Mathematica* notebook can be found in Appendix B.

4.5 Simulation Outputs

The outputs of the simulation are the way in which the model is both compared to other models such as [2],[3], and [5], and then, the outputs are compared to experimental results. To achieve these comparisons several different outputs are provided. A profile of the pump intensity $I_P(z, \nu_p)$ is shown throughout the entire cell. $I_+(z, \nu_p, \nu_l)$ and $I_-(z, \nu_p, \nu_l)$ are plotted. The population densities, $N_1(z, \nu_p)$, $N_2(z, \nu_p)$, and $N_3(z, \nu_p)$ are plotted. The output lasing intensity (I_{out}) is determined. The simulation selects the lasing mode with the greatest gain and outputs its fre-

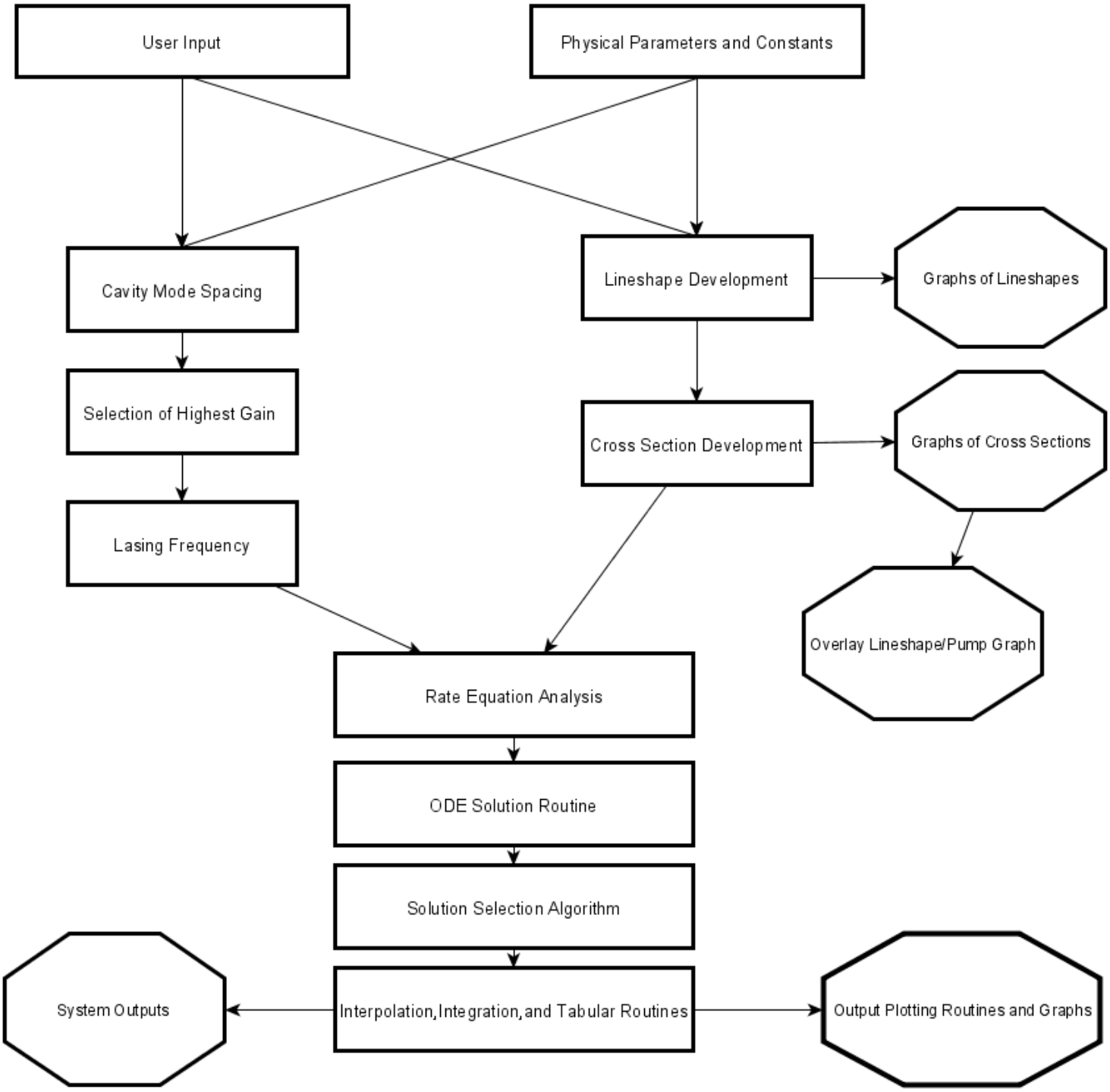

Figure 8. The architecture used to develop the simulation of the DPAL model. Octagons are output plots or printed output system characteristics. Rectangles are algorithms.

quency, as this is the frequency of the laser's output. $\gamma_\nu(z)$ is plotted for the system. The average value of γ_ν over z is compared to α and should be found to be roughly equivalent. A determination of the degree to which the chosen solution matches the boundary conditions is provided.

V. Results and Simulation Comparisons

5.1 Chapter Overview

To validate the model this thesis develops, which is henceforth known as the three level numerical model; it must be tested against similar previously vetted systems like the Lewis model and the Hager model. If the outputs of the model developed are comparable to those developed by Lewis and Hager in the regime where those models are known to operate well, then the model's output outside of those regimes is more believable. The model will also be tested against experimental results. Further, the model will be shown to simulate a DPAL with an extremely high initial pump intensity and other features typically found only during pulsed operation. The model will also perform Rigord analysis for a general DPAL case. Together these outputs will show the effectiveness and utility of the model and its simulation.

5.2 Comparison to Lewis Model

5.2.1 Inputs.

The inputs of Table 6 are derived from the DPAL quasi two level regime of Lewis's thesis [5]. The inputs are listed in the units used by Lewis in [5] rather than units used by the three level numerical model. If an input was not listed by Lewis, a suitable value was devised. This applies specifically to the temperature of the alkali for plots provided in [5]. The alkali used for this comparison was Rb, which is used throughout the comparison between the three level numerical model and the Lewis model. These inputs will be used throughout the comparison to Lewis's model and the three level numerical model for the remainder of this section unless otherwise noted. Lewis lists one of his buffer gases as ethane in [5]. However, his theortical development and plots list methane as the buffer gas used. Further [5] lists methane, not ethane, as his

buffer gas on all other tables. Therefore, methane, not ethane will be used for this development [5].

Table 6. Simulation Input Parameters from Lewis Model

Input Parameter	Units required	Value	Symbol
Temperature of Cell	K	455	T
Temperature of Methane	K	455	T_{meth}
Temperature of Helium	K	455	T_{He}
Temperature of Alkali	K	455	T_{alk}
Partial Pressure of Methane	$Torr$	600	M_{meth}
Partial Pressure of Helium	$Torr$	200	M_{He}
Partial Pressure of Alkali	$Torr$	0	M_{alk}
Total Alkali Number Density	cm^{-3}	6.1×10^{12}	N_t
Length of gain medium	cm	8.00	l_g
Transmission of windows around gain	Unitless	1.0	T_g
High Reflector Reflectivity	Unitless	1.0	R_1
Output Coupler Reflectivity	Unitless	1.0	R_2
Initial Pump Intensity at linecenter	Wcm^{-2}	200	I_p0
Diode Pump Line Center frequency	THz	384.23	ν_d
Diode Pump FWHM frequency	GHz	3	$\nu_{p_{fwhm}}$
Space Between Cavity Mirrors	cm	50	d_{mirror}

5.2.2 Cross Section Broadening Comparison.

Lewis details that the main mechanism for broadening in the DPAL system is the pressure of the buffer gas [5]. Lewis then investigates the effects of pressure broadening at several different pressures on the emission cross section of the 3 to 1 transition, σ_{31} shown in Figures 9 and 10. The analogous results for the three level numerical model are provided by accepting that the Lewis model neglects the terms f_{iso} and f_{ji} by assuming only one isotope is present and the hyperfine states all are equally populated in Figures 11 and 12. The Lewis model uses units of cm^2 as opposed to m^2 which will induce a shift of 10^{-4} when comparing cross sections between the Lewis model to the three level numerical model. Notice that Figures 9 and 11 differ slightly most likely due to a difference in temperature as Lewis did not list the temperature

he used to create Figure 9. Figures 10 and 12 are identical. This implies that the lineshapes and cross sections developed by the three level numerical model agree well with those of the Lewis model especially at high pressures. Note Figures 9, 10, 11, and 12 are all offset in frequency space by ν_{31}.

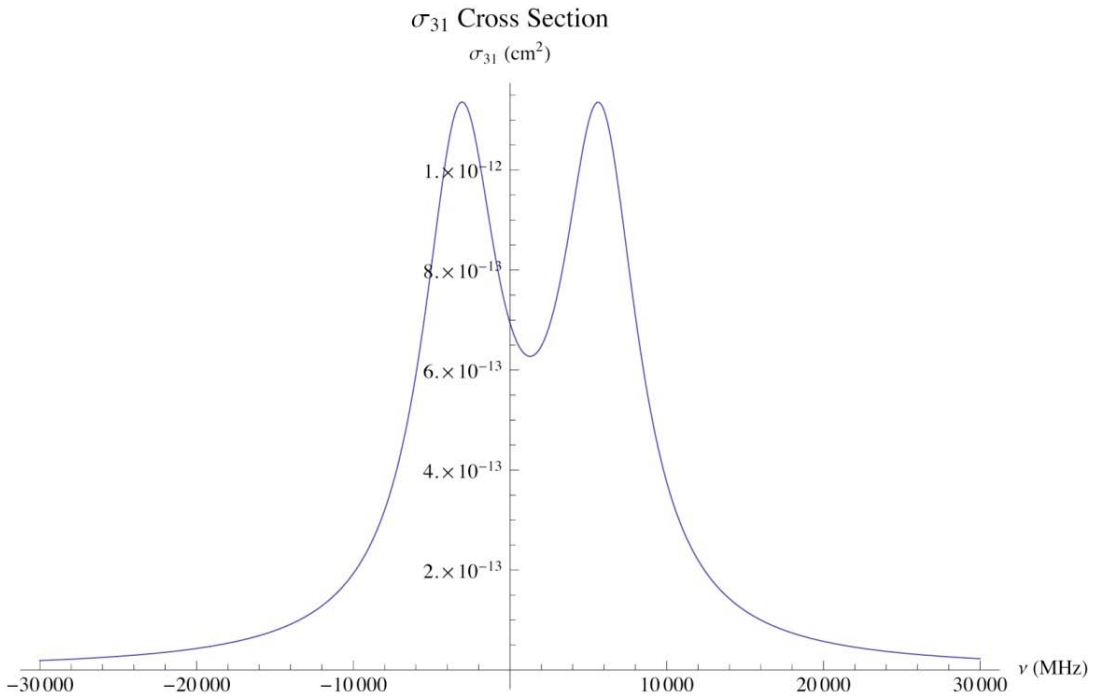

Figure 9. σ_{31} **for 100** $Torr$ **helium and 100** $Torr$ **methane from the Lewis model [5]**

5.2.3 Absorption Profile Comparison.

The absorption profiles for the DPAL regime from the Lewis model are given by Figure 13 from [5]. The same inputs were provided to the three level numerical model and the comparable output is given by Figure 14. Notice that the frequency axis in Figure 13 is offset based on pump line center frequency ν_d, the intensity is in Wcm^{-2}, and the position within the gain medium (z) is in cm. Figure 13's units are based on the MKS system. Figure 14 shows similar features to Figure 13, however, small changes from the more complete rate equation analysis and the use of the terms f_{iso} and f_{ji} are noticeable at the far end of the cell. Hence, the Lewis model captures a

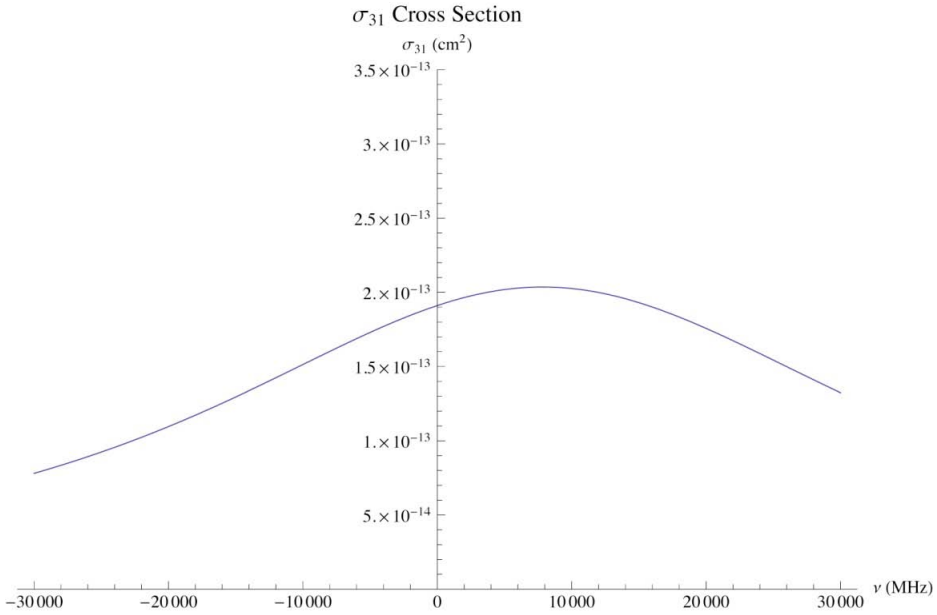

Figure 10. σ_{31} **for 1000** $Torr$ **helium and 1000** $Torr$ **methane from the Lewis model [5]**

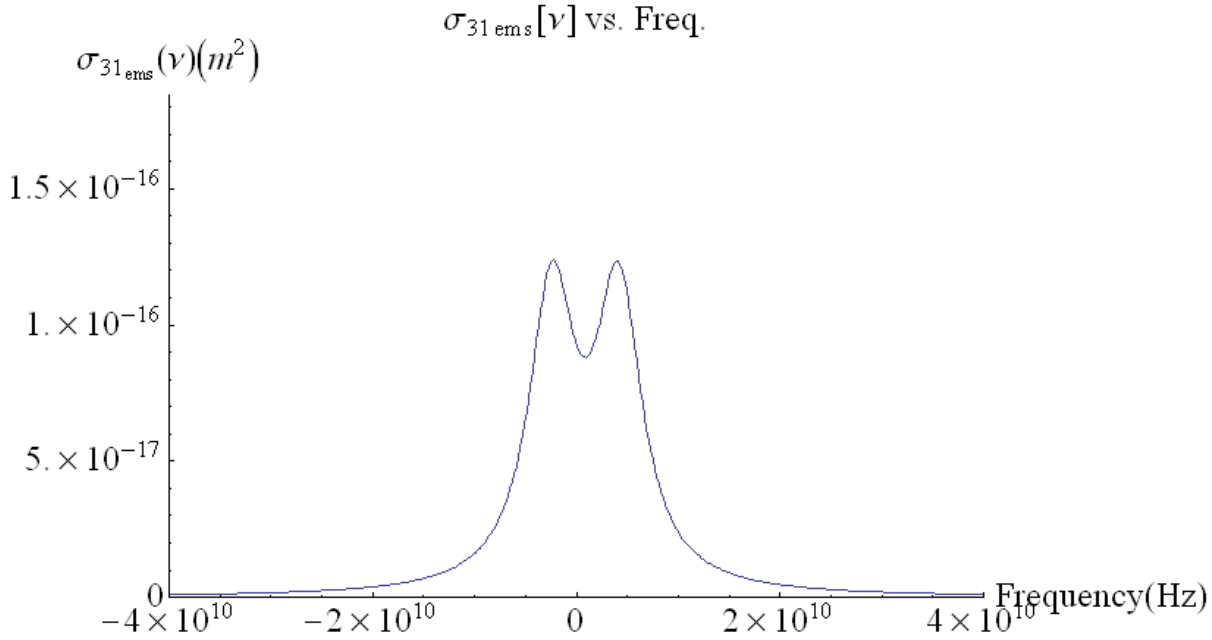

Figure 11. σ_{31} **for 100** $Torr$ **helium and 100** $Torr$ **methane from the three level numerical model**

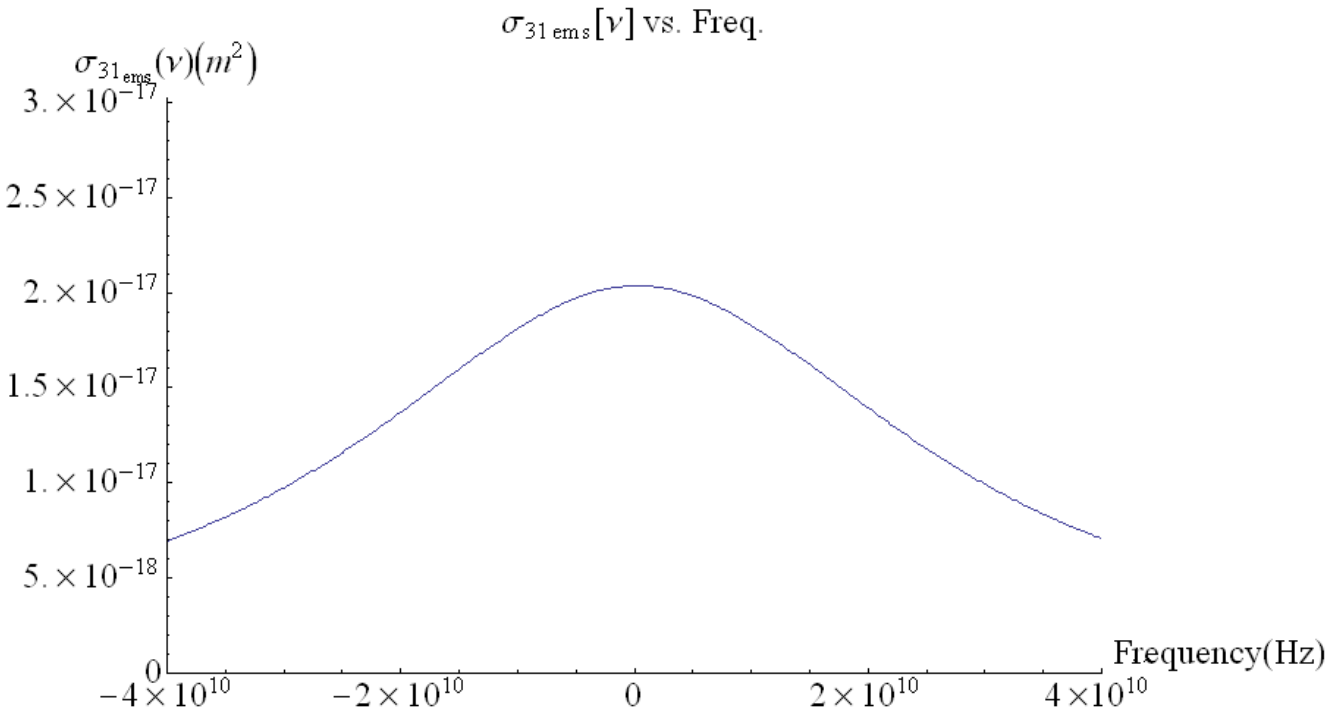

Figure 12. σ_{31} **for 1000** $Torr$ **helium and 1000** $Torr$ **methane from the three level numerical model**

great deal of the absorption effects within the gain medium, but it does not develop a wholly accurate picture of the attenuation of the pump wave.

The Lewis model also develops the attenuation of the pump intensity under the quasi-two level approach (QTLA), and based upon the QTLA assumption, is able to develop the amount of attenuation of the pump intensity due to lasing. This development is somewhat $ad-hoc$, and will not work properly at threshold and will not give a spectral profile for the occurrence of lasing. That is, the pump is assumed to cause lasing to occur and then will be attenuated to a greater degree based upon an assumed lasing intensity which will occur over all pump frequencies to an equal degree. This effect can be seen in Figure 15 with the inputs of Table 6. In actuality only those pump photons which cause lasing to occur in the gain medium will see this effect. Hence, only certain pump frequencies will exhibit this effect; those that induce lasing to occur. Those pump frequencies which do not provide enough energy

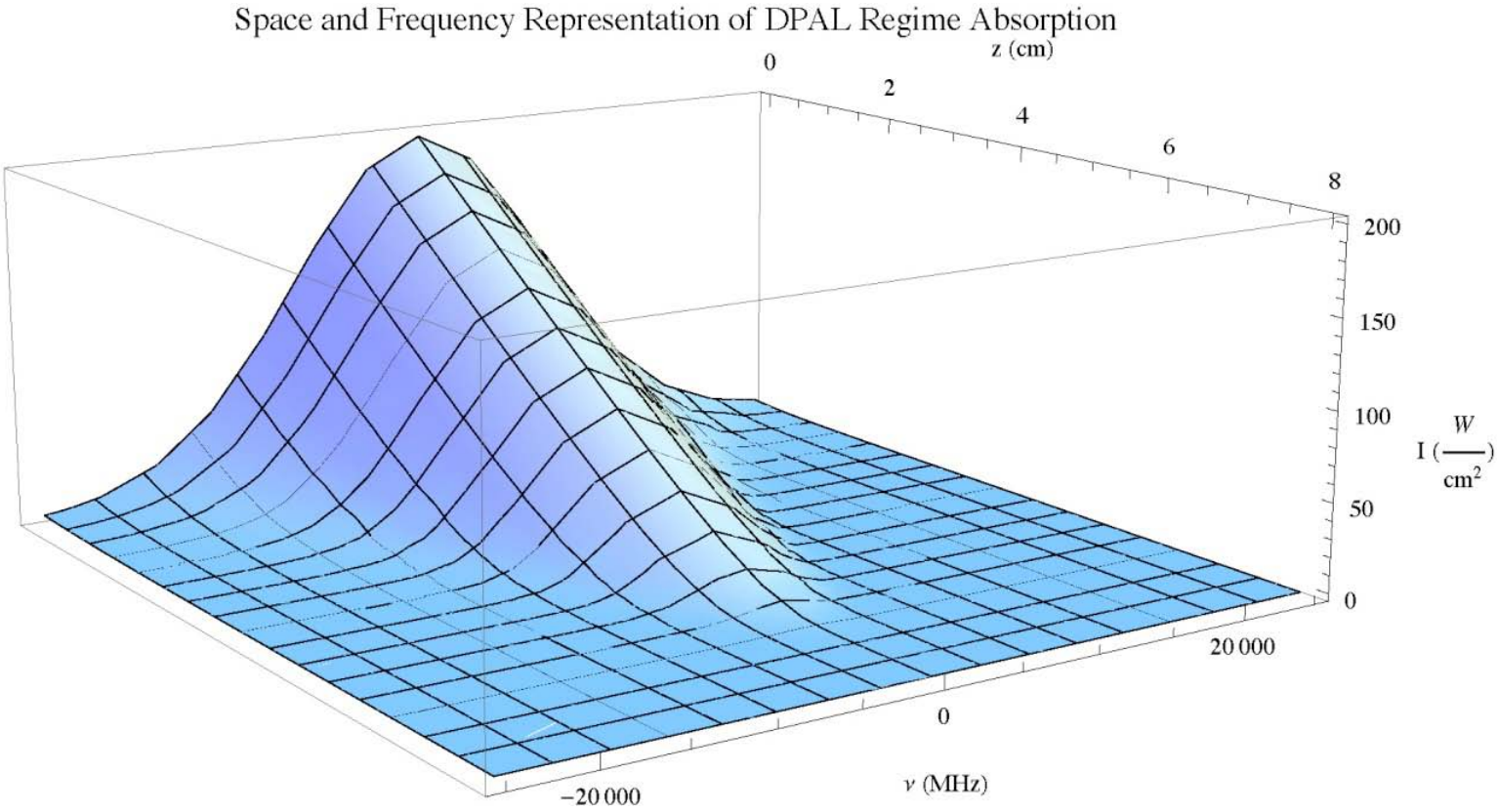

Figure 13. The Lewis model 3D absorption profile without lasing for inputs of Table 6. Note the units of the plot are not MKS and the frequency is offset by ν_d [5].

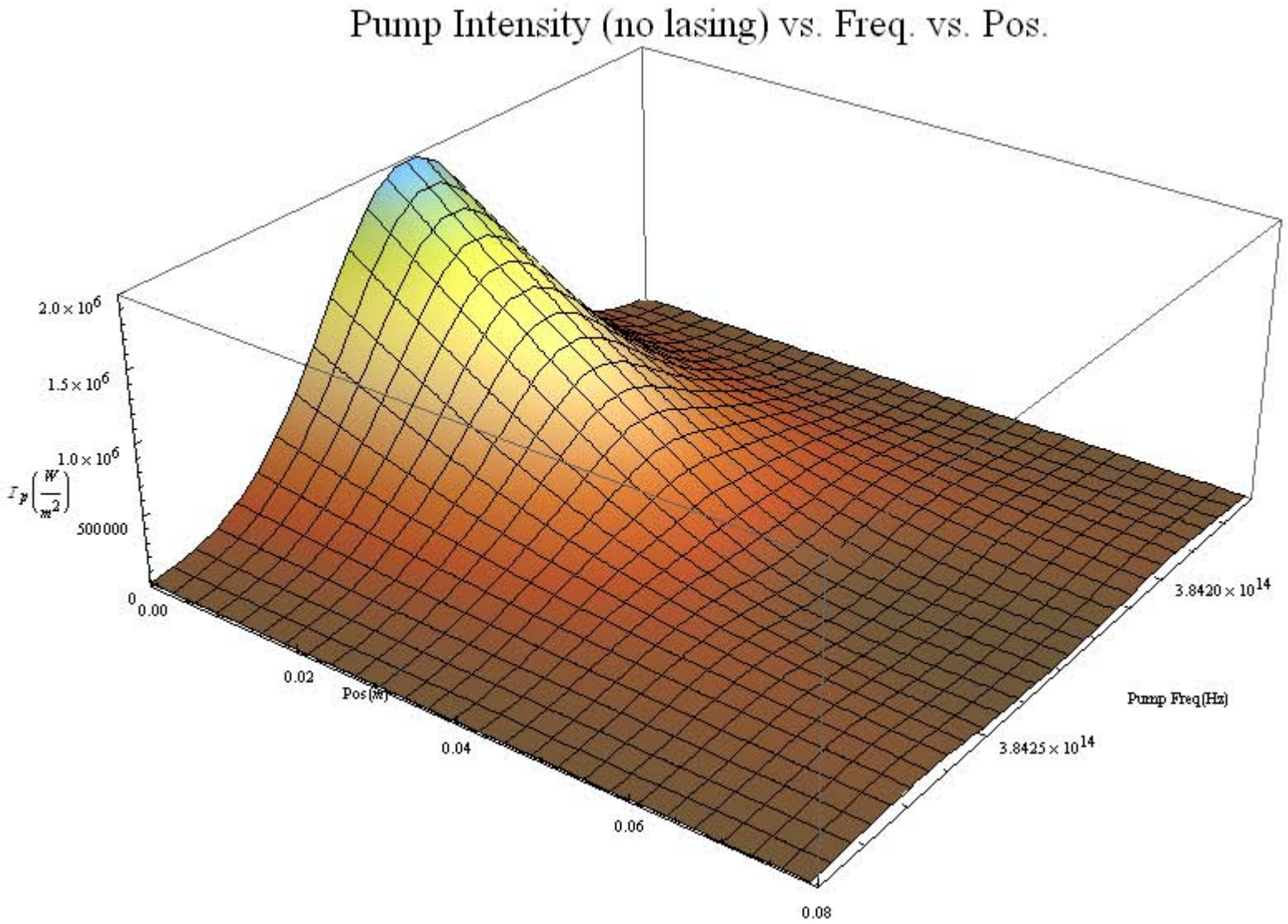

Figure 14. The three level numerical model 3D absorption profile without lasing for inputs of Table 6

to maintain gain above loss will not observe this effect. This can be seen in Figure 16, created with the inputs of Table 6 by the three level numerical model. Lasing is observed to occur in the frequency domain between the two peak features which propagate through to the end of the cell. Also, note that it appears that the pump intensity in the area without lasing has grown between Figures 14 and 16. This is simply an optical illusion due to the degree to which a discontinuity appears in frequency space due to achieving threshold inversion. A close inspection of Figures 14 and 16 will reveal this fact. By comparing Figures 15 and 16, one can see that the Lewis model is able to only approximate the effect of the attenuation of the pump due to intra-cavity lasing. This effect is negligible well above threshold (30 times I_{sat}). The three level numerical model also simulated $\gamma(z)$ for the lasing region of Figure 16 given in Figure 17. Figure 17 only shows the area with positive gain. An effective laser should end when gain dips below zero as the intra-cavity lasing waves will be absorbed beyond this point.

5.3 Comparison to Hager Model

5.3.1 Spectral Profile Comparison.

In [3], Hager develops a spectral line profile of the absorption of the D1 transition for all hyperfine states of Rb. The data Hager presents is based upon experimental data and is then fit to his development of the Voigt profile. The absorption profile calculated by Hager is given in Figure 18. The analogous emission spectra is provided for the three level numerical model in Figure 19. Figure 18's absorption features are shown to be exactly mirrored in the emission profile given by Figure 19. Thus, the three level model is able to fit both experimental lineshape data and the Hager model lineshape for a spectra including all of the naturally occurring isotopes of Rb and all of the hyperfine transitions of the D1 manifold.

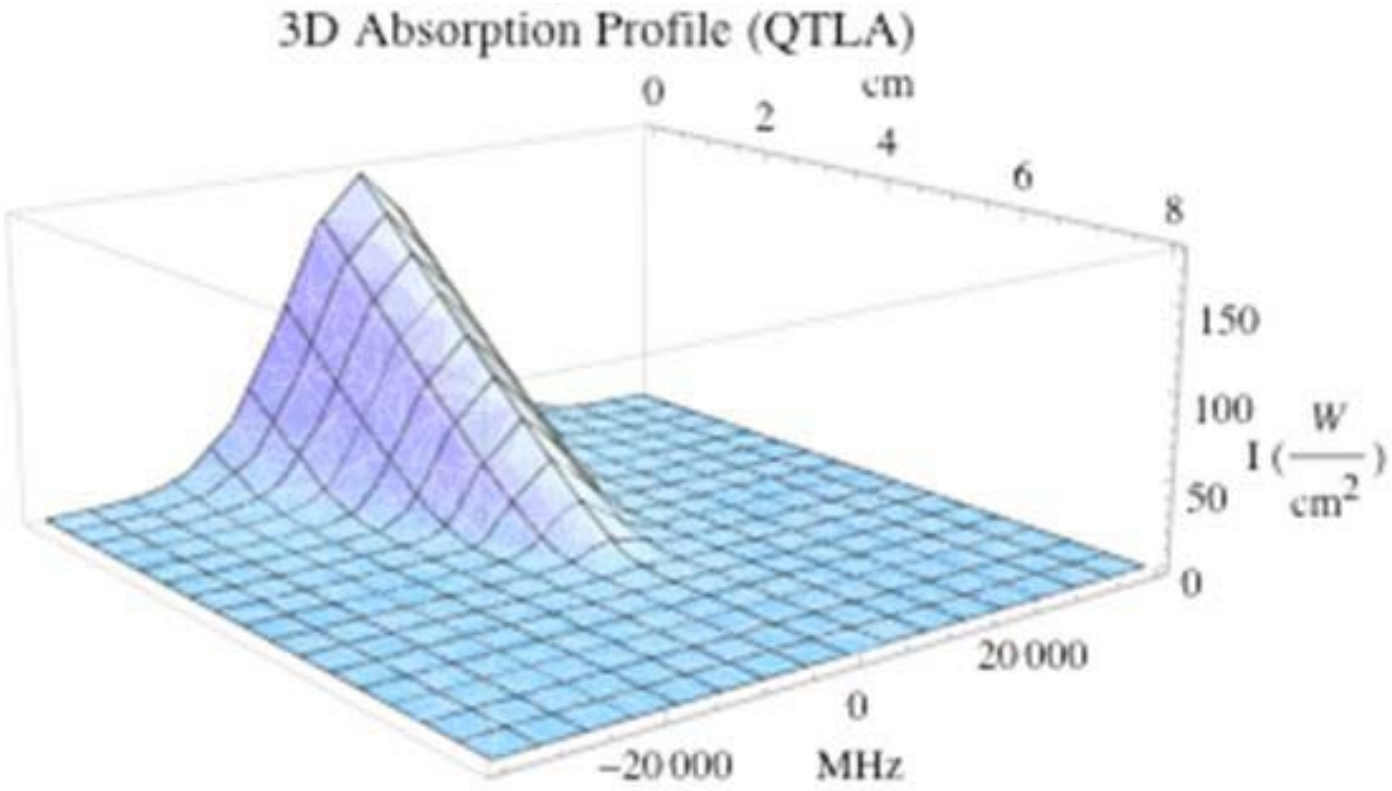

Figure 15. The Lewis model 3D absorption profile with QTLA lasing inputs of Table 6. Note the units of the plot are not MKS and the frequency is offset by ν_d [5].

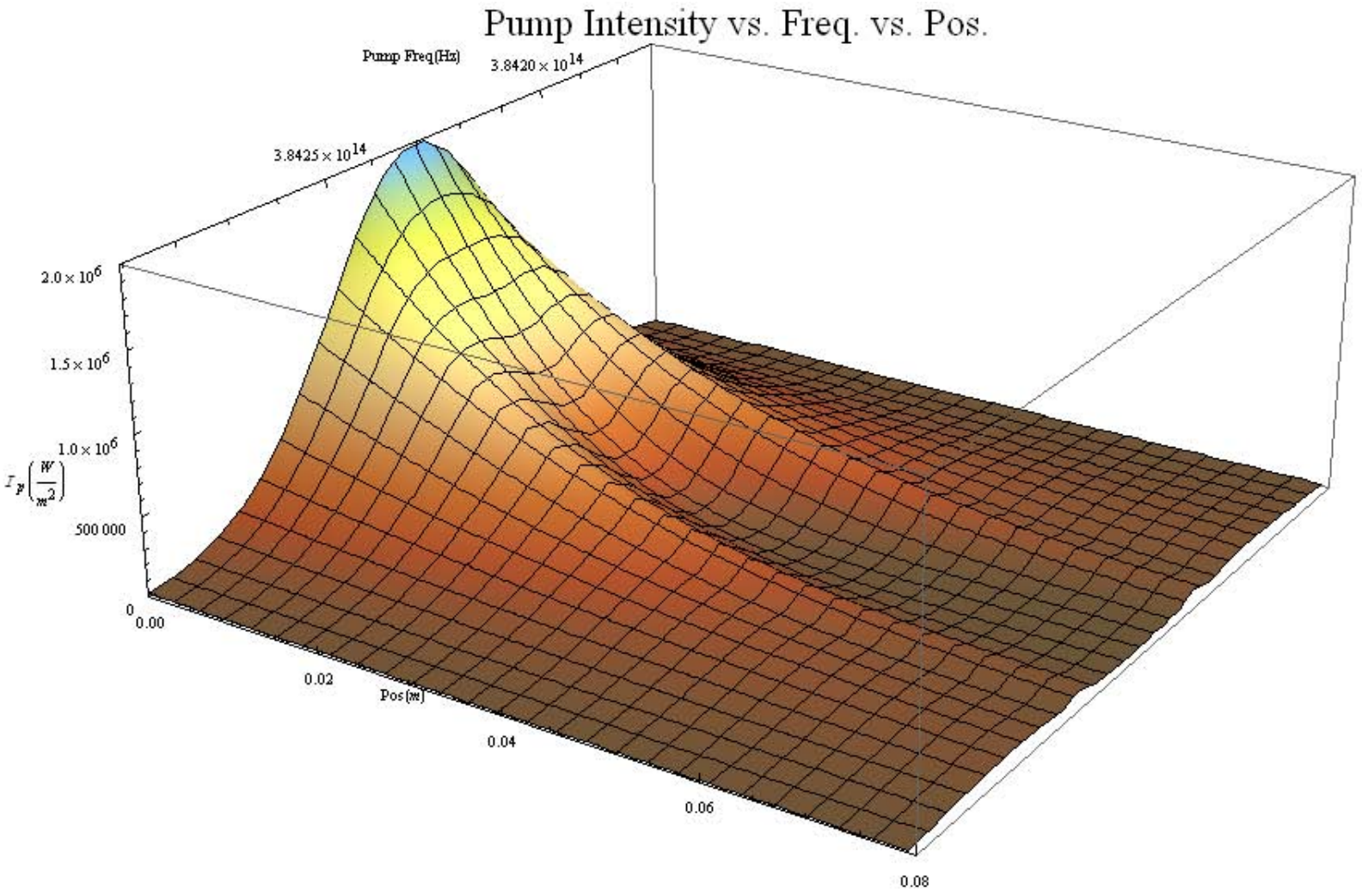

Figure 16. The three level numerical model 3D absorption profile with lasing for inputs of Table 6. Lasing is only occurring, in frequency space, in the region between the two peak features which propagate throughout the cell.

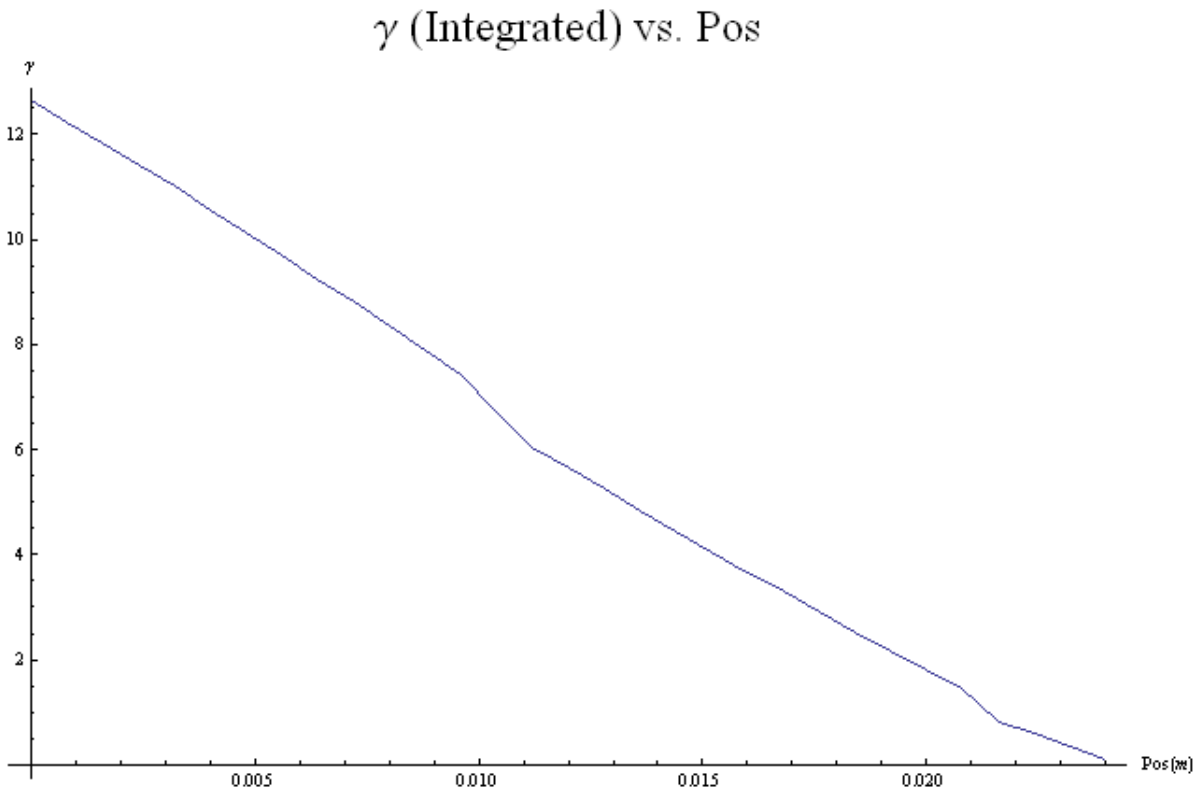

Figure 17. The three level numerical model determination of $\gamma(z)$ for inputs of Table 6 within the lasing region. Notice that the gain is only provided while γ is above zero.

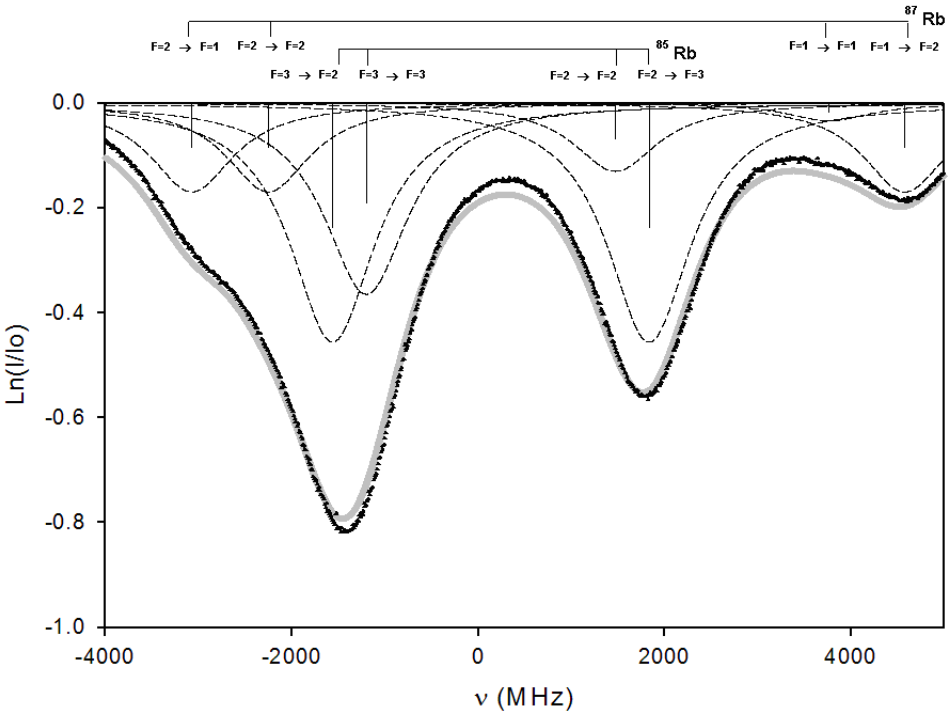

Figure 18. The hyperfine absorption profile for the Rb. D1 manifold offset by ν_{21} [3]

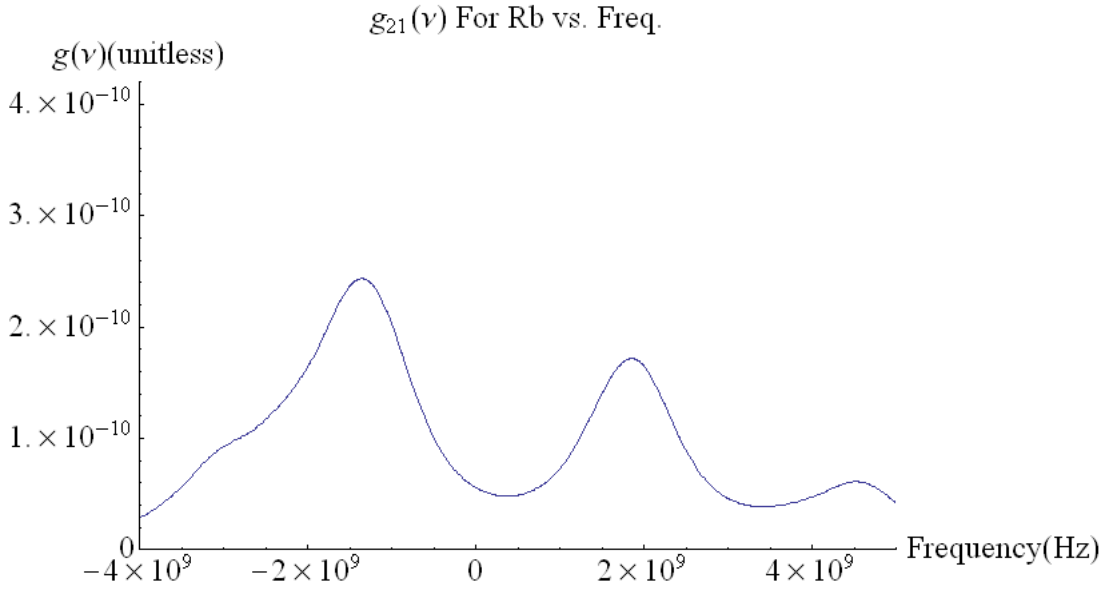

Figure 19. The three level numerical model lineshape for the Rb. D1 manifold offset by ν_{21}

5.4 CW Simulation of a Pulsed System

Pulsed DPAL systems typically operate at extremely high intensities compared to CW systems, however, as long as the population densities reach their equilibrium values a CW simulation is apt for a pulsed system. Even in systems which do not achieve equilibrium, the rate equations for the population concentrations remain unchanged from Chapter II. So, if the rate at which populations change with time is small with respect to the time scale of the pulse width of the diode and the populations are assumed to reach semi-equilibrium quickly after interaction with the pulse, then, this development is still at least somewhat valid. Hence, the three level numerical model can be applied to high intensity systems and may be used to give rough estimates of the characteristics of some pulsed DPAL systems. Typical inputs for the operation of a pulsed DPAL system can be found in Table 7.

Table 7. Simulation Input Parameters for CW Simulation of a Pulsed System

Input Parameter	Units required	Value	Symbol
Temperature of Cell	K	500	T
Temperature of Methane	K	500	T_{meth}
Temperature of Helium	K	500	T_{He}
Temperature of Alkali	K	500	T_{alk}
Partial Pressure of Methane	$Torr$	1000	M_{meth}
Partial Pressure of Helium	$Torr$	1000	M_{He}
Partial Pressure of Alkali	$Torr$	0	M_{alk}
Total Alkali Number Density	m^{-3}	3.79×10^{19}	N_t
Length of gain medium	m	0.01	l_g
Transmission of windows around gain	Unitless	1.0	T_g
High Reflector Reflectivity	Unitless	1.0	R_1
Output Coupler Reflectivity	Unitless	0.5	R_2
Initial Pump Intensity	GWm^{-2}	5	I_p0
Diode Pump Line Center frequency	THz	384.23	ν_d
Diode Pump FWHM frequency	GHz	50	$\nu_{p_{fwhm}}$
Space Between Cavity Mirrors	m	0.1	d_{mirror}

The outputs of the three level numerical model for the inputs of Table 7 are

given in Figures 20 - 23 and Table 8. Figure 20 provides the degree to which the diode pump lineshape was matched with the lineshape of the alkali atom. In this case, the areas overlap about 80 percent. In general, the pump lineshape should be well matched to the transition it is attempting to pump, otherwise energy will be lost. Based on Figure 21 most of the pump's input intensity is still present at the output coupler, implying that the gain cell should be extended if possible. Unlike in Figure 16, the pump intensity in Figure 21 is not observed to have a region which is being attenuated by laser operation and a region which is not. This is due to lasing occurring across the entire pump spectrum provided in Figure 21. Figure 22 shows the gain as a function of z. The gain can be seen to decrease as the pump attenuates. However, the gain does not decrease linearly with position, which implies that approximations such as LAND may not be valid in this case. The total gain in Table 8 is the average value of the gain in Figure 22. In Table 8 $\gamma(total)/\alpha$ is a measure to how well the system followed the approximation that gain equals loss. At infinite fidelity $\gamma(total)/\alpha$ should equal unity. So, $\gamma(total)/\alpha$ is a measure of merit of how well the system performed. The average residual in solutions listed in Table 8 is the of average of all residuals of the routine which chose the best adherence to the boundary condition at the output coupler, i.e. Equation (24). This average is only computed for those cases in which lasing is determined by the simulation to be occurring. Figure 23 shows the forward traveling wave (upper) and the backward traveling wave (lower). Notice that difference between the upper wave and the lower wave at the end of the cell is equal to the reflectivity of the output coupler times the square of the transmissivity of the gain cell, which in this case is 0.5.

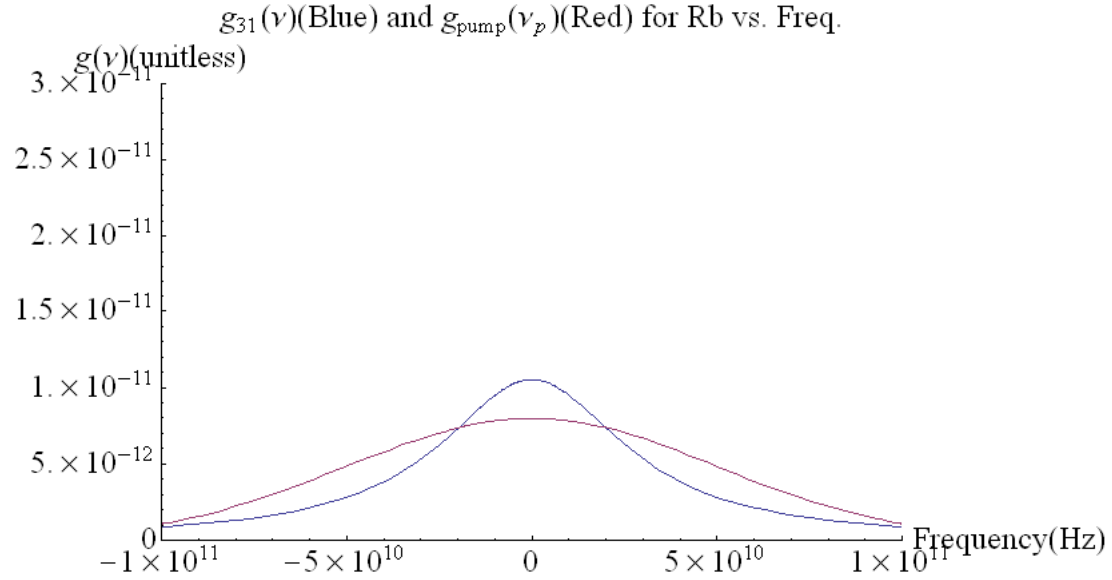

Figure 20. The lineshape g_{31} with the pump lineshape g_p overlayed to show the degree of area matching. Note the frequency is offset by ν_d [5].

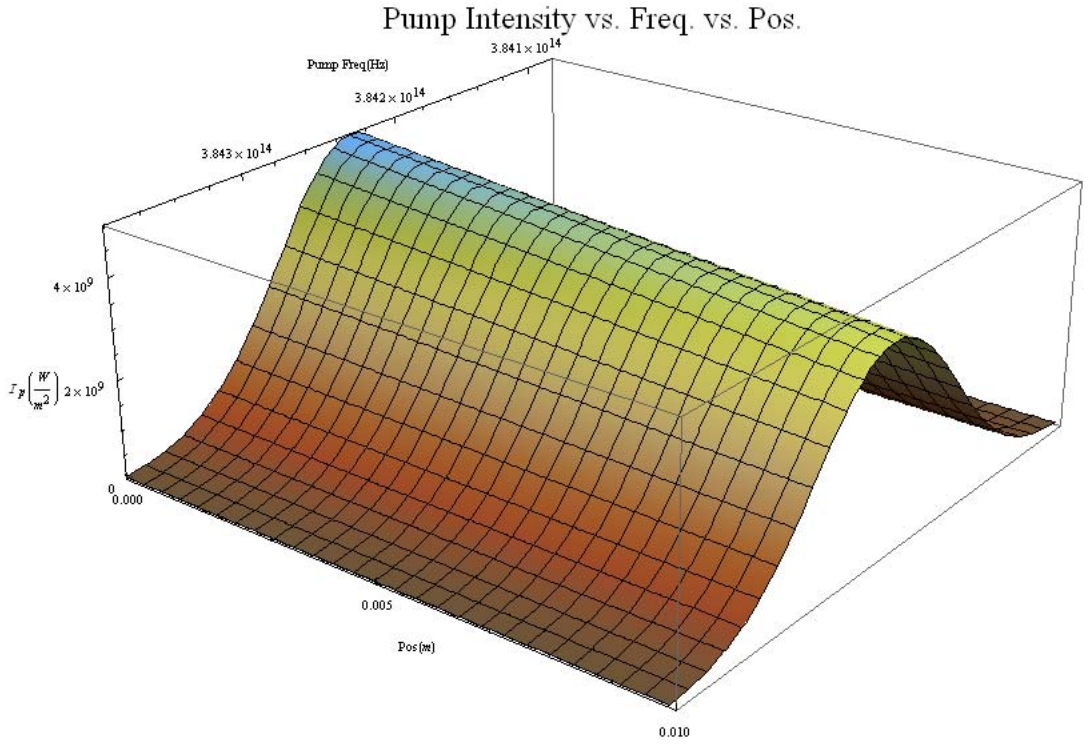

Figure 21. The intensity of the pump (I_P) as it propagates through the cell

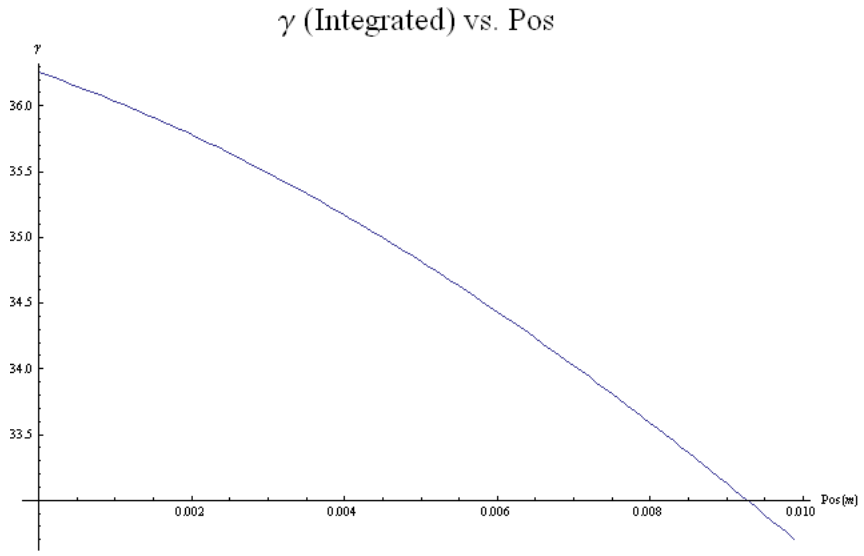

Figure 22. The gain γ as a function of z.

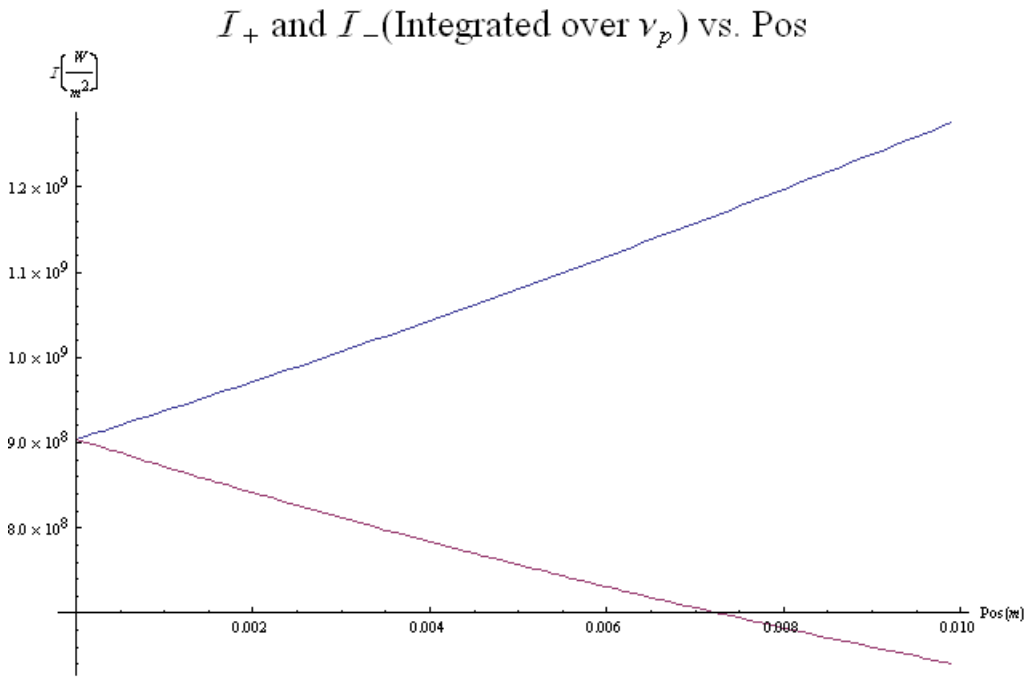

Figure 23. The Integrated Plus Wave Intensity(upper) and Minus Wave Intensity(lower) as functions of z. The output coupling is the space between the upper wave and lower wave at the edge of the graph.

Table 8. Simulation Outputs Characteristics for CW Simulation of a Pulsed System

Input Parameter	Units	Value	Symbol
Output Laser Intensity	MWm^{-2}	63.7	I_{out}
Output Laser Frequency	THz	377.107	ν_l
I_{out}/I_p	Out of 1	0.128	n/a
I_p/I_{sat}	n/a	5002.	n/a
$\gamma(total)/\alpha$	n/a	1.001	n/a
Average residual in solutions	n/a	0.0094	n/a

5.5 Simulation of a System Near Threshold

One of the more difficult regimes to model in most cases is the regime at or near threshold. The three level numerical model is able to simulate threshold systems effectively. The inputs for three level numerical model for a threshold system are given by Table 9. Under these conditions, only a the center bandwidth of the pump wave can induce a population inversion, and thus lasing. This effect is visible in Figure 24. The outputs of the three level numerical model are provided in Table 10. Near threshold the three level numerical model had difficulty obtaining an interpolation for $\gamma(total)$ so it is not listed. The difficulty seems to arise from the sharpness of the gain profile for a threshold case.

Table 9. Simulation Input Parameters for a Threshold System

Input Parameter	Units required	Value	Symbol
Temperature of Cell	K	450	T
Temperature of Methane	K	450	T_{meth}
Temperature of Helium	K	450	T_{He}
Temperature of Alkali	K	450	T_{alk}
Partial Pressure of Methane	$Torr$	500	M_{meth}
Partial Pressure of Helium	$Torr$	500	M_{He}
Partial Pressure of Alkali	$Torr$	0	M_{alk}
Total Alkali Number Density	m^{-3}	6.1×10^{18}	N_t
Length of gain medium	m	0.02	l_g
Transmission of windows around gain	Unitless	1.0	T_g
High Reflector Reflectivity	Unitless	1.0	R_1
Output Coupler Reflectivity	Unitless	0.9999	R_2
Initial Pump Intensity	kWm^{-2}	600	I_p0
Diode Pump Line Center frequency	THz	384.23	ν_d
Diode Pump FWHM frequency	GHz	5	$\nu_{p_{fwhm}}$
Space Between Cavity Mirrors	m	0.1	d_{mirror}

Table 10. Simulation Outputs Characteristics for a Threshold System

Input Parameter	Units	Value	Symbol
Output Laser Intensity	Wm^{-2}	11.2	I_{out}
Output Laser Frequency	THz	377.109	ν_l
I_{out}/I_p	Out of 1	0.000020	n/a
I_p/I_{sat}	n/a	1.25	n/a
$\gamma(total)/\alpha$	n/a	n/a	n/a
Average residual in solutions	n/a	0.35	n/a

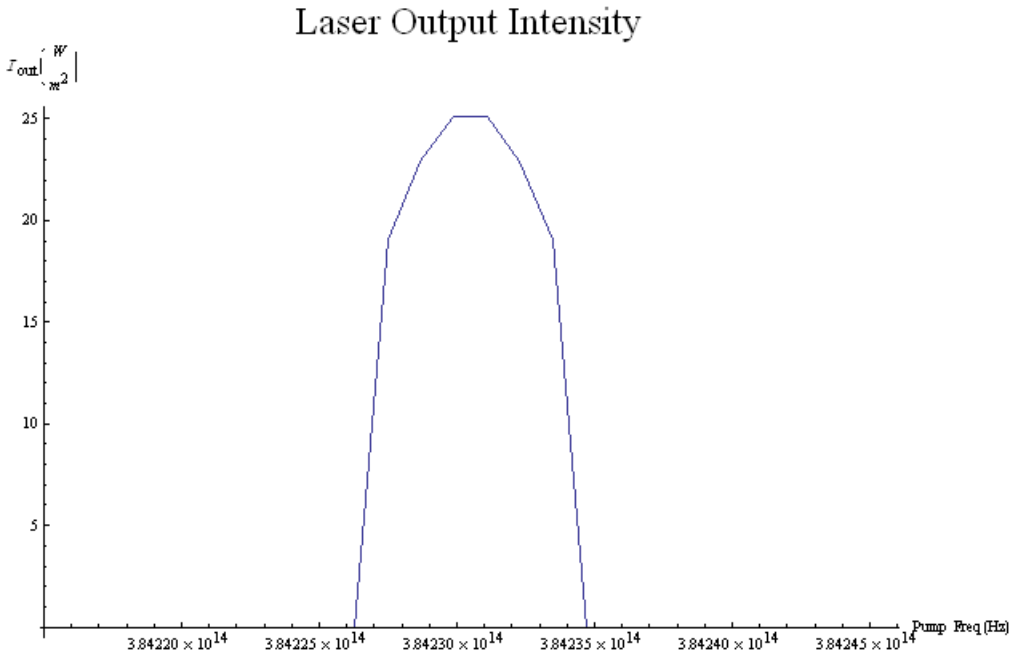

Figure 24. The laser output intensity's spectral width within the pump profile. To get total output intensity one must multiply by g_p and integrate over all space.

VI. Conclusions

6.1 Comparison to Other Models

The three level numerical model is able to replicate the results of both the Lewis model and the Hager model and to produce expected results that neither of these models are able to. The three level numerical model offers a much higher fidelity under many circumstances, but with that added fidelity comes a much more cumbersome development and a lack of intuitive understanding of the problem, which is a hallmark of the Lewis and Hager models. Hence, the three level numerical model provides another option for the simulation of DPAL systems, but does not supersede previous developments.

6.2 Use as a Research Tool

Though the three level numerical model can be somewhat difficult to utilize and to interpret, it provides a great deal of fidelity for research into many areas which no other DPAL simulation can provide. The three level numerical model handles broad-band pumping, produces a complete analysis of the rate equations for the three level DPAL system, selects preferential gain from cavity mode spacing, develops the hyperfine lineshape for multiple isotopes, allows the use of multiple buffer gases, allows for quenching to be simulated, and solves a set of three coupled non-linear transcendental differential equations to characterize any three level CW DPAL system under any regime to high fidelity. Hence, the three level numerical model is an excellent tool for the simulation and characterization of any CW DPAL system. Further, the three level numerical model can be used as a tool to approximate the parameters of many pulsed systems.

6.3 Future Model Development

6.3.1 Mode Volume.

The three level numerical model does not account for the incomplete filling of cavity mode volumes by the pump and currently does not have the ability to simulate the lost energy from this effect. Any further iteration of the three level numerical model should include this effect as it is a persistent issue for DPAL systems and without its effects a model cannot hope to completely capture the effects observed experimentally. The main hurdle to implementation is the lack of references on the subject of mode volume characterization for DPAL systems.

6.3.2 Pulsed DPAL Systems.

Probably the most important addition to the three level numerical model would be the addition of time dependence. Though this would add a great deal of complexity any high power system will most likely utilize pulsed operation. Much of the current research in DPAL systems involves the use of pulse operated DPAL system. Therefore, any further development of the model should include the ability for pulsed operation. While theoretical models do exist for the pulsed operation of lasers the inherent complexity of a time dependent laser system forces super-computing as a near necessity for any high fidelity systems.

Appendix A. *Mathematica* Code to Solve Rate Equations

DPAL 3-Level Modeling Rate Equation Solution

I. Rate Equations

```
ClearAll[N1, N2, N3, Reqn1, Reqn2, Reqn3, Reqn4, f, z]
Reqn1[N1_, N2_, N3_] := N3 * A31[iso] + N2 * A21[iso] + N3 * k31 + N2 * k21 +
  (-B13[νpump, iso] * N1 * Ip[z] * gIp0loop / (c / ng) + B31[νpump, iso] * N3 * Ip[z] * gIp0loop / (c / ng) +
    B21[νlaser, iso] * Il[z] * gapproxfixtotal21loop / (c / ng) * (N2 - g2 / g1 N1))

Reqn2[N1_, N2_, N3_] := N3 * k32[species, iso] * M[species] - N2 * k23[species, iso] * M[species] -
  N2 * A21[iso] - N2 * k21 - B21[νlaser, iso] * Il[z] * gapproxfixtotal21loop / (c / ng) * (N2 - g2 / g1 N1)

Reqn3[N1_, N2_, N3_] :=
 -N3 * k32[species, iso] * M[species] + N2 * k23[species, iso] * M[species] - N3 * A31[iso] -
  N3 * k31 + B13[νpump, iso] * Ip[z] * gIp0loop / (c / ng) * N1 - B31[νpump, iso] * N3 * Ip[z] * gIp0loop / (c / ng)

Reqn4[N1_, N2_, N3_] := N1 + N2 + N3
f = N2 / (N2 + N3);

Solve[{Reqn1[N1, N2, N3], Reqn2[N1, N2, N3], Reqn4[N1, N2, N3]} == {0, 0, Nt}, {N1, N2, N3}]

{{𝒩1 → 𝒩t + (g2 gapproxfixtotal21loop ng 𝒩t ℬ21[νlaser, iso] ℐl[z]) /
    (c g1 (-k21 - 𝒜21[iso] - gapproxfixtotal21loop ng ℬ21[νlaser, iso] ℐl[z] / c -
      g2 gapproxfixtotal21loop ng ℬ21[νlaser, iso] ℐl[z] / (c g1) - k23[species, iso] 𝒩[species])) +
```

$$\left(-\frac{1}{c\,g1}\,g2\,\text{gapproxfixtotal21loop}\,ng\,\mathcal{N}t\,\mathcal{B}21[\nu\text{laser},\text{iso}]\,\mathcal{I}l[z]\right.$$
$$\left(k21+\mathcal{R}21[\text{iso}]+\frac{\text{gapproxfixtotal21loop}\,ng\,\mathcal{B}21[\nu\text{laser},\text{iso}]\,\mathcal{I}l[z]}{c}+\right.$$
$$\frac{g2\,\text{gapproxfixtotal21loop}\,ng\,\mathcal{B}21[\nu\text{laser},\text{iso}]\,\mathcal{I}l[z]}{c\,g1}+$$
$$\left.\frac{g\mathcal{I}p0\text{loop}\,ng\,\mathcal{B}13[\nu\text{pump},\text{iso}]\,\mathcal{I}p[z]}{c}\right)+$$
$$\mathcal{N}t\left(-\frac{g2\,\text{gapproxfixtotal21loop}\,ng\,\mathcal{B}21[\nu\text{laser},\text{iso}]\,\mathcal{I}l[z]}{c\,g1}-\right.$$
$$\left.\frac{g\mathcal{I}p0\text{loop}\,ng\,\mathcal{B}13[\nu\text{pump},\text{iso}]\,\mathcal{I}p[z]}{c}\right)$$
$$\left(-k21-\mathcal{R}21[\text{iso}]-\frac{\text{gapproxfixtotal21loop}\,ng\,\mathcal{B}21[\nu\text{laser},\text{iso}]\,\mathcal{I}l[z]}{c}-\right.$$
$$\frac{g2\,\text{gapproxfixtotal21loop}\,ng\,\mathcal{B}21[\nu\text{laser},\text{iso}]\,\mathcal{I}l[z]}{c\,g1}-$$
$$\left.\left.k23[\text{species},\text{iso}]\,\mathcal{M}[\text{species}]\right)\right)\Big/$$
$$\left(\left(\left(k31+\mathcal{R}31[\text{iso}]+\frac{g2\,\text{gapproxfixtotal21loop}\,ng\,\mathcal{B}21[\nu\text{laser},\text{iso}]\,\mathcal{I}l[z]}{c\,g1}+\right.\right.\right.$$
$$\left.\left.\frac{g\mathcal{I}p0\text{loop}\,ng\,\mathcal{B}13[\nu\text{pump},\text{iso}]\,\mathcal{I}p[z]}{c}+\frac{g\mathcal{I}p0\text{loop}\,ng\,\mathcal{B}31[\nu\text{pump},\text{iso}]\,\mathcal{I}p[z]}{c}\right)\right.$$
$$\left(-k21-\mathcal{R}21[\text{iso}]-\frac{\text{gapproxfixtotal21loop}\,ng\,\mathcal{B}21[\nu\text{laser},\text{iso}]\,\mathcal{I}l[z]}{c}-\right.$$
$$\left.\frac{g2\,\text{gapproxfixtotal21loop}\,ng\,\mathcal{B}21[\nu\text{laser},\text{iso}]\,\mathcal{I}l[z]}{c\,g1}-k23[\text{species},\text{iso}]\,\mathcal{M}[\text{species}]\right)-$$
$$\left(k21+\mathcal{R}21[\text{iso}]+\frac{\text{gapproxfixtotal21loop}\,ng\,\mathcal{B}21[\nu\text{laser},\text{iso}]\,\mathcal{I}l[z]}{c}+\right.$$
$$\frac{g2\,\text{gapproxfixtotal21loop}\,ng\,\mathcal{B}21[\nu\text{laser},\text{iso}]\,\mathcal{I}l[z]}{c\,g1}+$$
$$\left.\frac{g\mathcal{I}p0\text{loop}\,ng\,\mathcal{B}13[\nu\text{pump},\text{iso}]\,\mathcal{I}p[z]}{c}\right)$$
$$\left(-\frac{g2\,\text{gapproxfixtotal21loop}\,ng\,\mathcal{B}21[\nu\text{laser},\text{iso}]\,\mathcal{I}l[z]}{c\,g1}+\right.$$

$$\left(\left(-\frac{g2\ gapproxfixtotal21loop\ ng\ \mathcal{B}21[\nu laser, iso]\ \mathcal{I}l[z]}{c\ g1}+k32[species, iso]\ \mathcal{M}[species]\right)\right.$$
$$\left(-\frac{1}{c\ g1}\ g2\ gapproxfixtotal21loop\ ng\ \mathcal{N}t\ \mathcal{B}21[\nu laser, iso]\ \mathcal{I}l[z]\right.$$
$$\left(k21+\mathcal{A}21[iso]+\frac{gapproxfixtotal21loop\ ng\ \mathcal{B}21[\nu laser, iso]\ \mathcal{I}l[z]}{c}+\right.$$
$$\frac{g2\ gapproxfixtotal21loop\ ng\ \mathcal{B}21[\nu laser, iso]\ \mathcal{I}l[z]}{c\ g1}+$$
$$\left.\frac{g\mathcal{I}p0loop\ ng\ \mathcal{B}13[\nu pump, iso]\ \mathcal{I}p[z]}{c}\right)+$$
$$\mathcal{N}t\left(-\frac{g2\ gapproxfixtotal21loop\ ng\ \mathcal{B}21[\nu laser, iso]\ \mathcal{I}l[z]}{c\ g1}-\right.$$
$$\left.\frac{g\mathcal{I}p0loop\ ng\ \mathcal{B}13[\nu pump, iso]\ \mathcal{I}p[z]}{c}\right)$$
$$\left(-k21-\mathcal{A}21[iso]-\frac{gapproxfixtotal21loop\ ng\ \mathcal{B}21[\nu laser, iso]\ \mathcal{I}l[z]}{c}-\right.$$
$$\frac{g2\ gapproxfixtotal21loop\ ng\ \mathcal{B}21[\nu laser, iso]\ \mathcal{I}l[z]}{c\ g1}-$$
$$\left.\left.k23[species, iso]\ \mathcal{M}[species]\right)\right)\Big/$$
$$\left(\left(-k21-\mathcal{A}21[iso]-\frac{gapproxfixtotal21loop\ ng\ \mathcal{B}21[\nu laser, iso]\ \mathcal{I}l[z]}{c}-\right.\right.$$
$$\left.\frac{g2\ gapproxfixtotal21loop\ ng\ \mathcal{B}21[\nu laser, iso]\ \mathcal{I}l[z]}{c\ g1}-k23[species, iso]\ \mathcal{M}[species]\right)$$
$$\left(\left(k31+\mathcal{A}31[iso]+\frac{g2\ gapproxfixtotal21loop\ ng\ \mathcal{B}21[\nu laser, iso]\ \mathcal{I}l[z]}{c\ g1}+\right.\right.$$
$$\frac{g\mathcal{I}p0loop\ ng\ \mathcal{B}13[\nu pump, iso]\ \mathcal{I}p[z]}{c}+\frac{g\mathcal{I}p0loop\ ng\ \mathcal{B}31[\nu pump, iso]\ \mathcal{I}p[z]}{c}\Big)$$
$$\left(-k21-\mathcal{A}21[iso]-\frac{gapproxfixtotal21loop\ ng\ \mathcal{B}21[\nu laser, iso]\ \mathcal{I}l[z]}{c}-\right.$$
$$\left.\frac{g2\ gapproxfixtotal21loop\ ng\ \mathcal{B}21[\nu laser, iso]\ \mathcal{I}l[z]}{c\ g1}-k23[species, iso]\right.$$

$$\mathcal{M}[\text{species}]\Big) - \Big(\text{k21} + \mathcal{R}21[\text{iso}] + \frac{\text{gapproxfixtotal21loop ng}\,\mathcal{B}21[\nu\text{laser, iso}]\,\mathcal{I}\text{l}[z]}{c} + \frac{\text{g2 gapproxfixtotal21loop ng}\,\mathcal{B}21[\nu\text{laser, iso}]\,\mathcal{I}\text{l}[z]}{c\ \text{g1}} + \frac{\text{g}\mathcal{I}\text{p0loop ng}\,\mathcal{B}13[\nu\text{pump, iso}]\,\mathcal{I}\text{p}[z]}{c}\Big)$$

$$\Big(-\frac{\text{g2 gapproxfixtotal21loop ng}\,\mathcal{B}21[\nu\text{laser, iso}]\,\mathcal{I}\text{l}[z]}{c\ \text{g1}} + \text{k32}[\text{species, iso}]\,\mathcal{M}[\text{species}]\Big)\Big)\Big),$$

$$\mathcal{N}2 \to -(\text{g2 gapproxfixtotal21loop ng}\,\mathcal{N}\text{t}\,\mathcal{B}21[\nu\text{laser, iso}]\,\mathcal{I}\text{l}[z])\Big/$$

$$\Big(c\ \text{g1}\Big(-\text{k21} - \mathcal{R}21[\text{iso}] - \frac{\text{gapproxfixtotal21loop ng}\,\mathcal{B}21[\nu\text{laser, iso}]\,\mathcal{I}\text{l}[z]}{c} - \frac{\text{g2 gapproxfixtotal21loop ng}\,\mathcal{B}21[\nu\text{laser, iso}]\,\mathcal{I}\text{l}[z]}{c\ \text{g1}} - \text{k23}[\text{species, iso}]\,\mathcal{M}[\text{species}]\Big) +$$

$$\Big(\Big(-\frac{\text{g2 gapproxfixtotal21loop ng}\,\mathcal{B}21[\nu\text{laser, iso}]\,\mathcal{I}\text{l}[z]}{c\ \text{g1}} + \text{k32}[\text{species, iso}]\,\mathcal{M}[\text{species}]\Big)$$

$$\Big(-\frac{1}{c\ \text{g1}}\,\text{g2 gapproxfixtotal21loop ng}\,\mathcal{N}\text{t}\,\mathcal{B}21[\nu\text{laser, iso}]\,\mathcal{I}\text{l}[z]$$

$$\Big(\text{k21} + \mathcal{R}21[\text{iso}] + \frac{\text{gapproxfixtotal21loop ng}\,\mathcal{B}21[\nu\text{laser, iso}]\,\mathcal{I}\text{l}[z]}{c} + \frac{\text{g2 gapproxfixtotal21loop ng}\,\mathcal{B}21[\nu\text{laser, iso}]\,\mathcal{I}\text{l}[z]}{c\ \text{g1}} + \frac{\text{g}\mathcal{I}\text{p0loop ng}\,\mathcal{B}13[\nu\text{pump, iso}]\,\mathcal{I}\text{p}[z]}{c}\Big) +$$

$$\mathcal{N}\text{t}\Big(-\frac{\text{g2 gapproxfixtotal21loop ng}\,\mathcal{B}21[\nu\text{laser, iso}]\,\mathcal{I}\text{l}[z]}{c\ \text{g1}} - \frac{\text{g}\mathcal{I}\text{p0loop ng}\,\mathcal{B}13[\nu\text{pump, iso}]\,\mathcal{I}\text{p}[z]}{c}\Big)$$

$$\Big(-\text{k21} - \mathcal{R}21[\text{iso}] - \frac{\text{gapproxfixtotal21loop ng}\,\mathcal{B}21[\nu\text{laser, iso}]\,\mathcal{I}\text{l}[z]}{c} -$$

$$\frac{g2\ gapproxfixtotal21loop\ ng\ \mathcal{B}21[\nu laser, iso]\ \mathcal{I}l[z]}{c\ g1} -$$

$$k23[species, iso]\ \mathcal{M}[species]\Big)\Big)\Big) \Big/$$

$$\Big(\Big(-k21 - \mathcal{A}21[iso] - \frac{gapproxfixtotal21loop\ ng\ \mathcal{B}21[\nu laser, iso]\ \mathcal{I}l[z]}{c} -$$

$$\frac{g2\ gapproxfixtotal21loop\ ng\ \mathcal{B}21[\nu laser, iso]\ \mathcal{I}l[z]}{c\ g1} - k23[species, iso]\ \mathcal{M}[species]\Big)$$

$$\Big(\Big(k31 + \mathcal{A}31[iso] + \frac{g2\ gapproxfixtotal21loop\ ng\ \mathcal{B}21[\nu laser, iso]\ \mathcal{I}l[z]}{c\ g1} +$$

$$\frac{g\mathcal{I}p0loop\ ng\ \mathcal{B}13[\nu pump, iso]\ \mathcal{I}p[z]}{c} + \frac{g\mathcal{I}p0loop\ ng\ \mathcal{B}31[\nu pump, iso]\ \mathcal{I}p[z]}{c}\Big)$$

$$\Big(-k21 - \mathcal{A}21[iso] - \frac{gapproxfixtotal21loop\ ng\ \mathcal{B}21[\nu laser, iso]\ \mathcal{I}l[z]}{c} -$$

$$\frac{g2\ gapproxfixtotal21loop\ ng\ \mathcal{B}21[\nu laser, iso]\ \mathcal{I}l[z]}{c\ g1} - k23[species, iso]$$

$$\mathcal{M}[species]\Big) - \Big(k21 + \mathcal{A}21[iso] + \frac{gapproxfixtotal21loop\ ng\ \mathcal{B}21[\nu laser, iso]\ \mathcal{I}l[z]}{c} +$$

$$\frac{g2\ gapproxfixtotal21loop\ ng\ \mathcal{B}21[\nu laser, iso]\ \mathcal{I}l[z]}{c\ g1} +$$

$$\frac{g\mathcal{I}p0loop\ ng\ \mathcal{B}13[\nu pump, iso]\ \mathcal{I}p[z]}{c}\Big)$$

$$\Big(-\frac{g2\ gapproxfixtotal21loop\ ng\ \mathcal{B}21[\nu laser, iso]\ \mathcal{I}l[z]}{c\ g1} +$$

$$k32[species, iso]\ \mathcal{M}[species]\Big)\Big)\Big),$$

$$\mathcal{N}3 \to -\Big(-\frac{1}{c\ g1}\ g2\ gapproxfixtotal21loop\ ng\ \mathcal{N}t\ \mathcal{B}21[\nu laser, iso]\ \mathcal{I}l[z]$$

$$\Big(k21 + \mathcal{A}21[iso] + \frac{gapproxfixtotal21loop\ ng\ \mathcal{B}21[\nu laser, iso]\ \mathcal{I}l[z]}{c} +$$

$$\frac{g2\ gapproxfixtotal21loop\ ng\ \mathcal{B}21[\nu laser, iso]\ \mathcal{I}l[z]}{c\ g1} +$$

$$\frac{g\mathcal{I}p0loop\ ng\ \mathcal{B}13[\nu pump, iso]\ \mathcal{I}p[z]}{c}\Big) +$$

$$\mathcal{N}t\left(-\frac{g2\,\text{gapproxfixtotal21loop}\,ng\,\mathcal{B}21[\nu\text{laser},\text{iso}]\,\mathcal{I}l[z]}{c\,g1}-\frac{g\mathcal{I}p0\text{loop}\,ng\,\mathcal{B}13[\nu\text{pump},\text{iso}]\,\mathcal{I}p[z]}{c}\right)\left(-k21-\mathcal{R}21[\text{iso}]-\frac{\text{gapproxfixtotal21loop}\,ng\,\mathcal{B}21[\nu\text{laser},\text{iso}]\,\mathcal{I}l[z]}{c}-\frac{g2\,\text{gapproxfixtotal21loop}\,ng\,\mathcal{B}21[\nu\text{laser},\text{iso}]\,\mathcal{I}l[z]}{c\,g1}-k23[\text{species},\text{iso}]\,\mathcal{M}[\text{species}]\right)\Big/\left(\left(k31+\mathcal{R}31[\text{iso}]+\frac{g2\,\text{gapproxfixtotal21loop}\,ng\,\mathcal{B}21[\nu\text{laser},\text{iso}]\,\mathcal{I}l[z]}{c\,g1}+\frac{g\mathcal{I}p0\text{loop}\,ng\,\mathcal{B}13[\nu\text{pump},\text{iso}]\,\mathcal{I}p[z]}{c}+\frac{g\mathcal{I}p0\text{loop}\,ng\,\mathcal{B}31[\nu\text{pump},\text{iso}]\,\mathcal{I}p[z]}{c}\right)\left(-k21-\mathcal{R}21[\text{iso}]-\frac{\text{gapproxfixtotal21loop}\,ng\,\mathcal{B}21[\nu\text{laser},\text{iso}]\,\mathcal{I}l[z]}{c}-\frac{g2\,\text{gapproxfixtotal21loop}\,ng\,\mathcal{B}21[\nu\text{laser},\text{iso}]\,\mathcal{I}l[z]}{c\,g1}-k23[\text{species},\text{iso}]\,\mathcal{M}[\text{species}]\right)-\left(k21+\mathcal{R}21[\text{iso}]+\frac{\text{gapproxfixtotal21loop}\,ng\,\mathcal{B}21[\nu\text{laser},\text{iso}]\,\mathcal{I}l[z]}{c}+\frac{g2\,\text{gapproxfixtotal21loop}\,ng\,\mathcal{B}21[\nu\text{laser},\text{iso}]\,\mathcal{I}l[z]}{c\,g1}+\frac{g\mathcal{I}p0\text{loop}\,ng\,\mathcal{B}13[\nu\text{pump},\text{iso}]\,\mathcal{I}p[z]}{c}\right)\left(-\frac{g2\,\text{gapproxfixtotal21loop}\,ng\,\mathcal{B}21[\nu\text{laser},\text{iso}]\,\mathcal{I}l[z]}{c\,g1}+k32[\text{species},\text{iso}]\,\mathcal{M}[\text{species}]\right)\right)\Big\}\Big\}$$

II. Full Simplify of f

f is found to be a function of M, ν, and z

```
N3 :=
 -((-B13 Ip (-k21 - A21 - B21 Il - B21 g2 Il/g1 - k23Eth MEth) Nt +
     B21 g2 Il (-B13 Ip + k23Eth MEth) Nt/g1)/
   (-(-k21 - A21 - B21 Il - B21 g2 Il/g1 - k23Eth MEth) (-k31 - A31 - B13 Ip - B31 Ip - k32Eth MEth) +
     (-B13 Ip + k23Eth MEth) (-B21 g2 Il/g1 + k32Eth MEth)))
N2 := -B13 Ip Nt/(-B13 Ip + k23Eth MEth) + ((-k31 - A31 - B13 Ip - B31 Ip - k32Eth MEth)
      (-B13 Ip (-k21 - A21 - B21 Il - B21 g2 Il/g1 - k23Eth MEth) Nt +
        B21 g2 Il (-B13 Ip + k23Eth MEth) Nt/g1))/((-B13 Ip + k23Eth MEth)
      (-(-k21 - A21 - B21 Il - B21 g2 Il/g1 - k23Eth MEth) (-k31 - A31 - B13 Ip - B31 Ip - k32Eth MEth) +
        (-B13 Ip + k23Eth MEth) (-B21 g2 Il/g1 + k32Eth MEth)))
N1 := -(-k21 k31 g1 Nt - k31 A21 g1 Nt - k21 A31 g1 Nt - A21 A31 g1 Nt - k31 B21 g1 Il Nt -
      A31 B21 g1 Il Nt - k21 B31 g1 Ip Nt - A21 B31 g1 Ip Nt - B21 B31 g1 Il Ip Nt -
      k23Eth k31 g1 MEth Nt - k21 k32Eth g1 MEth Nt - k32Eth A21 g1 MEth Nt -
      k23Eth A31 g1 MEth Nt - k32Eth B21 g1 Il MEth Nt - k23Eth B31 g1 Ip MEth Nt) /
  (k21 k31 g1 + k31 A21 g1 + k21 A31 g1 + A21 A31 g1 + k31 B21 g1 Il + A31 B21 g1 Il +
    k31 B21 g2 Il + A31 B21 g2 Il + k21 B13 g1 Ip + A21 B13 g1 Ip + k21 B31 g1 Ip + A21 B31 g1 Ip +
    B13 B21 g1 Il Ip + B21 B31 g1 Il Ip + B21 B31 g2 Il Ip + k23Eth k31 g1 MEth + k21 k32Eth g1 MEth +
    k32Eth A21 g1 MEth + k23Eth A31 g1 MEth + k32Eth B21 g1 Il MEth + k23Eth B21 g2 Il MEth +
    k32Eth B21 g2 Il MEth + k23Eth B13 g1 Ip MEth + k32Eth B13 g1 Ip MEth + k23Eth B31 g1 Ip MEth)
FullSimplify[
 f]
```

```
(B21 g2 Il (k31 + A31 + B31 Ip) + k32Eth (B21 g2 Il + B13 g1 Ip) MEth) /
 ((k21 + A21) B13 g1 Ip + B21 Il (B13 g1 Ip + g2 (k31 + A31 + B31 Ip)) +
   (k23Eth + k32Eth) (B21 g2 Il + B13 g1 Ip) MEth)
```

III. Limiting Cases for f

1. Case Ip approaches 0

```
Limit[f, Ip → 0]
```

$$\frac{k31 + A31 + k32Eth\ MEth}{k31 + A31 + (k23Eth + k32Eth)\ MEth}$$

2. Case Il approaches 0

```
Limit[f, Il → 0]
```

$$\frac{k32Eth\ MEth}{k21 + \mathcal{F}21 + (k23Eth + k32Eth)\ MEth}$$

3. Case Ip approaches 0 and Il approaches 0 in said order

```
FullSimplify[Limit[Limit[f, Ip → 0 ], Il → 0]]
```

$$\frac{k31 + \mathcal{F}31 + k32Eth\ MEth}{k31 + \mathcal{F}31 + (k23Eth + k32Eth)\ MEth}$$

4. Case Ip approaches 0 and Il approaches 0 in said order

```
FullSimplify[Limit[Limit[f, Il → 0 ], Ip → 0]]
```

$$\frac{k32Eth\ MEth}{k21 + \mathcal{F}21 + (k23Eth + k32Eth)\ MEth}$$

5. Case MEth approaches ∞

```
FullSimplify[Limit[f, MEth → ∞ ]]
```

$$\frac{k32Eth}{k23Eth + k32Eth}$$

It is of note that if A31, k31, A21, k21 are relatively small (which they should be) and Ip and Il are zero then the same result is obtained for all 5 cases.

Appendix B. Three Level DPAL Model Notebook for Rb Sample Input and Without Sample Output

Three Level DPAL CW Model for Rb

I. User Inputs (in mks units)

```
Temperatureofcell = 450(*K of cell*);
TemperatureMeth = 450(*K of relaxtion gas Methane*);
TemperatureHe = 450(*K of relaxtion gas Helium*);
Alkalitemperature = 450(*K*);
TotalAlkaliConcentration = 1.5 * 10^19(*m^-3*);
Celllength = 0.03(*m*);
Celltransmission = 1.0(*Unitless*);
HRreflectivty = 1.0(*Unitless*);
OCreflectivty = 0.99(*Unitless*);
IntialPumpIntesnity = 50 000 000 (*In W/m^2*);
PartialPressureMethane = 10 * 6666(*Pa*);
PartialPressureAlkali = 0(*Pa*);
PartialPressureHelium = 10 * 6666(*Pa*);
Pumplinecenter = 384.2304844685 * 10^12(*frequency of pump line center in Hz*);
PumpFWHM = 25 * 10^9(*the FWHM of the pump in Hz*);
DistanceBetweenMirrors = 0.1(*in m*);
FidelityI = 10
 (*The Amount of Grid Points in I for 3-D Grid on which to place solution*);
Fidelityν = 10(*The Amount of Grid Points in ν pump for 3-
  D Grid on which to place solution*);
Fidelityz = 10(*The Amount of Grid Points in z for 3-D Grid on which to place solution*);
```

II. Constants

A. Common Physical Constants (in standard SI units mks)

```
c = 299 792 458 (*Wikipedia m/s*);
kb = 1.380650424 * 10^-23(*J/K*);
h = 6.6260689633 * 10^-34(*J/Hz*);
amu = 1.66053878283 * 10^-27(*kg*);
```

B. Einstein A Coeffcients

$$A21[85] = \frac{1}{27.679 * 10^{-9}} \text{ (*Lewis Hz*);}$$

$$A21[87] = \frac{1}{27.7 * 10^{-9}} \text{(*Lewis Hz*);}$$

$$A31[85] = \frac{1}{26.2348 * 10^{-9}} \text{(*Lewis Hz*);}$$

$$A31[87] = \frac{1}{26.24 * 10^{-9}} \text{(*Lewis Hz*);}$$

```
A32[85] = 0;
A32[87] = 0;
```

III. Parameters

A. Enviromental Paremeters

```
temp = 294.15(*K*);
tempcell = Temperatureofcell;
celloutsidepressure = 101.3 * 10^3 (*Pa*);
```

B. Design Parameters

```
celllength = Celllength(*m*);
celltransmission = Celltransmission(*Unitless*);
hrreflectivty = HRreflectivty(*Unitless*);
ocreflectivty = OCreflectivty(*Unitless*);
Atomicmass[87] = 86.909180527 (*Lewis amu*);
Atomicmass[85] = 84.911789738(*Lewis amu*);
n = 1. (*index of refraction Unitless*);
ng = 1.(* group index of refraction Unitless*);
ν21 = 377.1074635 * 10^12 (*frequency 21 tranisition Lewis in Hz*) ;
ν31 = 384.2304844685 * 10^12(*Lewis Hz*);
ν32 = 7.123020968 * 10^12(*Lewis Hz*);
distance = DistanceBetweenMirrors;
```

C. Laser and Cell Input Parameters

```
(*If you wish to add more species you must do so in II. C. , I. D., and in V. A.*)
TotalAlkaliConcentration = TotalAlkaliConcentration (*In m^-3*);

tempMeth = TemperatureMeth(*K*);
MMeth = PartialPressureMethane(*Partial Pressure of Methane in Pa*);
MMeth = 16.04246 * amu(*Mass of Methane Lewis kg*);
γMeth1 = 218 304.576(*For Rb87 and D1 manifold[iso?] in Hz/Pa Hager*);
γMeth2 = 196 549.137(*For Rb87 and D2 manifold[iso?]in Hz/Pa Hager*);
δMe1 = -59 459.4595; (*Hz/Pa Collision induced shift D1 Hager*)
δMe2 = -52 552.5526; (*Hz/Pa Collision induced shift D2 Hager*)

tempAlk = Alkalitemperature(*K*);
MAlk = PartialPressureAlkali; (*Partial Pressure of Alkali in Pa*)
MAlk = 85.4678; (*Mass of Alkali function of iso? in kg*)
γAlk1 = 0(* in Hz/Pa*);
γAlk2 = 0(* in Hz/Pa*);

tempHe = TemperatureHe(*K*);
MHe = PartialPressureHelium(*Partial Pressure of Helium in Pa*);
MHe = 4.002602 * amu(*Mass of Helium in kg*);
γHe1 = 141 785.446(*For Rb87 and D1 manifold[iso?] in Hz/Pa Hager*);
γHe2 = 150 037.509(*For Rb87 and D2 manifold[iso?] in Hz/Pa Hager*);
δHe1 = 35 333.8335; (*Hz/Pa Collision induced shift D1 Hager*)
δHe2 = 2775.69392; (*Hz/Pa Collision induced shift D2 Hager*)
```

D. Diode Input Lineshape

$$\text{gIp0}[\nu\_] := \left(\sqrt{\frac{\pi}{2}}\ \text{PumpFWHM}\left(1+\text{Erf}\left[\frac{\text{Pumplinecenter}}{\sqrt{2}\ \text{PumpFWHM}}\right]\right)\right)^{-1}\text{Exp}\left[-\frac{(\nu-\text{Pumplinecenter})^2}{2\,\text{PumpFWHM}^2}\right];$$

```
(*This is the Input Lineshape function for
 gaussian distribution normalized to 1 and is unitless*)
(*gIp0[ν_]:=UnitStep[ν-ν31+PumpFWHM/2]*UnitStep[ν31+PumpFWHM/2-ν]
(*This is a square wave and may be substituted*)*)
Ip0 = IntialPumpIntesnity (*W/m^2*);
Plot[gIp0[ν], {ν, ν31 - PumpFWHM * 3, ν31 + PumpFWHM * 3},
 PlotLabel → "g_pump(ν) vs. Freq. ", AxesLabel → {g_p[ν_p], Hz}]
```

IV. Kinetics

A. k Coeffcients (quenching rates only)

```
k21rate[1] = 0 / (kb * tempMeth)(* Methane Hz input the k rate in m^3/s*);
k31rate[1] = 0 / (kb * tempMeth)(* Methane Hz input the k rate in m^3/s*);
k21rate[2] = 0 / (kb * tempHe)(* Helium Hz input the k rate in m^3/s*);
k31rate[2] = 0 / (kb * tempHe)(* Helium Hz input the k rate in m^3/s*);
k21rate[3] = 0 / (kb * tempAlk)(* Alkali Hz input the k rate in m^3/s*);
k31rate[3] = 0 / (kb * tempAlk)(* Alkali Hz input the k rate in m^3/s*);
k21 := Sum[k21rate[species] * M[species], {species, 1, speciesmax, 1}];
k31 := Sum[k31rate[species] * M[species], {species, 1, speciesmax, 1}];
```

B. Energy Differences D manifold states

```
ΔE21 = h * ν21 (*J*);
ΔE31 = h * ν31 (*J*);
ΔE32 = h * ν32 (*J*);
```

C. Boltzmann Ratios

```
g3 = 4.(*Unitless*);
g2 = 2.(*Unitless*);
g1 = 2.(*Unitless*);
```

$$f21 = \frac{g1}{g2} * e^{\frac{-\Delta E21}{kb*temp}}(*\text{Unitless}*);$$

$$f31 = \frac{g1}{g3} * e^{\frac{-\Delta E31}{kb*temp}}(*\text{Unitless}*);$$

$$f32 = \frac{g2}{g3} * e^{\frac{-\Delta E32}{kb*temp}}(*\text{Unitless}*);$$

D. k Coeffcients (for partner species on the 3 and 2 levels)

```
(*If you wish to add more species you must do so in II. C. , I. D., and ine V. A.*)
k32Meth[85] = 3.16 * 10^-16 / (kb * tempMeth)(*Hager provided the number listed in m^3/s,
 but the value of the coeffcient is in Hz/Pa*);
k32Meth[87] = 3.16 * 10^-16 / (kb * tempMeth)(*Hager provided the number listed in m^3/s,
 but the value of the coeffcient is in Hz/Pa*);
k23Meth[85] = k32Meth[85] * f32(*Hz/Pa*);
k23Meth[87] = k32Meth[87] * f32(*Hz/Pa*);
k32He[85] = 1.1776 * 10^6(*Hz/Pa*);
k32He[87] = 1.1776 * 10^6(*Hz/Pa*);
k23He[85] = k32He[85] * f32(*Hz/Pa*);
k23He[87] = k32He[87] * f32(*Hz/Pa*);
k32Alk[85] = 0(*Hz/Pa*);
k32Alk[87] = 0(*Hz/Pa*);
k23Alk[85] = k32Alk[85] * f32(*Hz/Pa*);
k23Alk[87] = k32Alk[87] * f32(*Hz/Pa*);
```

V. Lineshape, Emission, and Absorbtion Cross Sections

A. Transition Lineshape

```
(*Einstein B coeffs based on the A coeff and the frequncy in Hz*)
B21[ν_, iso_] := c^3 * A21[iso] / (n^2 * ng * 8 π * h * ν^3)(*m^3/J*s^2 or m/kg which are the same*);
B12[ν_, iso_] := g2 / g1 * B21[ν, iso](*m^3/J*s^2 or m/kg*);
B31[ν_, iso_] := c^3 * A31[iso] / (n^2 * ng * 8 π * h * ν^3)(*m^3/J*s^2 or m/kg*);
B13[ν_, iso_] := g3 / g1 * B31[ν, iso](*m^3/J*s^2 or m/kg*);
τrad21[iso_] := (A21[iso])^-1(*s*);
τrad31[iso_] := (A31[iso])^-1(*s*);
τrad32 = ∞(*s*);

(*Lorentzian Linewidth for transitions*)
Δνl21[iso_] := 1/(2 π) (1/τrad21[iso]) + γMeth1 * MMeth * (tempMeth/temp)^1/2 +
    γHe1 * MHe * (tempHe/temp)^1/2 + γAlk1 * MAlk * (tempAlk/temp)^1/2 (*Hz*);
Δνl31[iso_] := 1/(2 π) (1/τrad31[iso]) + γMeth2 * MMeth * (tempMeth/temp)^1/2 +
    γHe2 * MHe * (tempHe/temp)^1/2 + γAlk2 * MAlk * (tempAlk/temp)^1/2 (*Hz*);
Mass[85] = 84.911789738 * amu(*Lewis in kg*);
Mass[87] = 86.909180527 * amu (*Lewis in kg*);
```

```
(*Hyperfine corrections to frequency for 87 and 85 rb indexed
 by F'' for low and F' for ups. Note: old  is F'' or S1/2 level*)
νhyD2low[2, 87] = 2.563005979089114 * 10^9 (*Hz*);
νhyD2low[1, 87] = -4.271676631815196 * 10^9 (*Hz*);
νhyD2up[3, 87] = 193.740846 * 10^6 (*Hz*);
νhyD2up[2, 87] = 72.911332 * 10^6 (*Hz*);
νhyD2up[1, 87] = -229.851856 * 10^6 (*Hz*);
νhyD2up[0, 87] = -302.073888 * 10^6 (*Hz*);
νhyD1low[2, 87] = 2.563005979089114 * 10^9 (*Hz*);
νhyD1low[1, 87] = -4.271676631815196 * 10^9 (*Hz*);
νhyD1up[2, 87] = 306.246 * 10^6 (*Hz*);
νhyD1up[1, 87] = -510.410 * 10^6 (*Hz*);

νhyD2low[3, 85] = 1.26488516325 * 10^9 (*Hz*);
νhyD2low[2, 85] = -1.770843922835 * 10^9 (*Hz*);
νhyD2up[4, 85] = 100.20544 * 10^6 (*Hz*);
νhyD2up[3, 85] = 20.43551 * 10^6 (*Hz*);
νhyD2up[2, 85] = -83.83534 * 10^6 (*Hz*);
νhyD2up[1, 85] = -113.20884 * 10^6 (*Hz*);
νhyD1low[3, 85] = 1.26488516325 * 10^9 (*Hz*);
νhyD1low[2, 85] = -1.770843922835 * 10^9 (*Hz*);
νhyD1up[3, 85] = 150.65971 * 10^6 (*Hz*);
νhyD1up[2, 85] = -210.492399 * 10^6 (*Hz*);
```

```
(*Line positions for hyperfine lines need several enteries 1,2,3,
4 for 𝔑ews  and 𝔒lds  (These are usually F' and F'' in literature where F is I ,
  the nucler spin, + J, the angular momentum*)
(*νhy21[𝔒ld ,𝔑ew ,𝔇,iso]=:;*)
(*νhy31[𝔒ld ,𝔑ew ,𝔇,iso]=:;*)
νhy21[𝔒ld_ , 𝔑ew_ , 𝔇_ , iso_] := ν21 - (νhyD1low[𝔒ld , iso]) + νhyD1up[𝔑ew , iso](*Hz*);
νhy31[𝔒ld_ , 𝔑ew_ , 𝔇_ , iso_] := ν31 - (νhyD2low[𝔒ld , iso]) + νhyD2up[𝔑ew , iso](*Hz*);
Δνd21[𝔒ld_ , 𝔑ew_ , 𝔇_ , iso_] :=
  νhy21[𝔒ld , 𝔑ew , 𝔇, iso] * (8 * kb * tempcell * Log[2] / (Mass[iso] * c^2))^(1/2) (*Hz*);
Δνd31[𝔒ld_ , 𝔑ew_ , 𝔇_ , iso_] := νhy31[𝔒ld , 𝔑ew , 𝔇, iso] * (8 * kb * tempcell * Log[2] / (Mass[iso] * c^2))^(1/2)
 (*Hz*);
a21[ν_, 𝔒ld_ , 𝔑ew_ , 𝔇_ , iso_] := (Log[2])^(1/2) * Δνl21[iso] / Δνd21[𝔒ld , 𝔑ew , 𝔇, iso] (*Unitless*);
u21[ν_, 𝔒ld_ , 𝔑ew_ , 𝔇_ , iso_] := 2 * (Log[2])^(1/2) *
    (ν - νhy21[𝔒ld , 𝔑ew , 𝔇, iso](*+δMe1*MMeth*(tempMeth/temp)^1/2+δHe1*MHe*(tempHe/temp)^1/2*)) /
     Δνd21[𝔒ld , 𝔑ew , 𝔇, iso](*Unitless*);
z21[ν_, 𝔒ld_ , 𝔑ew_ , 𝔇_ , iso_] := a21[ν, 𝔒ld , 𝔑ew , 𝔇, iso] + i * u21[ν, 𝔒ld , 𝔑ew , 𝔇, iso]
 (*Unitless*);

a31[ν_, 𝔒ld_ , 𝔑ew_ , 𝔇_ , iso_] := (Log[2])^(1/2) * Δνl31[iso] / Δνd31[𝔒ld , 𝔑ew , 𝔇, iso] (*Unitless*);
u31[ν_, 𝔒ld_ , 𝔑ew_ , 𝔇_ , iso_] := 2 * (Log[2])^(1/2) *
    (ν - νhy31[𝔒ld , 𝔑ew , 𝔇, iso](*+δMe2*MMeth*(tempMeth/temp)^1/2+δHe2*MHe*(tempHe/temp)^1/2*)) /
     Δνd31[𝔒ld , 𝔑ew , 𝔇, iso](*Unitless*);
z31[ν_, 𝔒ld_ , 𝔑ew_ , 𝔇_ , iso_] := a31[ν, 𝔒ld , 𝔑ew , 𝔇, iso] + i * u31[ν, 𝔒ld , 𝔑ew , 𝔇, iso]
 (*Unitless*);

(*The lineshape of each transition. These functions represent
 sets of functions for each transition indexed by there hyperfine
 compenents F' and F'' and D the manifold or 𝔑ew  and 𝔒ld  and 𝔇*)

g21[ν_, 𝔒ld_ , 𝔑ew_ , 1, iso_] := NIntegrate[(Mass[iso] / (2 π * kb * temp))^1/2 * 10^12 *
      Δνl21[iso] / (2 π * ((ν - νhy21[𝔒ld , 𝔑ew , 1, iso] - νhy21[𝔒ld , 𝔑ew , 1, iso] * νz / c)^2 +
           (Δνl21[iso] / 2)^2)), {νz, -10^6, 10^6}] / 10^12 (* in s*);

g31[ν_, 𝔒ld_ , 𝔑ew_ , 2, iso_] := NIntegrate[(Mass[iso] / (2 π * kb * temp))^1/2 * 10^12 *
      Δνl31[iso] / (2 π * ((ν - νhy31[𝔒ld , 𝔑ew , 2, iso] - νhy31[𝔒ld , 𝔑ew , 2, iso] * νz / c)^2 +
           (Δνl31[iso] / 2)^2)), {νz, -10^10, 10^10}] / 10^12 (*in s*);
```

```
g21approx[ν_, ℱold_ , ℱnew_ , 1, iso_] := (4 Log[2]/π)^(1/2) 1/(Δνd21[ℱold , ℱnew , 1, iso]
    Re[ℯ^(z21[ν,ℱold ,ℱnew ,1,iso])^2 Erfc[z21[ν, ℱold , ℱnew , 1, iso]]](*s*);
g31approx[ν_, ℱold_ , ℱnew_ , 2, iso_] := (4 Log[2]/π)^(1/2) 1/(Δνd31[ℱold , ℱnew , 2, iso]
    Re[ℯ^(z31[ν,ℱold ,ℱnew ,2,iso])^2 Erfc[z31[ν, ℱold , ℱnew , 2, iso]]](*s*);

gapproxfix21[ν_, ℱold_ , ℱnew_ , 1, iso_] :=
  If[g21approx[ν, ℱold , ℱnew , 1, iso] === Underflow[],
   0, g21approx[ν, ℱold , ℱnew , 1, iso]](*s*);
gapproxfix31[ν_, ℱold_ , ℱnew_ , 2, iso_] := If[g31approx[ν, ℱold , ℱnew , 2, iso] ===
    Underflow[], 0, g31approx[ν, ℱold , ℱnew , 2, iso]](*s*);

(*Plot[{gapproxfix21[ν,1,1,1,87],gapproxfix21[ν,1,2,1,87],gapproxfix21[ν,2,2,1,87],
   gapproxfix21[ν,2,1,1,87]},{ν,νhy21[2,2,1,87]+2*10^9,νhy21[1,1,1,87]-2*10^9},
  PlotRange→{{νhy21[1,2,1,87]-10^9,νhy21[2,1,1,87]+10^9},
    {0,gapproxfix21[νhy21[1,2,1,87],2,2,1,87]*2}}]

 Plot[{gapproxfix31[ν,1,0,2,87],gapproxfix31[ν,1,1,2,87],gapproxfix31[ν,1,2,2,87],
   gapproxfix31[ν,2,2,2,87],gapproxfix31[ν,2,1,2,87],gapproxfix31[ν,2,3,2,87]},
  {ν,νhy31[2,2,2,87]-2*10^9,νhy31[1,1,2,87]+2*10^9},
  PlotRange→{{νhy31[2,2,2,87]+2*10^9,νhy31[1,1,2,87]-2*10^9},
    {0,gapproxfix31[νhy31[2,2,2,87],2,2,2,87]*2}}]*)
```

B. Absorbtion Cross Section

i. Hyperfine Structure

```
(*S[mold ,mnew ,D,iso] is the relative line strength All are unitless*)
S[1, 1, 1, 87] = 1/6 (*Unitless*);
S[1, 2, 1, 87] = 5/6;
S[2, 2, 1, 87] = 1/2;
S[2, 1, 1, 87] = 1/2;
S[1, 0, 2, 87] = 1/6;
S[1, 1, 2, 87] = 5/12;
S[1, 2, 2, 87] = 5/12;
S[1, 3, 2, 87] = 0;
S[2, 0, 2, 87] = 0;
S[2, 1, 2, 87] = 1/20;
S[2, 2, 2, 87] = 1/4;
S[2, 3, 2, 87] = 7/10;
S[2, 2, 1, 85] = 2/9;
S[2, 3, 1, 85] = 7/9;
S[3, 2, 1, 85] = 5/9;
S[3, 3, 1, 85] = 4/9;
```

```
𝒮[2, 1, 2, 85] = 3/10;
𝒮[2, 2, 2, 85] = 7/18;
𝒮[2, 3, 2, 85] = 14/45;
𝒮[2, 4, 2, 85] = 0;
𝒮[3, 1, 2, 85] = 0;
𝒮[3, 2, 2, 85] = 5/63;
𝒮[3, 3, 2, 85] = 5/18;
𝒮[3, 4, 2, 85] = 9/14;
```

(*

$S_{F',F}$	^{87}Rb			^{85}Rb		
	F	**1**	**2**	**F**	**2**	**3**
$D_1\ ^2S_{1/2} \rightarrow\ ^2P_{1/2}$	**1**	1/6	1/2	**2**	2/9	5/9
	2	5/6	1/2	**3**	7/9	4/9
$D_2\ ^2S_{1/2} \rightarrow\ ^2P_{3/2}$	**0**	1/6	---	**1**	3/10	---
	1	5/12	1/20	**2**	7/18	5/63
	2	5/12	1/4	**3**	14/45	5/18
	3	---	7/10	**4**	---	9/14

*)

```
(*hyperfine line strengths for structure
  need them for each forbidden transitions S = 0*)
Plot[{gapproxfix21[ν, 1, 1, 1, 87] * 𝒮[1, 1, 1, 87] + gapproxfix21[ν, 1, 2, 1, 87] * 𝒮[1, 2, 1, 87] +
    gapproxfix21[ν, 2, 2, 1, 87] * 𝒮[2, 2, 1, 87] + gapproxfix21[ν, 2, 1, 1, 87] * 𝒮[2, 1, 1, 87]},
 {ν, νhy21[2, 2, 1, 87] + PumpFWHM, νhy21[1, 1, 1, 87] - PumpFWHM},
 PlotRange → {{νhy21[2, 2, 1, 87] + PumpFWHM, νhy21[1, 1, 1, 87] - PumpFWHM},
   {0, gapproxfix21[νhy21[2, 2, 1, 87], 2, 2, 1, 87] * 1}},
 PlotLabel → "g21(ν) vs. Freq. For 87Rb", AxesLabel → {Frequency [Hz], g[ν] [unitless]}]
Plot[{gapproxfix21[ν, 2, 2, 1, 85] * 𝒮[2, 2, 1, 85] + gapproxfix21[ν, 2, 3, 1, 85] * 𝒮[2, 3, 1, 85] +
    gapproxfix21[ν, 3, 3, 1, 85] * 𝒮[3, 3, 1, 85] + gapproxfix21[ν, 3, 2, 1, 85] * 𝒮[3, 2, 1, 85]},
 {ν, νhy21[3, 3, 1, 85] + PumpFWHM, νhy21[2, 2, 1, 85] - PumpFWHM},
 PlotRange → {{νhy21[3, 3, 1, 85] + PumpFWHM, νhy21[2, 2, 1, 85] - PumpFWHM},
   {0, gapproxfix21[νhy21[2, 2, 1, 85], 2, 2, 1, 85] * 1}},
 PlotLabel → "g21(ν) vs. Freq. For 85Rb", AxesLabel → {Frequency [Hz], g[ν] [unitless]}]
Plot[{gapproxfix31[ν, 1, 0, 2, 87] * 𝒮[1, 0, 2, 87] + gapproxfix31[ν, 1, 1, 2, 87] * 𝒮[1, 1, 2, 87] +
    gapproxfix31[ν, 1, 2, 2, 87] * 𝒮[1, 2, 2, 87] + gapproxfix31[ν, 2, 2, 2, 87] * 𝒮[2, 2, 2, 87] +
```

```
    gapproxfix31[ν, 2, 1, 2, 87] * S[2, 1, 2, 87] + gapproxfix31[ν, 2, 3, 2, 87] * S[2, 3, 2, 87]},
  {ν, νhy31[2, 2, 2, 87] + PumpFWHM, νhy31[1, 1, 2, 87] - PumpFWHM},
  PlotRange → {{νhy31[2, 2, 2, 87] + PumpFWHM, νhy31[1, 1, 2, 87] - PumpFWHM},
    {0, gapproxfix31[νhy31[2, 2, 2, 87], 2, 2, 2, 87] * 1}},
  PlotLabel → "g31(ν) vs. Freq. For 87Rb", AxesLabel → {Frequency [Hz], g[ν] [unitless]}]
Plot[{gapproxfix31[ν, 2, 1, 2, 85] * S[2, 1, 2, 85] + gapproxfix31[ν, 2, 2, 2, 85] * S[2, 2, 2, 85] +
    gapproxfix31[ν, 2, 3, 2, 85] * S[2, 3, 2, 85] + gapproxfix31[ν, 3, 3, 2, 85] * S[3, 3, 2, 85] +
    gapproxfix31[ν, 3, 2, 2, 85] * S[3, 2, 2, 85] + gapproxfix31[ν, 3, 4, 2, 85] * S[3, 4, 2, 85]},
  {ν, νhy31[3, 3, 2, 85] + PumpFWHM, νhy31[2, 2, 2, 85] - PumpFWHM},
  PlotRange → {{νhy31[3, 3, 2, 85] + PumpFWHM, νhy31[2, 2, 2, 85] - PumpFWHM},
    {0, gapproxfix31[ν31, 3, 3, 2, 85] * 15}},
  PlotLabel → "g31(ν) vs. Freq. For 85Rb", AxesLabel → {Frequency [Hz], g[ν] [unitless]}]
```

ii. Statistical isotope distribution

```
fiso[85] = 0.7217(*Unitless*);
fiso[87] = 0.2783(*Unitless*);

ℱnewmin [1, 87] = 1(*Unitless*);
ℱnewmax [1, 87] = 2(*Unitless*);
ℱoldmin [1, 87] = 1(*Unitless*);
ℱoldmax [1, 87] = 2(*Unitless*);

ℱnewmin [2, 87] = 0(*Unitless*);
ℱnewmax [2, 87] = 3(*Unitless*);
ℱoldmin [2, 87] = 1(*Unitless*);
ℱoldmax [2, 87] = 2(*Unitless*);

ℱnewmin [1, 85] = 2(*Unitless*);
ℱnewmax [1, 85] = 3(*Unitless*);
ℱoldmin [1, 85] = 2(*Unitless*);
ℱoldmax [1, 85] = 3(*Unitless*);

ℱnewmin [2, 85] = 1(*Unitless*);
ℱnewmax [2, 85] = 4(*Unitless*);
ℱoldmin [2, 85] = 2(*Unitless*);
ℱoldmax [2, 85] = 3(*Unitless*);

isomin = 85(*Unitless*);
isomax = 87(*Unitless*);
isostep = 2(*Unitless*);

EngD2[ℱold_ , iso_] := h * (ν31 - νhyD2low[ℱold , iso] )
 (*The energy of a given F'' state in J*);
EngD1[ℱold_ , iso_] := h * (ν21 - νhyD1low[ℱold , iso])(*J*);

ftotD1[85] = Sum[(2 ℱold + 1) * e^(-EngD1[ℱold ,85]/(kb*temp)), {ℱold, ℱoldmin[1,85], ℱoldmax[1,85]}] (*Unitless*);

ftotD1[87] = Sum[(2 ℱold + 1) * e^(-EngD1[ℱold ,87]/(kb*temp)), {ℱold, ℱoldmin[1,87], ℱoldmax[1,87]}] (*Unitless*);

ftotD2[85] := Sum[(2 ℱold + 1) * e^(-EngD2[ℱold ,85]/(kb*temp)), {ℱold, ℱoldmin[2,85], ℱoldmax[2,85]}] (*Unitless*);

ftotD2[87] := Sum[(2 ℱold + 1) * e^(-EngD2[ℱold ,87]/(kb*temp)), {ℱold, ℱoldmin[2,87], ℱoldmax[2,87]}] (*Unitless*);

ff21[ℱold_ , iso_] := (2 ℱold + 1) * e^(-EngD1[ℱold ,iso]/(kb*temp)) / ftotD1[iso]
(*stat dis among ℱ states will need several enteries for each(*Unitless*)*)

ff31[ℱold_ , iso_] := (2 ℱold + 1) * e^(-EngD2[ℱold ,iso]/(kb*temp)) / ftotD2[iso]
 (*stat dis among ℱ states will need several enteries for each(*Unitless*)*)
```

iii. Cross Sections (in m^2)

```
σ12abs[ν_] =
  Sum[Sum[Sum[Sum[(g2/g1) * ((c^2/ν^2 * 8 π) A21[iso] * S[𝔉old, 𝔉new, 𝔇, iso] *
          gapproxfix21[ν, 𝔉old, 𝔉new, 𝔇, iso] * ff21[𝔉old, iso] * fiso[iso]),
    {iso, isomin, isomax, isostep}] (*m^2*);
σ13abs[ν_] = Sum[Sum[Sum[Sum[(g3/g1) * ((c^2/ν^2 * 8 π) A31[iso] * S[𝔉old, 𝔉new, 𝔇,
          iso] * gapproxfix31[ν, 𝔉old, 𝔉new, 𝔇, iso] * ff31[𝔉old, iso] * fiso[iso])),
    , {iso, isomin, isomax, isostep}] (*m^2*);
```

C. Emission Cross Sections

```
σ21ems[ν_] = g1/g2 σ12abs[ν](*m^2*);
σ31ems[ν_] = g1/g3 σ13abs[ν](*m^2*);
(*Do[Print[σ21ems[νhy21[2,2,1,87]-10^6+i*10^5]],{i,100}];*)
(*trapend=2*10^11;
trapstep=10^9;
trapstart=νhy21[2,2,1,87]-10^9;
trapend/(trapend/trapstep)*Sum[σ21ems[νhy21[2,2,1,87]-10^11+l],{l,0,trapend,trapstep}]*)

(*Plot[{σ21ems[ν_]},{ν,νhy21[2,2,1,87]-10^9,νhy21[2,2,1,87]+10^9},
 PlotRange→{{νhy21[2,2,1,87]-10^9,νhy21[2,2,1,87]+10^9},{0,2*10^-7}}]*)
(*NIntegrate[σ21ems[ν_],{ν,νhy21[2,2,1,87],νhy21[1,1,1,87]},Method→"TrapezoidalRule"]*)
gapproxfixtotal21[ν_] =
  Sum[∑_{D=1}^{1} ∑_{ℜold=ℜoldmin[D,iso]}^{ℜoldmax[D,iso]} ∑_{ℜnew=ℜnewmin[D,iso]}^{ℜnewmax[D,iso]} gapproxfix21[ν, ℜold, ℜnew, D, iso] *
      S[ℜold, ℜnew, D, iso] * fiso[iso] * ff21[ℜold, iso], {iso, isomin, isomax, isostep}];

gapproxfixtotal31[ν_] = Sum[∑_{D=2}^{2} ∑_{ℜold=ℜoldmin[D,iso]}^{ℜoldmax[D,iso]} ∑_{ℜnew=ℜnewmin[D,iso]}^{ℜnewmax[D,iso]} gapproxfix31[
      ν, ℜold, ℜnew, D, iso] * S[ℜold, ℜnew, D, iso] *
     fiso[iso] ff31[ℜold, iso], {iso, isomin, isomax, isostep}];

Plot[{gapproxfixtotal31[ν31 + ν], gIp0[ν31 + ν]}, {ν, -2 * PumpFWHM, 2 * PumpFWHM},
 PlotRange → {{-PumpFWHM * 2, PumpFWHM * 2}, {0, gapproxfixtotal31[νhy31[2, 2, 2, 87]] * 3}},
 PlotLabel → Style["g31(ν)(Blue) and gpump(νp)(Red) for Rb vs. Freq.", 24],
 LabelStyle → Directive[Large], AxesLabel → {Frequency [Hz], g[ν] [unitless]},
 LabelStyle → Directive[Large], AxesOrigin → {-PumpFWHM * 2, 0}]
Plot[σ31ems[ν31 + ν], {ν, -2 * PumpFWHM, 2 * PumpFWHM},
 PlotRange → {{-2 * PumpFWHM, 2 * PumpFWHM}, {0, σ31ems[νhy31[2, 2, 2, 87]] * 3}},
 PlotLabel → Style["σ31ems[ν] vs. Freq.", 24], LabelStyle → Directive[Large],
 AxesLabel → {Frequency[Hz], σ31ems[ν] [m^2]}, LabelStyle → Directive[Large],
 AxesOrigin → {-2 * PumpFWHM, 0}, PlotPoints → 400]

Plot[gapproxfixtotal21[ν21 + ν], {ν, -1 / 5 * PumpFWHM, 1 / 4 * PumpFWHM},
 PlotLabel → Style["g21(ν) For Rb vs. Freq.", 24],
 AxesLabel → {Frequency [Hz], g[ν] [unitless]}, LabelStyle → Directive[Large],
 AxesOrigin → {-PumpFWHM * 1 / 5, 0}, PlotRange →
  {{-PumpFWHM * 1 / 5, PumpFWHM * 1 / 4}, {0, gapproxfixtotal21[νhy21[1, 1, 1, 87]] * 10}}]
Plot[σ21ems[ν21 + ν], {ν, -2 * PumpFWHM, +2 * PumpFWHM},
 PlotRange → {{-PumpFWHM * 2, PumpFWHM * 2}, {0, σ21ems[νhy21[1, 1, 1, 87]] * 6}},
 PlotLabel → Style["σ21ems(ν) vs. Freq.", 24], AxesLabel → {Frequency[Hz], σ21ems[ν] [m^2]},
 LabelStyle → Directive[Large], AxesOrigin → {-PumpFWHM * 2, 0}, PlotPoints → 400]
```

D. Cavity-Mode Spacing

```
Δνfsr = c / (2 * n * distance);
νmaxgain = ν /. Last[FindMaximum[σ21ems[ν], {ν, ν21 - 10^10, ν21 + 10^10}]];
qmaxgain = Round[νmaxgain / Δνfsr];
νlaser = qmaxgain * Δνfsr;
Plot[(νlaser / Pumplinecenter) (σ21ems[ν21 + ν] / σ31ems[Pumplinecenter + ν]), {ν, -2 * PumpFWHM, 2 * PumpFWHM},
 PlotLabel → Style["η The effciency factor vs. Frequency in Hz", 24],
 AxesLabel → {Freq[Hz], η}, LabelStyle → Directive[Large]]
```

VII. Rate Equations Analysis, ODE Solutions, and System Outputs

(*

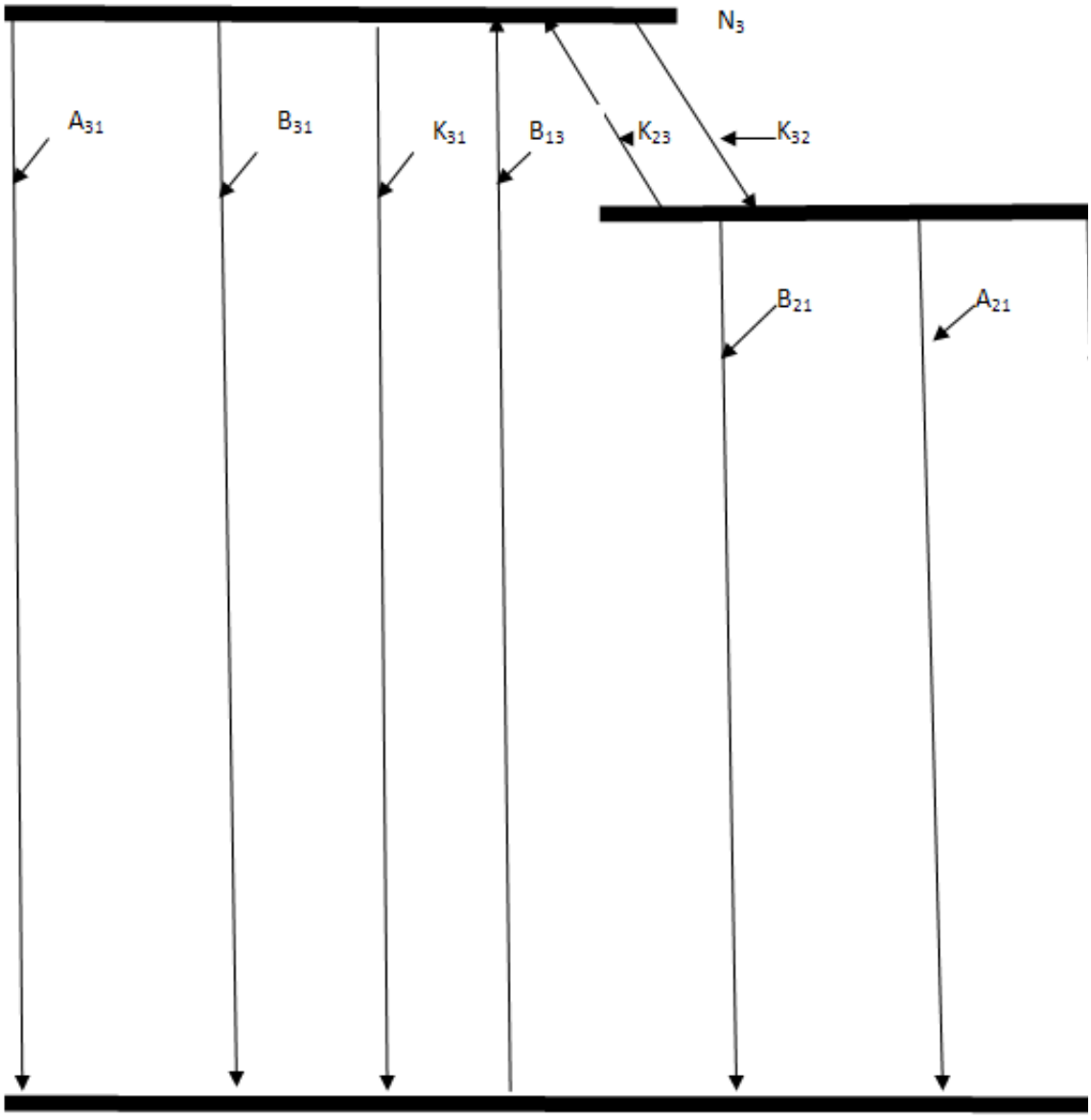

)

A. Species Setups

```
(*If you wish to add more species you must do so in II. C. ,
I. D., and in V. A. Also rember the species numer (1,2,3...)
 must be the same for all coeffs and pressures. [2] must always
 correspond to Heane for the species, but other sums do exist*)
k23[1, iso_] := k23Meth[iso](*Hz*);
k23[2, iso_] := k23He[iso](*Hz*);
k23[3, iso_] := k23Alk[iso](*Hz*);
k32[1, iso_] := k32Meth[iso](*Hz*);
k32[2, iso_] := k32He[iso](*Hz*);
k32[3, iso_] := k32Alk[iso](*Hz*);
M[1] = MMeth; (*Partial Pressures in Pa*)
M[2] = MHe(*Pa*);
M[3] = MAlk(*Pa*);
speciesmax = 3(*Unitless*);
```

B. Rate Equations and Populations

```
Nt = TotalAlkaliConcentration (*in m^-3*);
Il[z_] := Iplu[z] + Iminu[z] (*W/m^2*);
(*Reqn1[N1_ , N2_ , N3_ ] := ∫_-∞^∞ Σ_species=1^speciesmax N3 *A31+N2 *A21 +
  N3 *k31+N2 *k21+ (-B13[ν]*N1 *Ip+B31[ν]*N3 *Ip+B21[ν]*Il* (N2 - g2/g1 N1 )) dν;
Reqn2[N1_ , N2_ , N3_ ] := ∫_-∞^∞ Σ_species=1^speciesmax N3 *k32Meth*MMeth-N2 *k23Meth*MMeth-
  N2 *A21-N2 *k21 -B21[ν]*Il* (N2 - g2/g1 N1 ) dν;
Reqn3[N1_ , N2_ , N3_ ] := ∫_-∞^∞ Σ_species=1^speciesmax -N3 *k32Meth*MMeth+N2 *k23Meth*MMeth-
  N3 *A31-N3 *k31 +B13[ν]*Ip*N1 -B31[ν]*N3 *Ip dν;
Reqn4[N1_ , N2_ , N3_ ] := N1 +N2 +N3 ;
Solve[{Reqn2[N1 , N2 , N3 ],Reqn3[N1 , N2 , N3 ],Reqn4[N1 , N2 , N3 ]}=={0,0,Nt },{N1 , N2 , N3 }];
f= N2/(N2 +N3 );*)
```

$$
\begin{aligned}
\text{Pop3}[z\_, \nu\_, \nu\text{pump}\_] = \quad & \text{Sum}\Big[\text{Sum}\Big[\text{fiso}[\text{iso}] * \frac{1}{\text{speciesmax}} * \\
& \Big(-\Big(Nt\ \Big(-\text{k21} - \text{A21}[\text{iso}] - \text{k23}[\text{species}, \text{iso}]\, \text{M}[\text{species}] - \frac{\text{Il}[z]\, \sigma\text{21ems}[\nu\text{laser}]}{h\, \nu\text{laser}} - \\
& \frac{\text{g2}\, \text{Il}[z]\, \sigma\text{21ems}[\nu\text{laser}]}{\text{g1}\, h\, \nu\text{laser}}\Big)\Big)\Big(-\frac{\text{g2}\, \text{Il}[z]\, \sigma\text{21ems}[\nu\text{laser}]}{\text{g1}\, h\, \nu\text{laser}} - \frac{\text{g3}\, \text{Ip}[z]\, \sigma\text{31ems}[\nu\text{pump}]}{\text{g1}\, h\, \nu\text{pump}}\Big) - \\
& \frac{1}{\text{g1}\, h\, \nu\text{laser}}\, \text{g2}\, Nt\ \text{Il}[z]\, \sigma\text{21ems}[\nu\text{laser}]\ \Big(\text{k21} + \text{A21}[\text{iso}] + \frac{\text{Il}[z]\, \sigma\text{21ems}[\nu\text{laser}]}{h\, \nu\text{laser}} + \\
& \frac{\text{g2}\, \text{Il}[z]\, \sigma\text{21ems}[\nu\text{laser}]}{\text{g1}\, h\, \nu\text{laser}} + \frac{\text{g3}\, \text{Ip}[z]\, \sigma\text{31ems}[\nu\text{pump}]}{\text{g1}\, h\, \nu\text{pump}}\Big)\Big)\Big/ \\
& \Big(-\Big(\text{k32}[\text{species}, \text{iso}]\, \text{M}[\text{species}] - \frac{\text{g2}\, \text{Il}[z]\, \sigma\text{21ems}[\nu\text{laser}]}{\text{g1}\, h\, \nu\text{laser}}\Big)\Big(\text{k21} + \text{A21}[\text{iso}] + \\
& \frac{\text{Il}[z]\, \sigma\text{21ems}[\nu\text{laser}]}{h\, \nu\text{laser}} + \frac{\text{g2}\, \text{Il}[z]\, \sigma\text{21ems}[\nu\text{laser}]}{\text{g1}\, h\, \nu\text{laser}} + \frac{\text{g3}\, \text{Ip}[z]\, \sigma\text{31ems}[\nu\text{pump}]}{\text{g1}\, h\, \nu\text{pump}}\Big) + \\
& \Big(-\text{k21} - \text{A21}[\text{iso}] - \text{k23}[\text{species}, \text{iso}]\, \text{M}[\text{species}] - \frac{\text{Il}[z]\, \sigma\text{21ems}[\nu\text{laser}]}{h\, \nu\text{laser}} - \\
& \frac{\text{g2}\, \text{Il}[z]\, \sigma\text{21ems}[\nu\text{laser}]}{\text{g1}\, h\, \nu\text{laser}}\Big)\Big(\text{k31} + \text{A31}[\text{iso}] + \frac{\text{g2}\, \text{Il}[z]\, \sigma\text{21ems}[\nu\text{laser}]}{\text{g1}\, h\, \nu\text{laser}} +
\end{aligned}
$$

```
                    Ip[z] σ31ems[νpump]        g3 Ip[z] σ31ems[νpump]
                   ---------------------  +  ------------------------  ))))),
                      h νpump                   g1 h νpump

      {species, 1, speciesmax, 1}], {iso, isomin, isomax, isostep}] (*m^-3*);

Pop2[z_, ν_, νpump_] =      Sum[Sum[fiso[iso] * 1/speciesmax *

    (-(g2 Nt Il[z] σ21ems[νlaser])) / (g1 h νlaser (-k21 - A21[iso] -

          k23[species, iso] M[species] - Il[z] σ21ems[νlaser]/(h νlaser) - g2 Il[z] σ21ems[νlaser]/(g1 h νlaser))) +

    (((k32[species, iso] M[species] - g2 Il[z] σ21ems[νlaser]/(g1 h νlaser))

       (Nt (-k21 - A21[iso] - k23[species, iso] M[species] - Il[z] σ21ems[νlaser]/(h νlaser) -

          g2 Il[z] σ21ems[νlaser]/(g1 h νlaser)) (-g2 Il[z] σ21ems[νlaser]/(g1 h νlaser) - g3 Ip[z] σ31ems[νpump]/(g1 h νpump)) -

       1/(g1 h νlaser) g2 Nt Il[z] σ21ems[νlaser] (k21 + A21[iso] + Il[z] σ21ems[νlaser]/(h νlaser) +

          g2 Il[z] σ21ems[νlaser]/(g1 h νlaser) + g3 Ip[z] σ31ems[νpump]/(g1 h νpump))))) /

     (((-k21 - A21[iso] - k23[species, iso] M[species] - Il[z] σ21ems[νlaser]/(h νlaser) -

          g2 Il[z] σ21ems[νlaser]/(g1 h νlaser))

       (-(k32[species, iso] M[species] - g2 Il[z] σ21ems[νlaser]/(g1 h νlaser)) (k21 + A21[iso] +

          Il[z] σ21ems[νlaser]/(h νlaser) + g2 Il[z] σ21ems[νlaser]/(g1 h νlaser) + g3 Ip[z] σ31ems[νpump]/(g1 h νpump)) +

       (-k21 - A21[iso] - k23[species, iso] M[species] - Il[z] σ21ems[νlaser]/(h νlaser) -

          g2 Il[z] σ21ems[νlaser]/(g1 h νlaser)) (k31 + A31[iso] + g2 Il[z] σ21ems[νlaser]/(g1 h νlaser) +

          Ip[z] σ31ems[νpump]/(h νpump) + g3 Ip[z] σ31ems[νpump]/(g1 h νpump))))),

      {species, 1, speciesmax, 1}], {iso, isomin, isomax,
```

```
    isostep}](*m^-3*);

Pop1[z_, ν_, νpump_] =      Sum[Sum[fiso[iso] * 1/speciesmax *
    (Δt + (g2 Δt Il[z] σ21ems[νlaser])) / (g1 h νlaser (-k21 - A21[iso] -
          k23[species, iso] M[species] - Il[z] σ21ems[νlaser]/(h νlaser) - g2 Il[z] σ21ems[νlaser]/(g1 h νlaser))) +
     (Δt (-k21 - A21[iso] - k23[species, iso] M[species] - Il[z] σ21ems[νlaser]/(h νlaser) -
        g2 Il[z] σ21ems[νlaser]/(g1 h νlaser)) (-g2 Il[z] σ21ems[νlaser]/(g1 h νlaser) - g3 Ip[z] σ31ems[νpump]/(g1 h νpump)) -
      1/(g1 h νlaser) g2 Δt Il[z] σ21ems[νlaser] (k21 + A21[iso] + Il[z] σ21ems[νlaser]/(h νlaser) +
        g2 Il[z] σ21ems[νlaser]/(g1 h νlaser) + g3 Ip[z] σ31ems[νpump]/(g1 h νpump))) /
    (-(k32[species, iso] M[species] - g2 Il[z] σ21ems[νlaser]/(g1 h νlaser)) (k21 + A21[iso] +
        Il[z] σ21ems[νlaser]/(h νlaser) + g2 Il[z] σ21ems[νlaser]/(g1 h νlaser) + g3 Ip[z] σ31ems[νpump]/(g1 h νpump)) +
     (-k21 - A21[iso] - k23[species, iso] M[species] - Il[z] σ21ems[νlaser]/(h νlaser) -
        g2 Il[z] σ21ems[νlaser]/(g1 h νlaser)) (k31 + A31[iso] + g2 Il[z] σ21ems[νlaser]/(g1 h νlaser) +
        Ip[z] σ31ems[νpump]/(h νpump) + g3 Ip[z] σ31ems[νpump]/(g1 h νpump)) -
    ((k32[species, iso] M[species] - g2 Il[z] σ21ems[νlaser]/(g1 h νlaser))
       (Δt (-k21 - A21[iso] - k23[species, iso] M[species] - Il[z] σ21ems[νlaser]/(h νlaser) -
          g2 Il[z] σ21ems[νlaser]/(g1 h νlaser)) (-g2 Il[z] σ21ems[νlaser]/(g1 h νlaser) - g3 Ip[z] σ31ems[νpump]/(g1 h νpump)) -
        1/(g1 h νlaser) g2 Δt Il[z] σ21ems[νlaser] (k21 + A21[iso] + Il[z] σ21ems[νlaser]/(h νlaser) +
```

```
        (g2 Il[z] σ21ems[νlaser])/(g1 h νlaser) + (g3 Ip[z] σ31ems[νpump])/(g1 h νpump))))) /
    (((-k21 - A21[iso] - k23[species, iso] M[species] - (Il[z] σ21ems[νlaser])/(h νlaser) -
        (g2 Il[z] σ21ems[νlaser])/(g1 h νlaser))
      (-(k32[species, iso] M[species] - (g2 Il[z] σ21ems[νlaser])/(g1 h νlaser)) (k21 + A21[iso] +
          (Il[z] σ21ems[νlaser])/(h νlaser) + (g2 Il[z] σ21ems[νlaser])/(g1 h νlaser) + (g3 Ip[z] σ31ems[νpump])/(g1 h νpump)) +
        (-k21 - A21[iso] - k23[species, iso] M[species] - (Il[z] σ21ems[νlaser])/(h νlaser) -
          (g2 Il[z] σ21ems[νlaser])/(g1 h νlaser)) (k31 + A31[iso] + (g2 Il[z] σ21ems[νlaser])/(g1 h νlaser) +
          (Ip[z] σ31ems[νpump])/(h νpump) + (g3 Ip[z] σ31ems[νpump])/(g1 h νpump))))),
  {species, 1, speciesmax, 1}], {iso, isomin, isomax,
  isostep}] (*m^-3*);
```

C. f(stat dis) and Differential Equations in z for I_+, I_-, and I_p

```
Isat[νpump_] := (h * νpump)/(σ31ems[νpump]) * (1/(τrad31[85]) * fiso[85] + 1/(τrad31[87]) * fiso[87]) (*Wm^-2*);
fpop[z_, ν_] = (Pop2[z, ν])/(Pop2[z, ν] + Pop3[z, ν]) (*Unitless*);
α = 1/(2 * celllength) * Log[1/(r1 * r2 * t1^4)]; (*Loss Coeff*)
Deqn1[z_, ν_, νpump_] :=
  σ31ems[νpump] ((Pop3[z, ν, νpump]) - 2 * Pop1[z, ν, νpump] ) * Ip[z] (*m^-1*);
Deqn2[z_, ν_, νpump_] := (σ21ems[ν] ((Pop2[z, ν, νpump]) - Pop1[z, ν, νpump])) * Iplu[z]
  (*m^-1*);
Deqn3[z_, ν_, νpump_] := -(σ21ems[ν] ((Pop2[z, ν, νpump]) - Pop1[z, ν, νpump])) * Iminu[z]
  (*m^-1*);
(*Ip[0]=20000000;
Iminu[0]=1750000;
Iplu[0]=1750000;
νpump=ν31;
νlaser=νhy21[2,2,1,87];
gapproxfixtotal21loop=gapproxfixtotal21[νlaser];
gIp0loop=gIp0[νpump];
Pop1[0,νhy21[2,2,1,87],νpump];
Pop2[0,νhy21[2,2,1,87],νpump];
Pop3[0,νhy21[2,2,1,87],νpump];
Pop3[0,νhy21[2,2,1,87],νpump]-2*Pop1[0,νhy21[2,2,1,87],νpump];
Pop2[0,νhy21[2,2,1,87],νpump]-Pop1[0,νhy21[2,2,1,87],νpump]
   Pop1[0,νhy21[2,2,1,87],νpump]+
  Pop2[0,νhy21[2,2,1,87],νpump]+Pop3[0,νhy21[2,2,1,87],νpump];*)
```

D. NDSolve Routine for I_+, I_-, and I_p

```
(*Ip[znot]==Ip0*gIp0[ν31],Iplu[znot]==Iminu[znot],
refl*Iplu[zfinal]==Iminu[zfinal],Iplu[z]*Iminu[z]==Constant*)
t1 = celltransmission(*Unitless*);
r1 = hrreflectivty(*Unitless*);
r2 = ocreflectivty(*Unitless*);
znot = 0.0(*m*);
zfinal = znot + celllength(*m*);

νrange = 3 * PumpFWHM;
νsteps = Fidelityν;
Iplusteps = FidelityI;
Iplustepsize[νpump_] = (Ip0 * gIp0[νpump] / gIp0[Pumplinecenter]) / Iplusteps;
(*Ip0*gIp0[νpump]/gIp0[ν31]
      νlaser=νhy21[2,2,1,87];
    νpump=ν31;
    σ21emsloop=σ21ems[νlaser];
    σ31emsloop=σ31ems[νpump];
    gapproxfixtotal21loop=gapproxfixtotal21[νlaser];
    gIp0loop=gIp0[νpump];
Intenfunc=NDSolve[{Deqn1[z,νlaser,νpump]==Ip'[z],Deqn2[z,νlaser,νpump]==Iplu'[z],
   Deqn3[z,νlaser,νpump]==Iminu'[z],Ip[znot]==Ip0*gIp0[νpump]/gIp0[ν31],Iplu[znot]==1000,
   Iplu[znot]==r1*t1^2*Iminu[znot]},{Ip[z],Iplu[z],Iminu[z]},{z,znot,zfinal}]*)
```

```
Percentdone = 0;
νpumpcount = 1;
Do[{Iplucount = 1;
    σ21emsloop = σ21ems[νlaser];
    σ31emsloop = σ31ems[νpump];
    gapproxfixtotal21loop = gapproxfixtotal21[νlaser];
    gIp0loop = gIp0[νpump];
    νarray[νpumpcount] = νpump;
    Do[
      {
   Intenfunc = NDSolve[{Deqn1[z, νlaser, νpump] == Ip'[z],
      Deqn2[z, νlaser, νpump] == Iplu'[z], Deqn3[z, νlaser, νpump] == Iminu'[z], Ip[znot] ==
       Ip0 * gIp0[νpump] / gIp0[Pumplinecenter], Iplu[znot] + Iminu[znot] == Ipluindex,
      Iplu[znot] == r1 * t1^2 * Iminu[znot]}, {Ip, Iplu, Iminu}, {z, znot, zfinal}];
   SaveIntenfunc[νpumpcount, Iplucount] = Intenfunc,
       Iplucount = Iplucount + 1;
   (*        Percentdone2=Percentdone+100./νsteps*(Iplucount-1/Iplusteps),
       Print[Percentdone2,"% Completed"]*)
       }
      , {Ipluindex, 0, Ip0 * gIp0[νpump] / gIp0[Pumplinecenter], Iplustepsize[νpump]}],
     Percentdone = 100 * (νpumpcount - 1./νsteps),
     Print[Percentdone, "% Completed"] ,
     νpumpcount = νpumpcount + 1}
  , {νpump, Pumplinecenter - νrange, Pumplinecenter + νrange,
    ((Pumplinecenter + νrange) - (Pumplinecenter - νrange))/νsteps}
]
```

```
0.% Completed
10.% Completed
20.% Completed
30.% Completed
40.% Completed
50.% Completed
60.% Completed
70.% Completed
80.% Completed
```

E. Routine for Selecting the Best Solution from NDSolve

```
ClearAll[CurrentRoot, Rootfindeqn]
Percentdone = 0;
Do[
 {Rootfindeqn[νpumpcount2] = Ip0,
  Do[
   {(*Print[  Evaluate[Iplu[zfinal]/.SaveIntenfunc[νpumpcount2,Iplucount2]]==={0.}],*)
        zarraytest[νpumpcount2, Iplucount2] = znot,
        Iparraytest[νpumpcount2, Iplucount2] =
     Evaluate[Ip[zarraytest[νpumpcount2, Iplucount2]] /.
         SaveIntenfunc[νpumpcount2, Iplucount2]][[1]],
         Ipnolasingarraytest[νpumpcount2, Iplucount2] = Evaluate[
        Ip[zarraytest[νpumpcount2, Iplucount2]] /. SaveIntenfunc[νpumpcount2, 1]][[1]],
         Ipluarraytest[νpumpcount2, Iplucount2] =
     Evaluate[Iplu[zarraytest[νpumpcount2, Iplucount2]] /.
         SaveIntenfunc[νpumpcount2, Iplucount2]][[1]],
         Iminuarraytest[νpumpcount2, Iplucount2] =
     Evaluate[Iminu[zarraytest[νpumpcount2, Iplucount2]] /.
         SaveIntenfunc[νpumpcount2, Iplucount2]][[1]],
       N1arraytest [νpumpcount2, Iplucount2] =
     Pop1[zarraytest[νpumpcount2, Iplucount2], νlaser, νarray[νpumpcount2]] /.
      {Ip[zarraytest[νpumpcount2, Iplucount2]] → Iparraytest[νpumpcount2, Iplucount2],
       Iplu[zarraytest[νpumpcount2, Iplucount2]] → Ipluarraytest[νpumpcount2, Iplucount2],
       Iminu[zarraytest[νpumpcount2, Iplucount2]] →
        Iminuarraytest[νpumpcount2, Iplucount2]},
       N2arraytest [νpumpcount2, Iplucount2] =
     Pop2[zarraytest[νpumpcount2, Iplucount2], νlaser, νarray[νpumpcount2]] /.
      {Ip[zarraytest[νpumpcount2, Iplucount2]] → Iparraytest[νpumpcount2, Iplucount2],
       Iplu[zarraytest[νpumpcount2, Iplucount2]] → Ipluarraytest[νpumpcount2, Iplucount2],
       Iminu[zarraytest[νpumpcount2, Iplucount2]] →
        Iminuarraytest[νpumpcount2, Iplucount2]},
       N3arraytest [νpumpcount2, Iplucount2] =
     Pop3[zarraytest[νpumpcount2, Iplucount2], νlaser, νarray[νpumpcount2]] /.
      {Ip[zarraytest[νpumpcount2, Iplucount2]] → Iparraytest[νpumpcount2, Iplucount2],
       Iplu[zarraytest[νpumpcount2, Iplucount2]] → Ipluarraytest[νpumpcount2, Iplucount2],
       Iminu[zarraytest[νpumpcount2, Iplucount2]] →
        Iminuarraytest[νpumpcount2, Iplucount2]},
        γtest[νpumpcount2, zarraytest[νpumpcount2, Iplucount2]] = σ21ems[νlaser] *
      (N2arraytest [νpumpcount2, Iplucount2] - N1arraytest [νpumpcount2, Iplucount2]),
     If[
```

```
            Evaluate[Iplu[zfinal] /. SaveIntenfunc[νpumpcount2, Iplucount2]][[1]] >= 0.,
          CurrentRoot[νpumpcount2, Iplucount2] =
           (r2 * t1^2 * Evaluate[Iplu[zfinal] /. SaveIntenfunc[νpumpcount2, Iplucount2]][[1]]) /
             ((Evaluate[Iminu[zfinal] /. SaveIntenfunc[νpumpcount2, Iplucount2]][[1]]) +
               0.00001) - 1
            ],
         If[
          γtest[νpumpcount2, zarraytest[νpumpcount2, Iplucount2]] - α > 0,
          {If[Iplucount2 > 1,
            If[
             Abs[CurrentRoot[νpumpcount2, Iplucount2]] < Rootfindeqn[νpumpcount2],
             {Rootfindeqn[νpumpcount2] = Abs[CurrentRoot[νpumpcount2, Iplucount2]],
              Iplubest[νpumpcount2] = Iplucount2}
                ]
          ]},
          If[Rootfindeqn[νpumpcount2] == Ip0, {Rootfindeqn[νpumpcount2] =
             Abs[CurrentRoot[νpumpcount2, 1]], Iplubest[νpumpcount2] = 1}]
         ]
        },
        {Iplucount2, 1, Iplucount - 1, 1}
       ],
            Percentdone = 100 * (νpumpcount2 * 1. / (νpumpcount - 1)),
            Print[Percentdone, "% Completed"]
       (*,Print[Iplubest[νpumpcount2]]*), Print[Rootfindeqn[νpumpcount2]]},
     {νpumpcount2, 1, νpumpcount - 1, 1}
    ]
    Rootfindavg =
      1 / (νpumpcount - 1) Sum[Rootfindeqn[νpumpcount2], {νpumpcount2, 1, νpumpcount - 1, 1}];
9.09091% Completed
1.
18.1818% Completed
1.
27.2727% Completed
0.0815172
36.3636% Completed
2.15263
45.4545% Completed
3.1977
54.5455% Completed
3.44164
63.6364% Completed
3.1974
```

72.7273% Completed

2.15352

81.8182% Completed

0.0819762

90.9091% Completed

1.

100.% Completed

1.

F. Routine for Creating Arrays for Output Graphs Based on the Best Solutions

```
zcountfinal = Fidelityz;
γabove1 = 0;
Percentdone = 0;
Do[
 {
  γabove1a = 0,
  Do[
   {
    zarray2[zcountg] = zcountg * (zfinal - znot)/zcountfinal + znot - (zfinal - znot)/zcountfinal,
    zarray[νpumpcountg, zcountg] = zcountg * (zfinal - znot)/zcountfinal + znot - (zfinal - znot)/zcountfinal,
    Iparray[νpumpcountg, zcountg] = Evaluate[Ip[zarray[νpumpcountg, zcountg]] /.
     SaveIntenfunc[νpumpcountg, Iplubest[νpumpcountg]]][[1]],
    Ipnolasingarray[νpumpcountg, zcountg] =
  Evaluate[Ip[zarray[νpumpcountg, zcountg]] /. SaveIntenfunc[νpumpcountg, 1]][[1]],
    Ipluarray[νpumpcountg, zcountg] = Evaluate[Iplu[zarray[νpumpcountg, zcountg]] /.
     SaveIntenfunc[νpumpcountg, Iplubest[νpumpcountg]]][[1]],
    Iminuarray[νpumpcountg, zcountg] = Evaluate[Iminu[zarray[νpumpcountg, zcountg]] /.
     SaveIntenfunc[νpumpcountg, Iplubest[νpumpcountg]]][[1]],
   Λ1array [νpumpcountg, zcountg] = Pop1[zarray[νpumpcountg, zcountg], νlaser, νarray[
     νpumpcountg]] /. {Ip[zarray[νpumpcountg, zcountg]] → Iparray[νpumpcountg, zcountg],
    Iplu[zarray[νpumpcountg, zcountg]] → Ipluarray[νpumpcountg, zcountg],
    Iminu[zarray[νpumpcountg, zcountg]] → Iminuarray[νpumpcountg, zcountg]},
   Λ2array [νpumpcountg, zcountg] = Pop2[zarray[νpumpcountg, zcountg], νlaser, νarray[
     νpumpcountg]] /. {Ip[zarray[νpumpcountg, zcountg]] → Iparray[νpumpcountg, zcountg],
    Iplu[zarray[νpumpcountg, zcountg]] → Ipluarray[νpumpcountg, zcountg],
    Iminu[zarray[νpumpcountg, zcountg]] → Iminuarray[νpumpcountg, zcountg]},
   Λ3array [νpumpcountg, zcountg] = Pop3[zarray[νpumpcountg, zcountg], νlaser, νarray[
     νpumpcountg]] /. {Ip[zarray[νpumpcountg, zcountg]] → Iparray[νpumpcountg, zcountg],
    Iplu[zarray[νpumpcountg, zcountg]] → Ipluarray[νpumpcountg, zcountg],
    Iminu[zarray[νpumpcountg, zcountg]] → Iminuarray[νpumpcountg, zcountg]},
     γ[νpumpcountg, zarray[νpumpcountg, zcountg]] =
   σ21ems[νlaser] * (Λ2array [νpumpcountg, zcountg] - Λ1array [νpumpcountg, zcountg]),
  If[γabove1a == 0, νγpumpcountgmin = νpumpcountg]
   If[γ[νpumpcountg, zarray[νpumpcountg, zcountg]] > 0,
    {γabove1 = 1, γabove1a = 1, νγarray[νpumpcountg, zcountg] = νarray[νpumpcountg],
```

```
        νγpumpcountgmax = νpumpcountg}],
        γarray[νpumpcountg, zcountg] = γ[νpumpcountg, zarray[νpumpcountg, zcountg]]
        },
    {νpumpcountg, 1, νpumpcount - 1, 1}],
      Percentdone = 100 * (zcountg * 1. / zcountfinal),
      Print[Percentdone, "% Completed"],
    If[γabove1a == 1,
     {
      IpluTable = Table[{varray[νpumpcountg], Ipluarray[νpumpcountg, zcountg]},
        {νpumpcountg, νγpumpcountgmin, νγpumpcountgmax, 1}],
      IminuTable = Table[{varray[νpumpcountg], Iminuarray[νpumpcountg, zcountg]},
        {νpumpcountg, νγpumpcountgmin, νγpumpcountgmax, 1}],
      Ipluint = Interpolation[IpluTable],
      Iminuint = Interpolation[IminuTable],
      Ipluofz[zcountg] =
       NIntegrate[Ipluint[ν] * gIp0[ν], {ν, Min[Table[νγarray[νpumpcountg, zcountg],
            {νpumpcountg, νγpumpcountgmin, νγpumpcountgmax, 1}]], Max[Table[νγarray[
             νpumpcountg, zcountg], {νpumpcountg, νγpumpcountgmin, νγpumpcountgmax, 1}]]}],
      Iminuofz[zcountg] = NIntegrate[Iminuint[ν] * gIp0[ν],
        {ν, Min[Table[νγarray[νpumpcountg, zcountg], {νpumpcountg, νγpumpcountgmin,
             νγpumpcountgmax, 1}]], Max[Table[νγarray[νpumpcountg, zcountg],
            {νpumpcountg, νγpumpcountgmin, νγpumpcountgmax, 1}]]}],
      γTable = Table[ {varray[νpumpcountg], γ[νpumpcountg, zarray[νpumpcountg, zcountg]]},
        {νpumpcountg, νγpumpcountgmin, νγpumpcountgmax, 1}],
      γint = Interpolation[γTable], γofz[zcountg] = NIntegrate[γint[ν] * gIp0[ν],
        {ν, Min[Table[νγarray[νpumpcountg, zcountg], {νpumpcountg, νγpumpcountgmin,
             νγpumpcountgmax, 1}]], Max[Table[νγarray[νpumpcountg, zcountg],
            {νpumpcountg, νγpumpcountgmin, νγpumpcountgmax, 1}]]}]
       }
      ]
     },
    {zcountg, 1, zcountfinal, 1}] (*If you really need speed here comment out the sections
    on gain and their plotting routines. But you will lose alot of information.*)
10.% Completed
20.% Completed
30.% Completed
40.% Completed
50.% Completed
60.% Completed
70.% Completed
80.% Completed
90.% Completed
100.% Completed
```

G. Tabular and Plotting Routines for Best Solutions

```
Ipplot =
  Table[{νarray[νpumpcountg], zarray[νpumpcountg, zcountg], Iparray[νpumpcountg, zcountg]},
   {νpumpcountg, 1, νpumpcount - 1, 1}, {zcountg, 1, zcountfinal, 1}];
Ipnolasingplot = Table[{νarray[νpumpcountg], zarray[νpumpcountg, zcountg],
    Ipnolasingarray[νpumpcountg, zcountg]},
   {νpumpcountg, 1, νpumpcount - 1, 1}, {zcountg, 1, zcountfinal, 1}];
Ipluplot = Table[{νarray[νpumpcountg], zarray[νpumpcountg, zcountg],
    Ipluarray[νpumpcountg, zcountg]},
   {νpumpcountg, 1, νpumpcount - 1, 1}, {zcountg, 1, zcountfinal, 1}];
Iminuplot = Table[{νarray[νpumpcountg], zarray[νpumpcountg, zcountg],
    Iminuarray[νpumpcountg, zcountg]},
   {νpumpcountg, 1, νpumpcount - 1, 1}, {zcountg, 1, zcountfinal, 1}];
γplot = Table[{νarray[νpumpcountg], zarray[νpumpcountg, zcountg], γarray[νpumpcountg,
     zcountg]}, {νpumpcountg, 1, νpumpcount - 1, 1}, {zcountg, 1, zcountfinal, 1}];
αplot = Table[{νarray[νpumpcountg], zarray[νpumpcountg, zcountg], α},
   {νpumpcountg, 1, νpumpcount - 1, 1}, {zcountg, 1, zcountfinal, 1}];
Ilaseoutplot = Table[{νarray[νpumpcountg], (1 - r2) * Ipluarray[νpumpcountg, zcountfinal]},
   {νpumpcountg, 1, νpumpcount - 1, 1}];
Λ1plot = Table[{νarray[νpumpcountg], zarray[νpumpcountg, zcountg], Λ1array[νpumpcountg,
     zcountg]}, {νpumpcountg, 1, νpumpcount - 1, 1}, {zcountg, 1, zcountfinal, 1}];
Λ2plot = Table[{νarray[νpumpcountg], zarray[νpumpcountg, zcountg], Λ2array[νpumpcountg,
     zcountg]}, {νpumpcountg, 1, νpumpcount - 1, 1}, {zcountg, 1, zcountfinal, 1}];
Λ3plot = Table[{νarray[νpumpcountg], zarray[νpumpcountg, zcountg], Λ3array[νpumpcountg,
     zcountg]}, {νpumpcountg, 1, νpumpcount - 1, 1}, {zcountg, 1, zcountfinal, 1}];
Inv31plot = Table[{νarray[νpumpcountg], zarray[νpumpcountg, zcountg],
    Λ3array[νpumpcountg, zcountg] - Λ1array[νpumpcountg, zcountg]},
   {νpumpcountg, 1, νpumpcount - 1, 1}, {zcountg, 1, zcountfinal, 1}];
Inv21plot = Table[{νarray[νpumpcountg], zarray[νpumpcountg, zcountg],
    Λ2array[νpumpcountg, zcountg] - Λ1array[νpumpcountg, zcountg]},
   {νpumpcountg, 1, νpumpcount - 1, 1}, {zcountg, 1, zcountfinal, 1}];
γofzplot = Table[{zarray2[zcountg], γofz[zcountg]}, {zcountg, 1, zcountfinal, 1}];
Ipluofzplot = Table[{zarray2[zcountg], Ipluofz[zcountg]}, {zcountg, 1, zcountfinal, 1}];
Iminuofzplot = Table[{zarray2[zcountg], Iminuofz[zcountg]}, {zcountg, 1, zcountfinal, 1}];

ListPlot3D[Ipplot, DataRange → All, Mesh → 25,
 InterpolationOrder → All, ColorFunction → "SouthwestColors",
 PlotLabel → Style["Pump Intensity vs. Freq. vs. Pos.", 24],
 AxesLabel → {Pump Freq[Hz], Pos[m], I_p[W/m^2]}, (*LabelStyle→Directive[Large],*)
```

```
  PlotRange → {{Pumplinecenter - νrange, Pumplinecenter + νrange}, {0, celllength}, {0, Ip0}}]
ListPlot3D[Ipnolasingplot, DataRange → All, Mesh → 25,
  InterpolationOrder → All, ColorFunction → "SouthwestColors",
  PlotLabel → Style["Pump Intensity (no lasing) vs. Freq. vs. Pos.", 24],
  AxesLabel → {Pump Freq[Hz], Pos[m], Ip[W/m^2]}, (*LabelStyle→Directive[Large],*)
  PlotRange → {{Pumplinecenter - νrange, Pumplinecenter + νrange}, {0, celllength}, {0, Ip0}}]
ListPlot3D[Ipluplot, DataRange → All, Mesh → None,
  InterpolationOrder → All, ColorFunction → "SouthwestColors",
  PlotLabel → Style["Plus Wave Intensity vs. Freq. vs. Pos.", 24],
  AxesLabel → {Pump Freq[Hz], Pos[m], I+[W/m^2]}(*,LabelStyle→Directive[Large]*)]
ListPlot3D[Iminuplot, DataRange → All, Mesh → None,
  InterpolationOrder → All, ColorFunction → "SouthwestColors",
  PlotLabel → Style["Minus Wave Intensity vs. Freq. vs. Pos.", 24],
  AxesLabel → {Pump Freq[Hz], Pos[m], I-[W/m^2]}(*,LabelStyle→Directive[Large]*)]
ListPlot3D[N1plot , DataRange → All, Mesh → None, InterpolationOrder → All,
  ColorFunction → "SouthwestColors", PlotLabel → Style[N1 vs. Freq. vs. Pos., 24],
  AxesLabel → {Pump Freq[Hz], Pos[m], Conc[1/m^3]}(*,LabelStyle→Directive[Large]*)]
ListPlot3D[N2plot , DataRange → All, Mesh → None, InterpolationOrder → All,
  ColorFunction → "SouthwestColors", PlotLabel → Style[N2 vs. Freq. vs. Pos., 24],
  AxesLabel → {Pump Freq[Hz], Pos[m], Conc[1/m^3]}(*,LabelStyle→Directive[Large]*)]
ListPlot3D[N3plot , DataRange → All, Mesh → None, InterpolationOrder → All,
  ColorFunction → "SouthwestColors", PlotLabel → Style[N3 vs. Freq. vs. Pos., 24],
  AxesLabel → {Pump Freq[Hz], Pos[m], Conc[1/m^3]}(*,LabelStyle→Directive[Large]*)]
ListPlot3D[Inv31plot, DataRange → All, Mesh → None, InterpolationOrder → All,
  ColorFunction → "SouthwestColors", PlotLabel → Style[N3-N1 vs. Freq. vs. Pos., 24],
  AxesLabel → {Pump Freq[Hz], Pos[m], Conc[1/m^3]}(*,LabelStyle→Directive[Large]*)]
ListPlot3D[Inv21plot, DataRange → All, Mesh → None, InterpolationOrder → All,
  ColorFunction → "SouthwestColors", PlotLabel → Style[N2-N1 vs. Freq. vs. Pos., 24],
```

```
  AxesLabel → {Pump Freq[Hz], Pos[m], Conc[1/m^3]}(*,
  PlotRange→{Automatic,Automatic,{-10^17,10^17}}*)(*,LabelStyle→Directive[Large]*)]
ListPlot3D[{γplot, αplot}, DataRange → All, Mesh → None, ColorFunction → "SouthwestColors",
  InterpolationOrder → All, PlotLabel → Style["Gain Coeffcient vs. Freq. vs. Pos.", 24],
  AxesLabel → {Pump Freq[Hz], Pos[m], γ},
  PlotRange → {{Pumplinecenter - νrange, Pumplinecenter + νrange}, {0, celllength}, {-2 α, 2 α}}
  (*,LabelStyle→Directive[Large]*)]
ListLinePlot[{γofzplot}, PlotLabel → Style["γ (Integrated) vs. Pos", 24],
  AxesLabel → {Pos[m], γ}(*,LabelStyle→Directive[Large]*)]
ListLinePlot[{Ipluofzplot, Iminuofzplot},
  PlotLabel → Style["I+ and I-(Integrated over νp) vs. Pos", 24],
  AxesLabel → {Pos[m], I[W/m^2]}(*,LabelStyle→Directive[Large]*)]
ListLinePlot[Ilaseoutplot, PlotLabel → Style["Laser Output Intensity", 24],
  AxesLabel → {Pump Freq[Hz], Iout[W/m^2]}(*,LabelStyle→Directive[Large]*)]
```

H. Laser Output Power and Other System Outputs

```
Laseroutfunc = Interpolation[Ilaseoutplot];
Plot[Laseroutfunc[ν] * gIp0[ν], {ν, Pumplinecenter - νrange, Pumplinecenter + νrange}];
LasPower = NIntegrate[Laseroutfunc[ν] * gIp0[ν],
   {ν, Pumplinecenter - νrange, Pumplinecenter + νrange}];
γofzint = Interpolation[γofzplot];
γtotal = 1/(zfinal - znot) NIntegrate[γofzint[z], {z, znot, zfinal}];
OutputEfficiency = LasPower / Ip0;
(*Interpolation[ γplot]
  If[γabove1==1,γgain=NIntegrate[
     NIntegrate[Interpolation[ γplot]*gIp0[ν],{ν,Min[νγarray[νpumpcountg,zcountg]],
       Max[νγarray[νpumpcountg,zcountg]]}],{z,znot,zfinal}]];*)
Print[Style["1. The Output Laser Intensity of DPAL System Tested is predicted to be ",
  30, Bold], Style[LasPower, 30, Bold, Red], Style["W/m^2", 30, Bold, Red]]
Print[Style["2. The Output Lasing Frequency of DPAL System Tested is predicted to be ",
  30, Bold], Style[νlaser, 30, Bold, Red], Style["Hz", 30, Bold, Red]]
Print[Style["3. The Output Efficiency of the Tested DPAL System is predicted to be ",
  30, Bold], Style[OutputEfficiency * 100, 30, Bold, Red], Style["%", 30, Bold, Red]]
Print[Style["4. Ip0/Isat for this system is ", 30, Bold],
 Style[Ip0 / Isat[Pumplinecenter], 30, Bold, Red]]
Print[Style["5. γ(total)/α or Gain Divded by Loss for this system is ", 30, Bold],
 Style[γtotal / α, 30, Bold, Red]](*This is a measure of the accuracy of the simulation*)
Print[Style["6. The degree to which the boudary condition at z final was met was: ",
  30, Bold], Style[Rootfindavg, 30, Bold, Red]](*,
"Note The smaller this number is the better. Above 1 is bad and implies
  a solution set should be rerun with a longer/shorter cavity. "*)
(*This is a measure of the accuracy of the simulation*)
```

1. The Output Laser Intensity of DPAL System Tested is predicted to be $358130.\ W/m^2$
2. The Output Lasing Frequency of DPAL System Tested is predicted to be 3.77109×10^{14} Hz
3. The Output Efficiency of the Tested DPAL System is predicted to be 0.71626%
4. $\mathcal{I}_p0/\mathcal{I}_{sat}$ for this system is 103.782
5. γ(total)/α or Gain Divded by Loss for this system is 154.126
6. The degree to which the boudary condition at z final was met was: 1.66422

Bibliography

[1] Beach R.J., V.K. Kanz S.A. Payne M.A. Dubinski, W.F. Krupke and L.D. Merkle. *Opt Soc Am B*, 21, 2004.

[2] Hager, Gordon D. "A Three Level Analytic Model for Alkali Metal Vapor Lasers". *Air Force Institute of Technology*, Draft Aug 2008.

[3] Hager, Gordon D. "A quasi-two level analytic model for end pumped alkali metal vapor lasers". *Air Force Institute of Technology*, Draft May 2008.

[4] Krupke W.F., V.K. Kanz, R.J. Beach and S.A. Payne. *Opt Lett*, 28, 2003.

[5] Lewis, Charlton D. "A theoretical model analysis of absorption of a three level diode pumped alkali laser". *Air Force Institute of Technology (Thesis)*, 2009.

[6] Readle J.D., J.T. Verdeyen T.M. Spinka D.L. Carroll, C.J. Wagner and J.G. Eden. "Pumping of atomic alkali lasers by photoexicitation of a resonance line blue satellite and alkali-rare gas excimer dissociation". *Applied Physics Letters*, 94, 2009.

[7] Thompson, W.J. "Numerous neat algorithms for the voigt profile function". *Computers in Physics*, 7, 1993.

[8] Verdeyen, Joseph T. *Laser Electronics*. Prentice Hall, 2002.

[9] Zhdanov, B.V. *Opt Lett*, 33, 2008.

[10] Zhdanov B.V., R.J. Knize. *Opt Lett*, 32, 2007.

REPORT DOCUMENTATION PAGE

Form Approved
OMB No. 0704–0188

1. REPORT DATE *(DD–MM–YYYY)*	2. REPORT TYPE	3. DATES COVERED *(From — To)*
27–03–2010	Master's Thesis	Aug 2008 — Mar 2010

4. TITLE AND SUBTITLE

Simulation of a Diode Pumped Alkali Laser, A Three Level Numerical Approach

5a. CONTRACT NUMBER

5b. GRANT NUMBER

5c. PROGRAM ELEMENT NUMBER

6. AUTHOR(S)

Hackett, Shawn W. , 2Lt., USAF

5d. PROJECT NUMBER

5e. TASK NUMBER

5f. WORK UNIT NUMBER

7. PERFORMING ORGANIZATION NAME(S) AND ADDRESS(ES)

Air Force Institute of Technology
Graduate School of Engineering and Management (AFIT/EN)
2950 Hobson Way
WPAFB OH 45433-7765

8. PERFORMING ORGANIZATION REPORT NUMBER

AFIT/GAP/ENP/10-M06

9. SPONSORING / MONITORING AGENCY NAME(S) AND ADDRESS(ES)

HEL-JTO
901 University Blvd SE Ste 100
Albuquerque, NM 87106
505-248-8200 ,hel-jto@jto.hpc.mil

10. SPONSOR/MONITOR'S ACRONYM(S)

HEL-JTO

11. SPONSOR/MONITOR'S REPORT NUMBER(S)

12. DISTRIBUTION / AVAILABILITY STATEMENT

APPROVED FOR PUBLIC RELEASE; DISTRIBUTION UNLIMITED.

13. SUPPLEMENTARY NOTES

14. ABSTRACT

This paper develops a three level model for a continuous wave diode pumped alkali laser by creating rate equations based on a three level system. Differential equations for intra-gain pump attenuation and intra-gain laser growth are developed in the fashion done by Rigrod. Using *Mathematica* 7.0, these differential equations are solved numerically and a diode pumped alkali laser system is simulated.The results of the simulation are compared to previous experimental results and to previous computational results for similar systems. The absorption profile for the three level numerical model is shown to have excellent agreement with previous absorption models. The lineshapes of the three level numerical model are found to be nearly identical to previous developments excepting those models assumptions. The three level numerical model provides results closer to experimental results than previous systems and provides results which observe effects not previously modeled, such as the effects of lasing on pump attenuation.

15. SUBJECT TERMS

Diode Pumped Alkali Laser, Numerical Modelling, Rate Equation Analysis, Three Level Systems

16. SECURITY CLASSIFICATION OF:			17. LIMITATION OF ABSTRACT	18. NUMBER OF PAGES	19a. NAME OF RESPONSIBLE PERSON
a. REPORT	b. ABSTRACT	c. THIS PAGE			LtCol. Jeremy C. Holtgrave
U	U	U	UU	111	19b. TELEPHONE NUMBER *(include area code)* (937) 255-3636; jeremy.holtgrave@afit.edu